

SYNTHESIS AND CHARACTERIZATION OF ELECTROCHEMICALLY
POLYMERIZED METAL-FREE, NICKEL AND ZINC CONTAINING
PHTHALOCYANINE DERIVATIVES

A THESIS SUBMITTED TO
THE GRADUATE SCHOOL OF NATURAL AND APPLIED SCIENCES
OF
MIDDLE EAST TECHNICAL UNIVERSITY

BY

ARZU YAVUZ

IN PARTIAL FULFILLMENT OF THE REQUIREMENTS
FOR
THE DEGREE OF DOCTOR OF PHILOSOPHY
IN
POLYMER SCIENCE AND TECHNOLOGY

JULY 2009

Approval of the thesis:

**SYNTHESIS AND CHARACTERIZATION OF
ELECTROCHEMICALLY POLYMERIZED METAL-FREE,
NICKEL AND ZINC CONTAINING PHTHALOCYANINE
DERIVATIVES**

submitted by **ARZU YAVUZ** in partial fulfillment of the requirements for the degree of **Doctor of Philosophy of Science in Polymer Science and Technology Department, Middle East Technical University** by,

Prof. Dr. Canan Özgen
Dean, Graduate School of **Natural and Applied Sciences**

Prof. Dr. Cevdet Kaynak
Head of Department, **Polymer Science and Technology**

Prof. Dr. Leyla Aras
Supervisor, **Chemistry Department, METU**

Examining Committee Members:

Prof. Dr. Ahmet M. Önal
Chemistry Dept., METU

Prof. Dr. Leyla Aras
Chemistry Dept., METU

Assoc. Prof. Dr. Göknur Bayram
Chemical Engineering Dept., METU

Assoc. Prof. Dr. Cemil Alkan
Chemistry Dept., GOU

Assoc. Prof. Dr. Atilla Cihaner
Chemistry Group, Atılım University

Date: July 10, 2009

I hereby declare that all information in this document has been obtained and presented in accordance with academic rules and ethical conduct. I also declare that, as required by these rules and conduct, I have fully cited and referenced all materials and rules that are not original to this work.

Name, Last Name : Arzu YAVUZ

Signature :

ABSTRACT

SYNTHESIS AND CHARACTERIZATION OF ELECTROCHEMICALLY POLYMERIZED METAL-FREE, NICKEL AND ZINC CONTAINING PHTHALOCYANINE DERIVATIVES

Yavuz, Arzu

Ph.D., Department of Polymer Science and Technology

Supervisor: Prof. Dr. Leyla Aras

July 2009, 93 pages

In the first part of this study, 4-(2,5-di-2-thiophen-2-yl-pyrrol-1-yl)-phthalonitrile (SNS-PN) was synthesized by utilizing 1,4-di(2-thienyl)-1,4-butadione (SOOS) and 4-aminophthalonitrile via Knorr-Paal Reaction. Nuclear magnetic resonance (^1H NMR and ^{13}C NMR) and fourier transform infrared (FTIR) spectroscopies were utilized for the characterization of this compound. SNS-PN monomer was then electrochemically polymerized in acetonitrile/0.2 M LiClO_4 solvent/electrolyte couple. Characterizations of the resulting polymer P(SNS-PN) were carried out by cyclic voltammetry (CV), UV-vis and FTIR spectroscopic techniques. Spectroelectrochemical studies revealed that P(SNS-PN) has an electronic band gap of 2.5 eV and exhibits electrochromic behaviour. The switching ability of polymer was also monitored. It was also found that P(SNS-PN) was fluorescent and its fluorescence intensity enhanced in the presence of cations.

In the second part, novel tetrakis (4-(2,5-di-2-thiophen-2-yl-pyrrol-1-yl)) substituted metal-free ($\text{H}_2\text{Pc-SNS}$), zinc (ZnPc-SNS) and nickel phthalocyanine (NiPc-SNS) complexes were synthesized and characterized by elemental analysis, FTIR and UV-

Vis spectroscopies. The solution redox properties of these complexes were also studied by using CV and differential pulse voltammetry. All of the complexes showed two reversible reduction peaks having ligand-based character and one irreversible oxidation peak. Also, the electrochemical polymerization of these complexes was performed in dichloromethane/tetrabutylammonium perchlorate solvent/electrolyte couple. Resulting polymer films were characterized by UV–vis and FTIR spectroscopic techniques and their electrochemical behaviors were investigated utilizing CV. *In-situ* spectroelectrochemical investigations revealed that all the polymer films could be reversibly cycled and exhibit electrochromic behavior. Furthermore, the band gap of P(H₂Pc-SNS), P(ZnPc-SNS) and P(NiPc-SNS) were calculated as 2.38 eV, 2.25 eV and 2.69 eV, respectively. Moreover, the fluorescence property of the P(ZnPc-SNS) was investigated in dimethyl sulfoxide and toluene.

Keywords: Phthalocyanines, Spectroelectrochemistry, Electrochemical Polymerization, Electrochromism, Fluorescence Spectroscopy.

ÖZ

ELEKTROKİMYASAL OLARAK POLİMERLEŞTİRİLEN METALSİZ, NİKEL ve ÇİNKO İÇEREN FTALOSİYANİN TÜREVLERİNİN SENTEZ VE KARAKTERİZASYONU

Yavuz, Arzu

Doktora, Polimer Bilim ve Teknolojisi Bölümü

Tez Yöneticisi: Prof. Dr. Leyla Aras

Temmuz 2009, 93 sayfa

Bu çalışmanın ilk kısmında 1,4-di(2-thienyl)-1,4- butadione (SOOS) ve 4-aminophthalonitrile'in Knorr-Paal reaksiyonu sonucu 4-(2, 5-di-2-thiophen-2-yl-pyrrol-1-yl) phthalonitrile (SNS-PN) sentezlenmiştir. Bu malzemenin yapısı Nükleer Manyetik Rezonans ($^1\text{H-NMR}$ ve $^{13}\text{C-NMR}$) ve Fourier Dönüşüm Kızılötesi Spektroskopileri (FTIR) kullanılarak karakterize edilmiştir. SNS-PN daha sonra asetonitril/0.2 M LiClO_4 çözücü/elektrolit çifti içerisinde elektrokimyasal olarak polimerleştirilmiştir. Elde edilen polimerin, P(SNS-PN), karakterizasyonu, döngülü voltametre (CV), UV-Vis ve FTIR spektroskopik teknikleriyle gerçekleştirilmiştir. Spektroelektrokimyasal çalışmalar göstermiştir ki P(SNS-PN) 2.5 eV değerinde bir bant aralığına sahiptir ve elektrokromik özellik göstermektedir. Polimerin anahtarlama özelliği de çalışılmıştır. P(SNS-PN) floresan özellik göstermiş ve katyonların varlığında floresan şiddeti artmıştır.

İkinci kısımda ise yeni, (4-(2, 5-di-2-thiophen-2-yl-pyrrol-1-yl)) eklenmiş metalsiz ($\text{H}_2\text{Pc-SNS}$), çinko (ZnPc-SNS) ve nikel ftalosyanin (NiPc-SNS), kompleksleri

sentezlenmiş ve elemental analiz, FTIR ve Uv-Vis spektroskopileri kullanılarak karakterize edilmişlerdir. Komplekslerin çözelti redoks özellikleri CV ve diferansiyel puls voltametri ile çalışılmıştır. Bütün komplekslerde ftalosyanin halkasından kaynaklanan iki adet tersinir indirgenme ve bir adet tersinmez yükseltgenme piki gözlenmiştir. Bu komplekslerin elektrokimyasal polimerleşmeleri de diklorometan/tetrabütülamonyum perklorat çözücü/elektrolit çifti içerisinde gerçekleştirilmiştir. Oluşan polimer filmleri, P(H₂Pc-SNS), P(ZnPc-SNS) ve P(NiPc-SNS), UV-vis ve FTIR spektroskopik teknikleriyle karakterize edilmiş ve elektrokimyasal davranımları CV tekniği ile incelenmiştir. Spektroelektrokimyasal çalışmalar, polimer filmlerinin tersinir bir şekilde indirgenmiş ve oksitlenmiş hallerine dönüştürüldüğünü ve elektrokromik özellik gösterdiğini açığa çıkartmıştır. Bununla birlikte, P(H₂Pc-SNS), P(ZnPc-SNS) ve P(NiPc-SNS) filmlerinin bant aralıkları sırasıyla 2.38 eV, 2.25 eV ve 2.69 eV olarak hesaplanmıştır. Ayrıca P(ZnPc-SNS)'in floresan özelliği dimetilsülfoksit ve toluen içerisinde incelenmiştir.

Anahtar Kelimeler: Ftalosyanin, Spektroelektrokimya, Elektrokimyasal Polimerleşme, Elektrokromizm, Floresan Spektroskopisi

To My Beloved Husband
For his love and patience

To My Parents
For their endless support

ACKNOWLEDGEMENTS

I would like to give many thanks to my supervisor, Prof. Dr. Leyla Aras, for her patience, valuable guidance and enthusiasm throughout the success of this work. Her continual encouragement allowed me to improve my abilities and become a better chemist.

I give great thanks to the members of my Ph.D. examining committee, Prof. Dr. Ahmet M. Önal for his support, guidance and helps for electrochemical measurements and Assoc. Prof. Dr. Göknur Bayram, for their time and deliberative consideration of this work.

Special thanks go to my dear friend Buket Bezgin for her endless help during electrochemical study and bighearted friendship.

I also wish to express my thanks to my friends Cemil Alkan, Tuba Ecevit, Gözde Tuzcu, Ayşegül Elmacı, Asuman Aybey and Fadile Kapaklı for their friendship, moral supports and encouragement.

For being a hospitable laboratory, many thanks go to the members of B-24 research group. For elemental analyses, I would like to give my thanks to Leyla Karabey Molu and Central Laboratory of METU.

Last, but not least, I thank my mother, father and brothers and my beloved husband for their patience, support and constant encouragement. Appreciation is extended to colleagues in the Department of Chemistry, METU.

TABLE OF CONTENTS

ABSTRACT	iv
ÖZ	vi
ACKNOWLEDGEMENTS	ix
TABLE OF CONTENTS	x
LIST OF FIGURES	xiv
LIST OF TABLES	xviii
ABBREVIATIONS	xix

CHAPTERS

1. INTRODUCTION.....	1
1.1 Phthalocyanines	1
1.1.1 History of Phthalocyanines	1
1.1.2 Structures of Phthalocyanines	3
1.1.3 Synthesis of Phthalocyanines	6
1.1.3.1 Soluble Phthalocyanines	9
1.1.3.1.1 Tetra-Substituted Phthalocyanines	10
1.1.3.1.2 Octa-Substituted Phthalocyanines	11
1.1.4 Mechanism of Phthalocyanine formation	11
1.1.5 Application of Phthalocyanines	14
1.2 Chemistry of Phthalocyanines	15
1.2.1 Spectral Properties	15
1.2.1.1 Absorption Spectra of Phthalocyanines	15
1.2.1.2 Infrared Spectroscopy	17
1.2.2 Electrochemistry of Phthalocyanines	17
1.3 Phthalocyanine Polymers	18
1.3.1 Polymeric Phthalocyanines by Cyclotetramerization Reactions.....	18

1.3.2 Polymeric Phthalocyanines by Electropolymerization	20
1.3.2.1 The Electrochemical Polymerization Strategy	20
1.4 Electrochemical Basics	22
1.4.1 Cyclic Voltammetry	22
1.4.2 Constant Potential Methods (Potentiostatic)	24
1.4.3 Constant Current Methods (Galvanostatic)	25
1.4.4 Differential Pulse Voltammetry (DPV)	25
1.4.5 Spectroelectrochemistry	26
1.4.6 Electrochromism	27
1.5 Aim of the study	28
2. EXPERIMENTAL	30
2.1 Materials	30
2.2 Instrumentation	30
2.2.1 Nuclear Magnetic Resonance (NMR) Spectrometer	30
2.2.2 Fourier Transform Infrared (FTIR) Spectrometer	31
2.2.3 Fluorescence Spectrophotometer	31
2.2.4 Scanning Electron Microscopy	31
2.2.5 Elemental Analyzer	31
2.3 Electropolymerization and Characterization	32
2.3.1 Electropolymerization of SNS-PN	32
2.3.2 Electropolymerization of H ₂ Pc-SNS, ZnPc-SNS and NiPc-SNS ...	33
2.3.3 Spectroelectrochemistry	33
2.3.4 Switching Properties of Polymers	35
2.4 Experimental Procedure	35
2.4.1 Synthesis of 4-aminophthalonitrile	35
2.4.2 Synthesis of 1,4-di(2-thienyl)-1,4-butadione (SOOS)	36
2.4.3 Synthesis of 4-(2,5-di-2-thiophen-2-yl-pyrrol-1-yl)phthalonitrile (SNS-PN)	37

2.4.4 Synthesis of tetrakis(4-(2,5-di-2-thiophen-2-yl-pyrrol-1-yl)) phthalocyanine (H ₂ Pc-SNS).....	38
2.4.5 Synthesis of tetrakis(4-(2,5-di-2-thiophen-2-yl-pyrrol-1-yl)) phthalocyaninato zinc (ZnPc-SNS).....	38
2.4.6 Synthesis of tetrakis(4-(2,5-di-2-thiophen-2-yl-pyrrol-1-yl)) phthalocyaninato nickel (NiPc-SNS)	39
3. RESULTS AND DISCUSSION	41
3.1 Spectroscopic Characterizations.....	42
3.1.1 SNS-PN and P(SNS-PN).....	42
3.1.1.1 ¹ H and ¹³ C NMR Spectroscopies	42
3.1.1.2 Infrared Spectrometry	44
3.1.1.3 Elemental Analysis	45
3.1.2 H ₂ Pc-SNS, ZnPc-SNS and NiPc-SNS	46
3.1.2.1 ¹ H and ¹³ C NMR Spectroscopies	46
3.1.2.2 Elemental Analysis	46
3.1.2.3 UV-Vis Absorption Spectroscopy	47
3.1.2.4 Infrared Spectrometry	49
3.1.3 P(H ₂ Pc-SNS), P(ZnPc-SNS) and P(NiPc-SNS).....	53
3.2 Electrochemical Characterization.....	55
3.2.1 H ₂ Pc-SNS, ZnPc-SNS and NiPc-SNS	55
3.3 Electropolymerization	60
3.3.1 SNS-PN	60
3.3.2 H ₂ Pc-SNS, ZnPc-SNS and NiPc-SNS	63
3.4 Spectroelectrochemistry	71
3.4.1 P(SNS-PN)	71
3.4.2 P(H ₂ Pc-SNS), P(ZnPc-SNS) and P(NiPc-SNS).....	73
3.5 Electrochromic Switching	76
3.5.1 P(SNS-PN)	77

3.5.2 P(H ₂ Pc-SNS), P(ZnPc-SNS) and P(NiPc-SNS).....	78
3.6 Fluorescence Study.....	80
3.6.1 P(SNS-PN).....	80
3.6.2 P(ZnPc-SNS).....	82
3.7 Morphologies of P(H ₂ Pc-SNS), P(ZnPc-SNS) and P(NiPc-SNS)	83
4. CONCLUSION.....	85
REFERENCES.....	87
VITA	93

LIST OF FIGURES

FIGURES

Figure 1.1 The accidental discovery of phthalocyanine from <i>o</i> -cyanobenzamide.....	2
Figure 1.2 The accidental discovery of CuPc from <i>o</i> -dibromobenzene.....	2
Figure 1.3 Structures of pyrrole, porphyrin, Pc and MPc	4
Figure 1.4 Numbering in phthalocyanine molecule.....	5
Figure 1.5 Synthesis of phthalocyanines.....	7
Figure 1.6 Possible constitutional isomers of tetra-substituted Pcs	10
Figure 1.7 Structures of a) 1,4 and b) 2,3 -octa substituted Pcs.....	11
Figure 1.8 Mechanism of phthalocyanine formation in the presence of an alcohol [12].	13
Figure 1.9 Classic electronic absorption spectra of a) Pc and b) MPc with B and Q bands	16
Figure 1.10 Gouterman's four model showing electron transitions and the origin of Q and B bands for MPc	17
Figure 1.11 Typical cyclic voltammogram for a reversible process	23
Figure 1.12 Structure of SNS-PN.....	28
Figure 1.13 Structures of H ₂ SNS-Pc, ZnSNS-Pc and NiSNS-Pc	29
Figure 2.1 Schematic representation of a voltammetric cell.....	32
Figure 2.2 Schematic representation of a spectroelectrochemical cell	34
Figure 2.3 Synthetic route of 4-aminophthalonitrile.....	36
Figure 2.4 Synthetic route of 1,4-di(2-thienyl)-1,4-butanedione.....	37
Figure 2.5 Synthetic route of 4-(2,5-di-2-thienyl-1 <i>H</i> -pyrrol-1-yl)phthalonitrile.....	37
Figure 2.6 Synthetic route of H ₂ Pc-SNS, ZnPc-SNS and NiPc-SNS	39
Figure 3.1 Synthesis of all of the compounds	41
Figure 3.2 ¹ H NMR spectrum of SNS-PN	43
Figure 3.3 ¹³ C NMR spectrum of SNS-PN	43

Figure 3.4 FTIR spectra of (a) SNS-PN and (b) P(SNS-PN).....	45
Figure 3.5 UV-vis spectra of 1.0×10^{-4} mol.L ⁻¹ for H ₂ Pc-SNS, ZnPc-SNS and NiPc-SNS in DCM	48
Figure 3.6 FTIR spectra of SNS-PN and H ₂ Pc-SNS.....	50
Figure 3.7 FTIR spectra of SNS-PN and ZnPc-SNS	50
Figure 3.8 FTIR spectra of SNS-PN and NiPc-SNS	51
Figure 3.9 FTIR spectra of H ₂ Pc-SNS, ZnPc-SNS and NiPc-SNS.....	52
Figure 3.10 FTIR spectra of H ₂ Pc-SNS and P(H ₂ Pc-SNS).....	53
Figure 3.11 FTIR spectra of ZnPc-SNS and P(ZnPc-SNS)	54
Figure 3.12 FTIR spectra of Pc-SNS and P(NiPc-SNS).....	54
Figure 3.13 Cyclic voltammogram of H ₂ Pc-SNS on a Pt disc electrode at 100 mVs ⁻¹ in 0.1 M TBAP / DCM.....	57
Figure 3.14 DPV of H ₂ Pc-SNS in 0.1 M TBAP/DCM.....	57
Figure 3.15 Cyclic voltammogram of ZnPc-SNS on a Pt disc electrode at 100 mVs ⁻¹ in 0.1 M TBAP/DCM.....	58
Figure 3.16 DPV of ZnPc-SNS in 0.1 M TBAP/DCM.....	58
Figure 3.17 Cyclic voltammogram of NiPc-SNS on a Pt disc electrode at 100 mVs ⁻¹ in 0.1 M TBAP / DCM.....	59
Figure 3.18 DPV of NiPc-SNS in 0.1 M TBAP/DCM	59
Figure 3.19 Repeated scan electrochemical polymerization of 2.0×10^{-3} M SNS-PN	60
Figure 3.20 Cyclic voltammogram of P(SNS-PN) film on a Pt disc electrode at 100 mV/s in acetonitrile solution containing 0.2 M LiClO ₄	61
Figure 3.21 Cyclic voltammogram of P(SNS-PN) film (25 mC/cm ²) on a Pt disc electrode in acetonitrile containing 0.2 M LiClO ₄ , NaClO ₄ , and TBAP.....	62
Figure 3.22 Repeated potential scan electropolymerization of 0.1 mM H ₂ Pc-SNS on a Pt disc electrode at 100 mVs ⁻¹ in 0.1 M TBAP/DCM	64
Figure 3.23 Repeated potential scan electropolymerization of 0.1 mM ZnPc-SNS on a Pt disc electrode at 100 mVs ⁻¹ in 0.1 M TBAP/DCM	64

Figure 3.24 Repeated potential scan electropolymerization of 0.1 mM NiPc-SNS on a Pt disc electrode at 100 mVs ⁻¹ in 0.1 M TBAP/DCM	65
Figure 3.25 Scan rate dependence of P(H ₂ Pc-SNS) films (25 cycle) on a Pt disc electrode in 0.1M TBAP/DCM at different scan rates between 20 mV/s and 100 mV/s	66
Figure 3.26 Scan rate dependence of P(ZnPc-SNS) film (25 cycle) on a Pt disc electrode in 0.1M TBAP/DCM at different scan rates between 20 mV/s and 100 mV/s.	66
Figure 3.27 Scan rate dependence of P(NiPc-SNS) film (25 cycle) on a Pt disc electrode in 0.1M TBAP/DCM at different scan rates between 20 mV/s and 100 mV/s.	67
Figure 3.28 Relationship of anodic (I _{ac}) and cathodic (I _{cc}) current peaks as a function of scan rate for neutral and oxidized H ₂ Pc-SNS in 0.1 M TBAP/DCM.....	68
Figure 3.29 Relationship of anodic (I _{ac}) and cathodic (I _{cc}) current peaks as a function of scan rate for neutral and oxidized ZnPc-SNS in 0.1 M TBAP/DCM.....	69
Figure 3.30 Relationship of anodic (I _{ac}) and cathodic (I _{cc}) current peaks as a function of scan rate for neutral and oxidized NiPc-SNS in 0.1 M TBAP / DCM.....	69
Figure 3.31 Cyclic voltammogram of P(H ₂ Pc-SNS) film (10 cycle) on a Pt disc electrode in DCM containing 0.1 M zinc (II) acetate and TBAP	70
Figure 3.32 <i>In-situ</i> absorption spectra of P(SNS-PN) (55 mC/cm ²) recorded in acetonitrile containing 0.2 M LiClO ₄ at various applied potentials.	72
Figure 3.33 Electronic absorption spectra of P(H ₂ Pc-SNS) (25 mC/ cm ²) on ITO in 0.1 M TBAP/DCM solution during anodic oxidation of the polymer film	74
Figure 3.34 Electronic absorption spectra of P(ZnPc-SNS) (25 mC/ cm ²) on ITO in 0.1 M TBAP/DCM solution during anodic oxidation of the polymer film.	75
Figure 3.35 Electronic absorption spectra of P(NiPc-SNS) (25 mC/ cm ²)	

on ITO in 0.1 M TBAP/DCM solution during anodic oxidation of the polymer film.	76
Figure 3.36 Absorption and emission spectra of P(SNS-PN) in DMSO	81
Figure 3.37 Emission spectra of P(SNS-PN) recorded in the presence of 3.3×10^{-5} M LiClO ₄ and NaClO ₄ in DMF	82
Figure 3.38 Emission spectra of P(ZnPc-SNS) (excited at 370 nm) in (a) DMSO and (b) toluene	83
Figure 3.39 SEM micrographs of solution side of (a) P(H ₂ Pc-SNS) (b) P(ZnPc-SNS) and (c) P(NiPc-SNS)	84

LIST OF TABLES

TABLES

Table 3.1 Elemental analysis data for SNS-PN.....	45
Table 3.2 Elemental analysis data for Pc complexes	46
Table 3.3 Summary of redox potentials ($E_{1/2}$ vs Ag/AgCl) of the Pc complexes in 0.1 M TBAP dissolved in DCM	56
Table 3.4 Voltammetric and spectroelectrochemical data for P(SNS-PN) recorded in AN containing 0.1 M LiClO ₄	78
Table 3.5 Voltammetric and spectroelectrochemical data for P(H ₂ Pc-SNS) recorded in DCM containing 0.1 M TBAP.....	79
Table 3.6 Voltammetric and spectroelectrochemical data for P(ZnPc-SNS) recorded in DCM containing 0.1 M TBAP.....	79
Table 3.7 Voltammetric and spectroelectrochemical data for P(NiPc-SNS) recorded in DCM containing 0.1 M TBAP.....	80

ABBREVIATIONS

Ag/AgCl	Silver/silver chloride
AN	Acetonitrile
CE	Coloration efficiency
CV	Cyclic voltammetry
DBN	1,5-Diazabicyclo[4.3.0]non-5-ene
DBU	1,8-Diazabicyclo[5.4.0]undec-7-ene
DCM	Dichloromethane
DMF	Dimethylformamide
DMAE	<i>N,N</i> -dimethylaminoethanol
DMSO	Dimethylsulfoxide
DPV	Differential pulse voltammetry
E_g	Band gap
E_{pa}	Anodic peak potential
E_{pc}	Cathodic peak potential
EQCM	Electrochemical quartz crystal microbalance
FTIR	Fourier transform infrared spectroscopy
H₂Pc	Metal-free phthalocyanine
H₂Pc-SNS	Tetrakis(4-(2,5-di-2-thiophen-2-yl-pyrrol-1-yl)) phthalocyanine
HOMO	Highest occupied molecular orbital
I_{pa}	Anodic peak current
I_{pc}	Cathodic peak current
IR	Infrared
ITO	Indium-tin oxide
LiClO₄	Lithium perchlorate
LUMO	Lowest unoccupied molecular orbital
MPc	Metallophthalocyanine

NaClO₄	Sodium perchlorate
NiPc-SNS	Tetrakis(4-(2,5-di-2-thiophen-2-yl-pyrrol-1-yl)) phthalocyaninato nickel
NMR	Nuclear magnetic resonance spectroscopy
OTTLE	Optically transparent thin layer electrode
Pc	Phthalocyanine
PDT	Photodynamic therapy
P(SNS-PN)	Poly((2,5-di-2-thiophen-2-yl-pyrrol-1-yl)-phthalonitrile)
PTSA	p-toluene sulfonic acid
SCE	Saturated calomel electrode
SEM	Scanning electron microscopy
SNS-PN	4-(2,5-di-2-thiophen-2-yl-pyrrol-1-yl)-phthalonitrile
SOOS	1,4-di(2-thienyl)-1,4-butadione
SPEL	Spectroelectrochemical
TBAP	Tetrabutylammonium perchlorate
UV	Ultraviolet
vis	Visible
ZnPc-SNS	Tetrakis(4-(2,5-di-2-thiophen-2-yl-pyrrol-1-yl)) phthalocyaninato zinc

CHAPTER 1

INTRODUCTION

1.1 Phthalocyanines

1.1.1 History of Phthalocyanines

The word phthalocyanine is derived from the Greek terms for naphtha (rock oil) and for cyanine (dark blue). Naphtha was mentioned in ancient Greek literature. Dioscorides stated naphtha to be a clear, combustible rock oil procured from Babylonian asphalt. Cyanine was in the written vocabulary of several ancient Greek writers, including Homer. The phthalocyanines (Pcs) (Figure 1.1) were discovered by chance. In 1907, Braun and Tscherniac [1], at the South Metropolitan Gas Company in London, upon examining the properties of o-cyanobenzamide which they made from the reaction of phthalimide and acetic anhydride, found a trace amount of a blue substance after heating o-cyanobenzamide, cooling, dissolving in alcohol, and filtration. This substance undoubtedly was phthalocyanine.

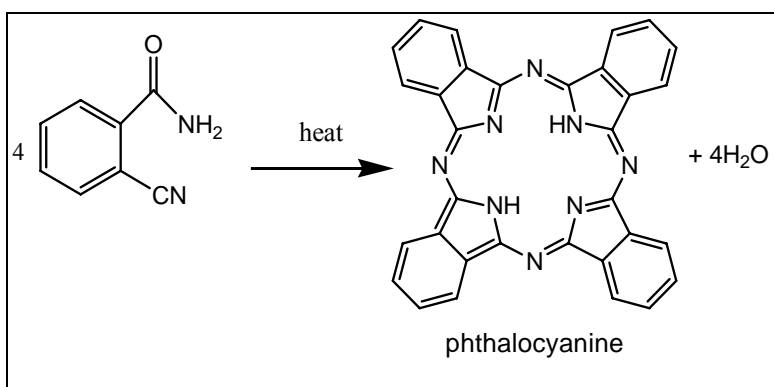


Figure 1.1 The accidental discovery of phthalocyanine from *o*-cyanobenzamide.

In a similar fashion, de Diesbach and von der Weid (1927) of Fribourg University, obtained a 23 % yield of an exceptionally stable and blue material during the preparation of *o*-dibromobenzene with copper (I) cyanide in refluxing pyridine (Figure 1.2) [2]. Analysis gave the formula of $C_{26}H_{18}N_6Cu$. The product undoubtedly was copper phthalocyanine (CuPc). De Diesbach and von der Weid also observed the remarkable stability of their product to alkalis, concentrated sulphuric acid and heat. De Diesbach and von der Weid appreciated the properties of this compound and ended their study with the hope that other colleagues would address themselves to the problem of determining its structure.

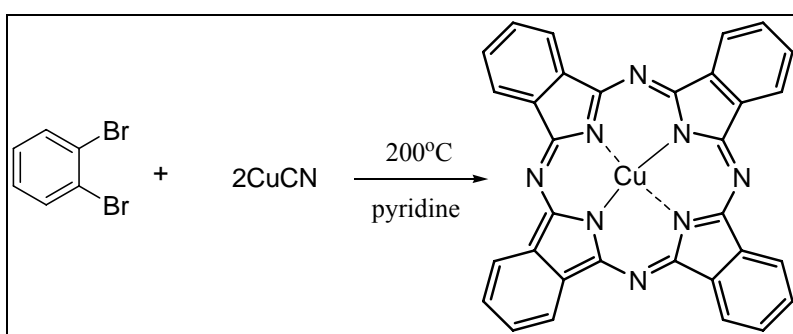


Figure 1.2 The accidental discovery of CuPc from *o*-dibromobenzene.

In 1929, another Pc derivative, iron (II) phthalocyanine, was found as a green/blue impurity coming from a defect in the iron vats of which phthalimide was being produced from phthalic anhydride and ammonia [3,4] Dandridge and Dunsworth reported that the compound was very stable, insoluble and resistant to heat (500°C) and concentrated acid. One year later, a patent for iron (II) phthalocyanine was granted to Dandridge, Drescher and Thomas of Scottish Dyes, Ltd., being the first for Pc compounds.

Up to 1929, none of the observers of the blue coloring matters attempted to determine its structure. Professor Linstead and his students, at the University of London, supported by grants from Imperial Chemical Industries, starting in 1929, determined and announced the structure of Pc and several metallophthalocyanines (MPcs) in 1933 and 1934 [5].

Not only are the Pcs a new class of organic compounds but also they constitute a new class of coloring matter or chromogen. Moderate cost of manufacture, good stability and tinctorial properties, in a region of the visible spectrum which had been lacking in chromogens of as good color properties, stability, and manufacturing cost, have led the Pcs to become, since 1934 and continuing to the present day, the object of intensive world-wide investigations, particularly with respect to applications in the field of color. Also, numerous production facilities for the manufacture of the principal Pc coloring matter, copper phthalocyanine have been constructed throughout the world.

1.1.2 Structures of Phthalocyanines

Linstead and co-workers were the first to investigate the molecular structure of Pcs [5]. Linstead used a combination of elemental analysis, ebullioscopic molecular mass determination and oxidative degradation (which produces phthalimide) to arrive at the correct structure of Pc. They reported the synthesis of many Pcs and suggested

that Pcs (**1**) and their metal analogues MPcs (**2**) (Figure 1.3) are macrocyclic 18 π -electron conjugated systems containing four isoindole groups which are linked by aza (-N=C-) group at the α -carbon of pyrrole unit and they are similar to naturally occurring porphyrins.

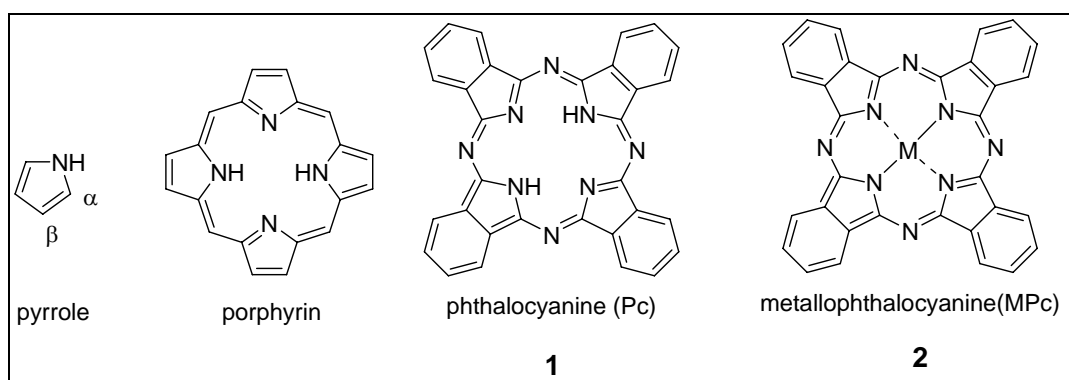


Figure 1.3 Structures of pyrrole, porphyrin, Pc and MPc.

Unlike porphyrin, which can be found in nature such as in hemoglobin, chlorophyll and vitamin B₁₂, Pcs do not occur in nature. In Pc system methine-bridges of porphyrin are replaced by aza-bridges and, therefore, Pcs are tetrabenzotetraazaporphyrins. There is a close connection between phthalocyanines and porphyrins: both are stable to alkalis, less so to acids; both are highly coloured and form complex metallic compounds; both can be degraded by oxidation to the imides of dibasic acids. Also, the order of stability of the metallic derivatives of the porphyrin and phthalocyanine series is similar.

The numbering seen in Figure 1.4 shows the accepted notation for the possible sites of substitution, which occur at the peripheral (2, 3, 9, 10, 16, 17, 23, 24) and non-peripheral (1, 4, 8, 11, 15, 18, 22, 25) positions of the benzo- units. These observations were verified by Robertson's investigations, making it the 'first organic structure' to yield an absolutely direct X-ray analysis [6].

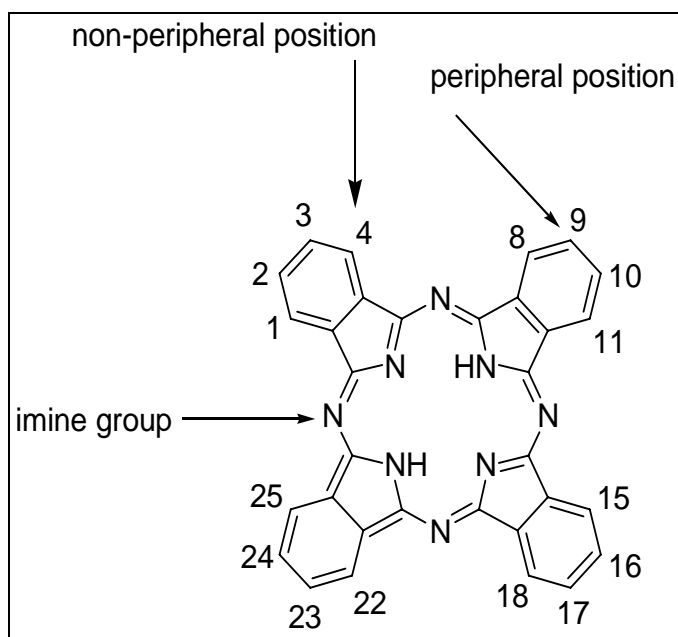


Figure 1.4 Numbering in phthalocyanine molecule.

Through substitution of hydrogen in metal-free Pc (H_2Pc) by metal atoms, MPcs are obtained. About 70 different elements could be coordinated with the Pc ligand, almost every metal, also some metalloids such as boron, silicon, germanium and arsenic. The individual natures of these atoms greatly affect the properties of the Pc ring, especially its solubility. Many MPcs have metal ions (e.g. Cu^{2+} , Fe^{2+}) that are bound very tightly to the ring making their removal impossible without destruction along with attributing to their insolubility. Solubility improves for MPcs containing two mono cations (e.g. K_2Pc) or large cations ($PbPc$), in which the central atom(s) lie outside the plane of the ring, or cations with axial ligands (Cl_3TaPc).

The coordination number of the square-planar Pc is four. In combination with metals, which prefer a higher coordination number, square-based pyramidal, tetrahedral or octahedral structures result. In such cases, the central metal is coordinated with one or two axial ligands such as chlorine, water or pyridine. Together with lanthanides and

actinides, complexes of a sandwich structure formed by two Pcs and one central metal with eight coordinated nitrogen atoms result [7].

1.1.3 Synthesis of Phthalocyanines

Synthesis of Pcs can be achieved using different routes depending on the type of Pcs to be synthesized; metal free, symmetrical and asymmetrical MPcs (Figure 1.5). Pcs have been commonly synthesized by cyclotetramerization reaction of phthalyl derivatives, namely, phthalic acid, phthalic anhydride, phthalimide, phthalonitrile, and 1,2-dibromobenzene or 1,3-diiminoisoindoline [8]. A fairly mild, clean and direct method for metal-free phthalocyanine (H_2Pc) synthesis involves heating of phthalonitrile with a base (1,8-diazabicyclo[5.4.0]undec-7-ene (DBU), 1,5-diazabicyclo[4.3.0]non-5-ene (DBN) or NH_3) in a solvent (e.g. 1-pentanol) or use of basic solvent *N,N*-dimethylaminoethanol (DMAE).

Of particular interest and value is the method in which lithium, sodium or magnesium alkoxides are used in primary alcohols (usually *n*- or *iso*-pentan-1-ol) for the cyclotetramerization. The metal ions are easily removed to give H_2Pc by acidic or aqueous work-up. Another approach involves reducing agent (usually inexpensive hydroquinone) that is melted together with phthalonitrile. The cyclotetramerization of 1,3- diiminoisoindoline is usually performed in a refluxing DMAE.

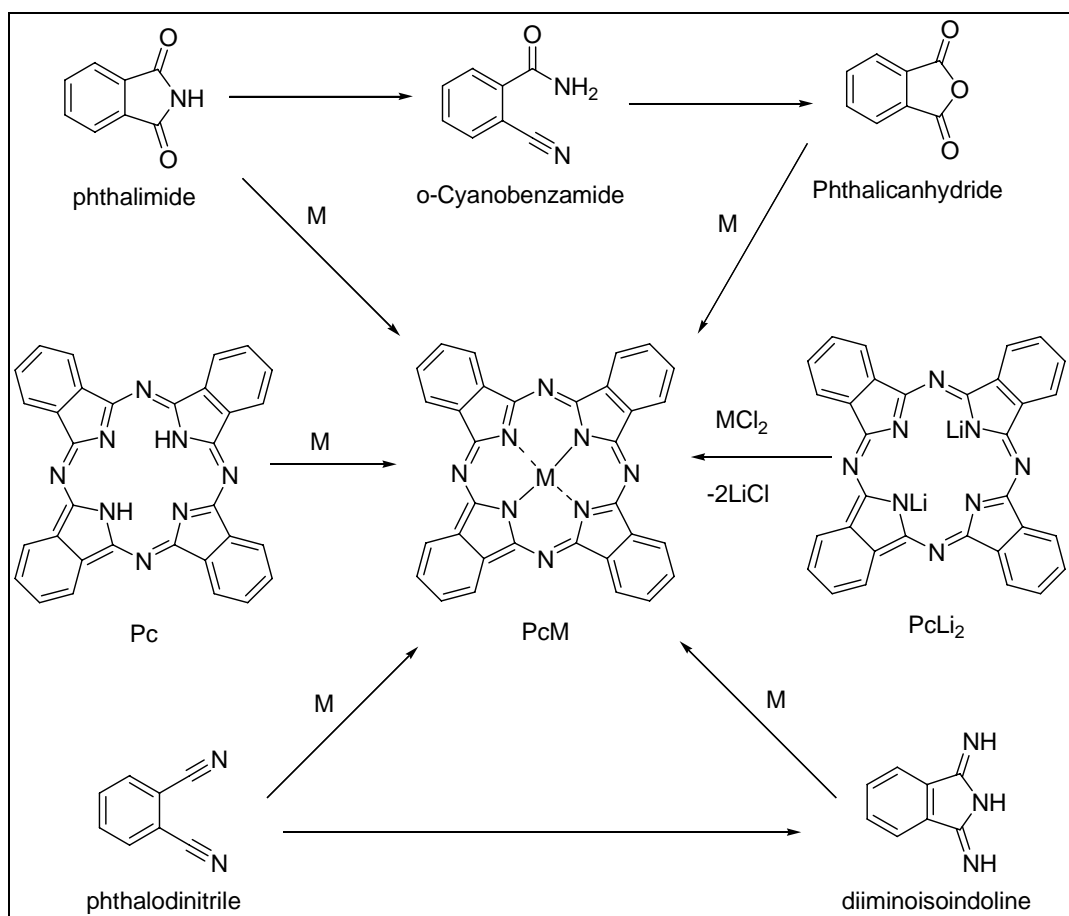


Figure 1.5 Synthesis of phthalocyanines.

A direct and in some cases convenient method for MPC synthesis is heating of phthalonitrile with a metal or metal salt. However, it is not suitable for substituents with low thermal stability, as it requires high temperatures. Moreover, the cyclotetramerization of phthalonitrile with metal salt can be achieved in a solvent. Of particular use are some high boiling solvents such as quinoline, dimethyl formamide (DMF), 1-chloronaphthalene, DMAE. In a modification to this method, the use of organic “super-bases” DBU and DBN in conjunction with a metal salt and a solvent gives good results in many cases.

Phthalimide, phthalic anhydride and phthalic acid have been used successfully for MPc synthesis. Of special interest is phthalic anhydride as a precursor, as most commercial processes are based upon this compound. Such reactions are commonly carried out in melted urea, which serves as a convenient source of nitrogen (ammonia). In addition to the appropriate metal salt, ammonium molybdate is usually added as a catalyst. Nitrobenzene has been used in some cases as a solvent. It is accepted that phthalic acid is converted to phthalimide via phthalic anhydride under the reaction conditions.

Diiminoisoindoline, prepared from the reaction of phthalonitrile and ammonia in the presence of catalytic amount of sodium methoxide, proved to be an excellent precursor for metal-containing phthalocyanines. It has been widely used for silicon and germanium phthalocyanine preparation. It is common to obtain some copper(II) phthalocyanine directly from 1,2- dibromobenzene. This reaction involves heating the dibromide with CuCN in a solvent, usually DMF or quinoline.

Historically, the eldest method for phthalocyanine synthesis is the reaction of 2-cyanobenzamide in the presence of metal or metal salt in a bulk reaction or in a solution. However, this method is limited to very few cases and has not received much attention in daily lab practice. The complexation of metal-free phthalocyanine is usually a clean and efficient reaction.

Additionally, subphthalocyanines can undergo ring expansion reaction to yield unsymmetrical phthalocyanines. Nearly every metal from the periodic system can replace two hydrogen atoms in the centre of the macrocycle. Moreover, the axial substituents can be attached to many metals. Additionally, multinuclear structures can be formed either through metal or through peripheral substituents. And finally, there are sixteen positions on the periphery that can be replaced by many substituents. Taking into account all these facts, today it is possible to prepare bespoke

phthalocyanine derivatives with highly tailored properties (*e.g.* Q-band position, solubility, light absorption, self-assembling, *etc.*). There are two excellent reviews on phthalocyanines preparation; one by Leznoff et al. [9] and the other, actually the most up-to-date, by Neil B. McKeown [10]. Pc and related compounds synthesis has been rapidly developing field with yearly appearing new achievements and publications.

1.1.3.1 Soluble Phthalocyanines

Unsubstituted Pcs are practically insoluble in common organic solvents due to strong interactions between ring systems. The introduction of substituents onto the phthalocyanine ring either on the peripheral (2,3) or non-peripheral (1,4) positions, (Figure 1.4) facilitates phthalocyanine solvation because they increase the distance between the stacked molecules [11]. Addition of axial substituents at the central metal atom which decreases the aggregation effect is another approach employed. By introduction of selected substituents, the physical and electrical properties of Pcs can be changed, resulting in the broadening of their applications.

The best investigated soluble substituted Pcs are the tetra- and octa-substituted ones. Substituting at the 1, 2, 3 or 4 positions of a phthalonitrile gives tetra substituted Pcs and substituting at the 2, 3 or 1, 4 positions gives octa substituted Pcs. In general, the solubility of tetra-substituted ones is higher than that of octa-substituted Pcs. This is due to the fact that tetra-substituted Pcs are prepared as a mixture of isomers consequently leading to a lower degree of order in the solid state, when compared to symmetrically octa-substituted Pcs. Moreover, the less symmetrical isomers have a higher dipole moment derived from the more unsymmetrical arrangement of the substituents on the periphery of the Pc ring.

1.1.3.1.1 Tetra-Substituted Phthalocyanines

Synthesis of tetra substituted Pcs can be achieved from 3- and 4-substituted phthalodinitriles, respectively, which results in a mixture of four constitutional isomers with different symmetries as shown in Figure 1.6.

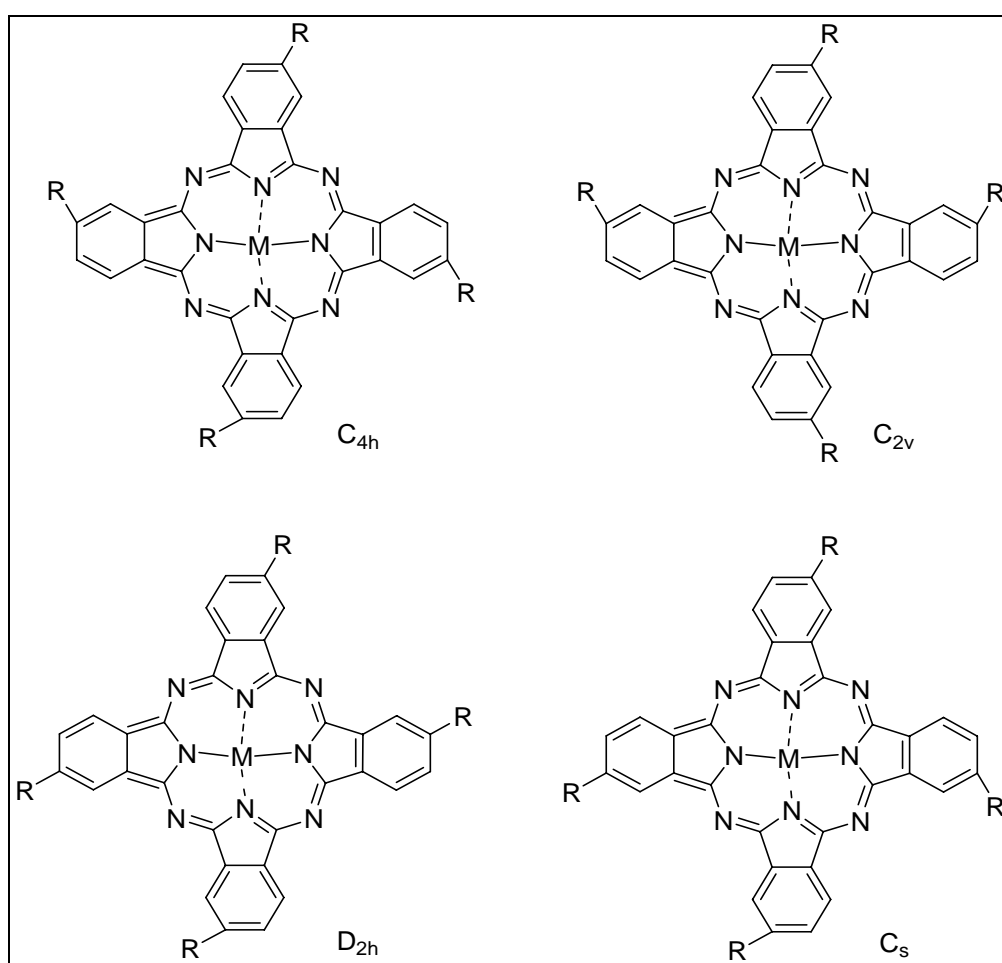


Figure 1.6 Possible constitutional isomers of tetra-substituted Pcs.

1.1.3.1.2 Octa-Substituted Phthalocyanines

The synthetic pathway for octa substituted Pcs is similar to that of tetra substituted ones, only that 3,6- and 4,5-disubstituted phthalodinitriles are used instead of 3- and 4- substituted derivatives, respectively. Two different types of products, one having substitution from 1,4,8,11,15,18,22,25- and the other from 2,3,9,10,16,17,23,24-positions, which are depicted as 1,4- and 2,3-octa substituted Pcs, respectively, are obtained. Their structures are represented in Figure 1.7.

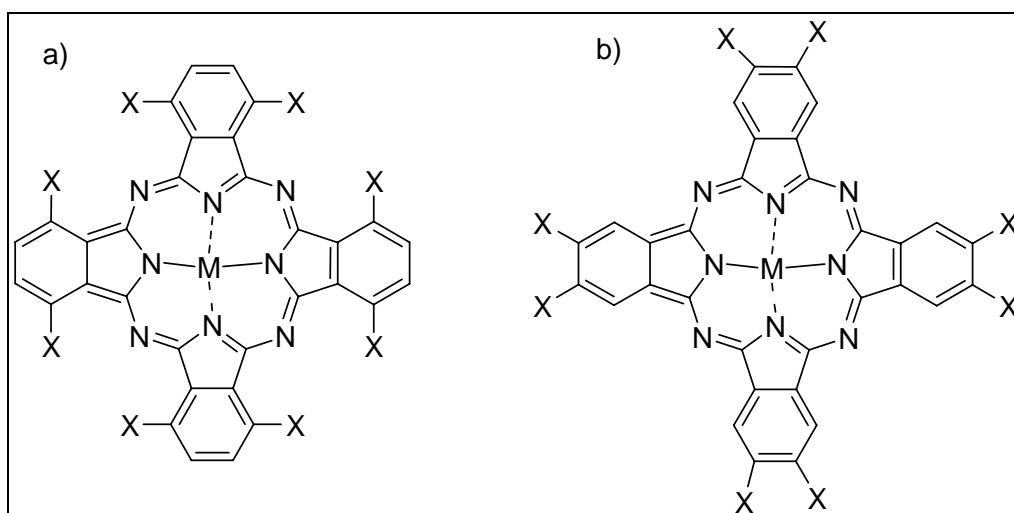


Figure 1.7 Structures of a) 1,4 and b) 2,3 -octa substituted Pcs.

1.1.4 Mechanism of Phthalocyanine formation

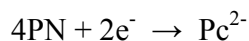
The synthesis of Pcs starting from phthalonitrile (PN) and related compounds proceeds through complex reaction pathways that involve the formation of reactive precursors, condensation to reactive intermediates, and ring-closure mechanism that leads to macrocyclic compounds. Although most of these methods use phthalonitrile

as starting material, the reaction conditions are fairly different and therefore they do not necessarily occur through identical mechanisms or intermediates. A detailed comprehension of the mechanism is difficult to achieve because of the reaction conditions employed in the synthesis of these compounds. In some synthetic routes, intermediates have been isolated, thus facilitating the understanding of the mechanism.

There are generally different suggested mechanisms for the Pc formation depending on the starting materials and the reaction promoters [12].

In presence of an alcohol, firstly, some basic promoters such as DBU or DBN deprotonate the alcohol forming strong nucleophilic alkoxide species **1**. These species then attack the nitrile or the imide linkage in case of phthalonitrile and diiminoisoindoline, respectively. The intermediates **2** and **3** are formed which are suggested to condense or add further phthalonitrile in a template reaction forming the intermediate **4**. Metal-ion template is surrounded by the two dimers of **4** to form the tetramer intermediate **5** which loses aldehyde and a hydride equivalent driven by the aromatization of the formed phthalocyanine molecule.

The template effect of the central metal ion and the resulting stabilization this complex causes, seem to be the driving force for the Pc macrocycle formation. The same mechanism is also suggested for the reactions, which involve the use of Li or Na. In this case the metal serves as electron donor for the template cyclization according to the following equation:



The Pc synthesis in presence of an alcohol is illustrated in Figure 1.8.

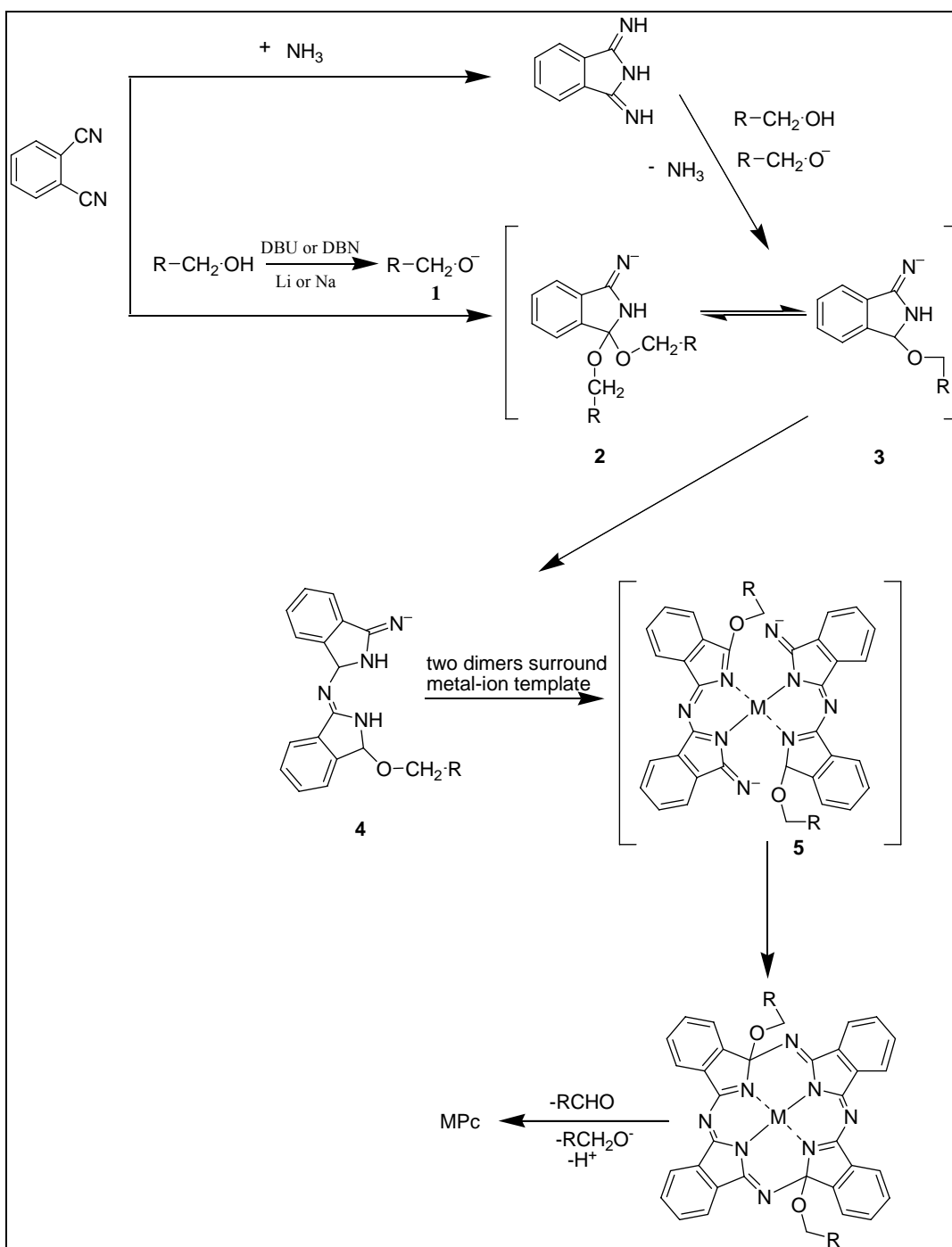


Figure 1.8 Mechanism of phthalocyanine formation in the presence of an alcohol [12].

The high temperature reactions of phthalonitrile with a metal or a metal salt, either neat or in a high boiling solvent, are likely to proceed by a similar mechanism to that shown in Figure 1.8.

1.1.5 Application of Phthalocyanines

Pcs and MPcs have been a subject of extensive study for many years in much detail because of their increasing diverse applications from industrial to biomedical.

- Owing to beautiful color, usually blue or green, considerable chemical and photochemical stability, Pcs are used worldwide as dyestuffs. They are an important industrial commodity. They are widely used in inks (ballpoint pens, printing inks etc.), coloring for plastics and metal surfaces as well as dyestuff for jeans and other clothing. Interestingly, copper phthalocyanine was certified as a food dyestuff in Germany and for coloring contact lenses in the United States [9].

- Photodynamic therapy (PDT) uses a combination of a photosensitizing drug (dye) and light in the presence of molecular oxygen to obtain a therapeutic effect that depends on selective cell injury. PDT has been developed as an alternative to conventional treatments such as radiotherapy and chemotherapy. The photosensitizer is harmless unless it is activated by light. Light can be therefore selectively focused on the tumor through an optical fiber, followed by the photosensitizer activation and cell destruction afforded in a predetermined area. Among the second-generation photosensitizers developed for PDT, the phthalocyanines have received particular attention due to their high molar absorption coefficient (ϵ ca. $10^5 \text{ M}^{-1} \cdot \text{cm}^{-1}$) in the red part of the spectrum (640- 710 nm), which allows increased tissue penetration of the activating light. Low toxicity of Pcs makes them promising for PDT application. Both lipophilic and water-soluble Pcs have been considered as candidates for PDT [13-15].

- Due to the narrow bandwidth, excellent thermal, chemical as well as photochemical stability and compatibility with semiconductor diode lasers, Pcs have been successfully applied as a laser-optical recording media. They are particularly attractive candidates for applications in long-term optical data storage (i.e. write once read many times (WORM) discs) [16].

- The phenomena of electrochromism relies on the reversible color change of the material upon application of an electric field. Many Pcs are famous for their electrochromic properties. Films of dyes can be switched over many colors which make them useful for display devices construction [17].

- Besides, Pcs find uses in the petroleum industry as catalysts in sulphur compounds oxidation (Merox process) [18-22].

- MPcs have several potential technological applications, including energy conversion [23-25], liquid crystal displays [26,27], gas sensing [9,28] and electrocatalysis in fuel cells [29,30]. Moreover, MPcs are widely used as photoconductors in the printer and photocopier industry [31,32] as well as non-linear optical devices [33-35].

1.2 Chemistry of Phthalocyanines

1.2.1 Spectral Properties

1.2.1.1 Absorption Spectra of Phthalocyanines

The main and most characteristic feature of the absorption spectra of Pcs is the presence of very intensive two bands; one in the visible region (600 – 800 nm) called

the Q-band and a weaker band in the UV region (300 – 500 nm) called B or the Soret band (Figure 1.9) [36, 37]. The assignment of the Q and B bands are based on the four-orbital model (Figure 1.10) proposed by Gouterman's group [38-40].

The Q band arises from $\pi - \pi^*$ transitions and can be best explained in terms of linear combination of transitions from a_{1u} and a_{2u} , the highest occupied molecular orbitals (HOMO) of the MPc ring to the lowest unoccupied molecular orbitals (LUMO), e_g^* . The symmetry of an H_2Pc , is less (because of the two protons in the cavity), and this results in the splitting of the Q band (Figure 1.9). As a result of the protons in the cavity of the H_2Pc , the e_g orbital loses its degeneracy resulting in two allowed transitions of different energies which gives a split Q band.

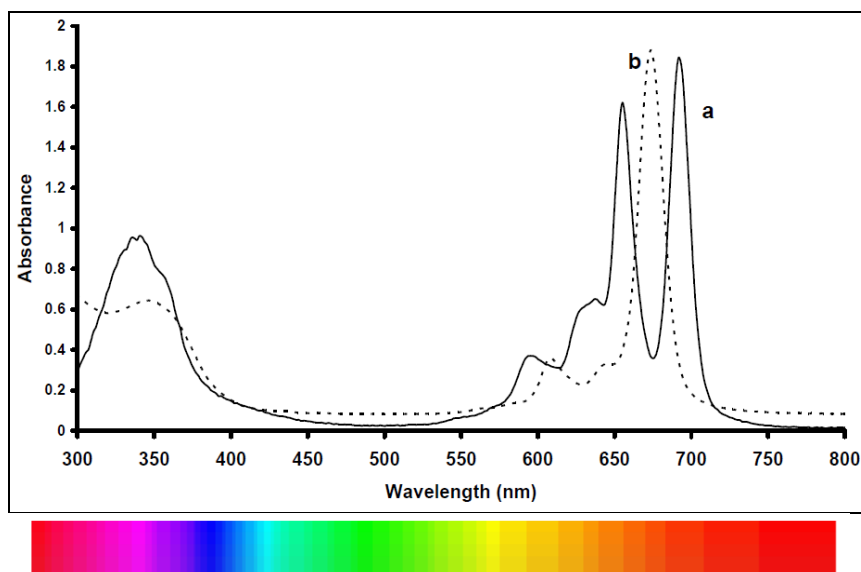


Figure 1.9 Classic electronic absorption spectra of a) Pc and b) MPc with B and Q bands.

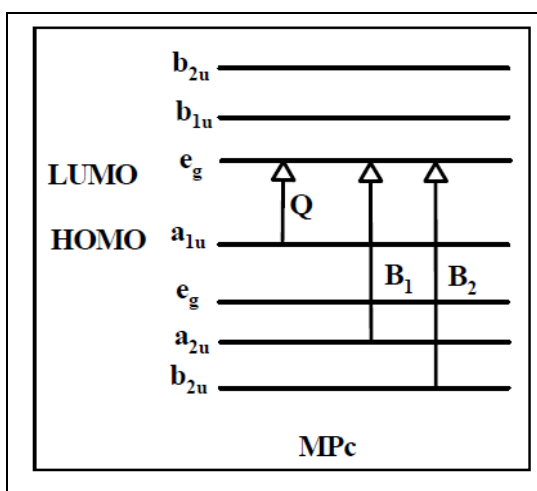


Figure 1.10 Gouterman's four model showing electron transitions and the origin of Q and B bands for MPc.

1.2.1.2 Infrared Spectroscopy

The infrared (IR) spectra of MPc complexes are typically complex but similar. The main bands are the C-H stretching vibration at around 3030 cm^{-1} , C-C ring skeletal stretching vibrations at around 1600 and 1475 cm^{-1} , C-H out of plane bending vibrations at around $750\text{-}790\text{ cm}^{-1}$, all these bands are from the aromatic ring of the MPc. The unmetallated Pcs can be distinguished from the metallated ones by the presence of N-H stretching vibration at around 3298 cm^{-1} in the former but absence of the band in the latter.

1.2.2 Electrochemistry of Phthalocyanines

The neutral form of Pc skeleton exists as a dianion, i.e. Pc^{2-} [41], which may be reduced or oxidized. The electrochemical activity of unmetallated Pcs is related to processes occurring on the ring; on the other hand, the MPcs containing electroactive

central metals exhibit electroactivity associated with the central metals, in addition to ring processes. Examples of electroactive metals include cobalt, iron and manganese while electrochemically inactive metals include zinc, nickel and magnesium.

Moreover, electroactive ligands substituted on the Pc also exhibit their own characteristic redox peaks or couples [42].

The redox activity of Pcs is directly related to HOMO and LUMO in the molecule. Oxidation is the removal of electron(s) from HOMO (a_{1u}) while reduction is the addition of electron(s) to the LUMO (Figure 1.10). Successive removal of up to two electrons from HOMO (a_{1u}) results in the formation of Pc(-1) and Pc(0). In the same way, successive gain of one to four electrons by the LUMO of the Pc complex results in the formation of Pc⁻³, Pc⁻⁴, Pc⁻⁵ and Pc⁻⁶ [43]. These processes can be monitored with electrochemical methods such as amperometry and complexes are influenced by: the nature of the substituents on the Pc ring; the nature and oxidation state of the central metal; the nature of any axial ligands and solvents [44].

1.3 Phthalocyanine Polymers

Polymeric Pcs are prepared by two methods: polycyclotetramerization of tetracarbonitriles and electropolymerization of suitably designed Pc monomer.

1.3.1 Polymeric Phthalocyanines by Cyclotetramerization Reactions

For polycyclotetramerization, bifunctional monomers based on tetracarbonitriles, various oxy-, arylenedioxy-, and alkylendioxy-bridged diphtalonitriles and other

nitriles or tetra carboxylic acid derivatives are employed mainly in the presence of metal salts or metals in bulk at higher temperatures.

The polymers exhibit good thermal stability under an inert gas atmosphere up to ≈ 500 °C and under oxidative conditions up to ≈ 350 °C. Low molecular weight phthalocyanines can be purified depending on either being unsubstituted or containing suitable substituents by zone sublimation or liquid chromatography. Common instrumental techniques are employed for their analytical characterization. In contrast, polymeric Pcs are not soluble in organic solvents (sometimes only partially soluble in conc. sulphuric acid) and are not vaporizable. Therefore, separation from unreacted monomers, metal salts and perhaps by-products is only possible by treatment with organic solvents (e. g., in a Soxhlet apparatus) or dilute acids. In the polycyclotetramerization of tetracarbonitriles, the formation of by-products, such as polyisoindolenine and polytriazine can occur. They are covalently incorporated into the polymers as co-units and cannot be separated from the Pc structural elements [45, 46]. Hence, a structurally uniform formation of polymeric Pcs is crucial.

For a complete characterization of the polymers, the following points must be considered: structural uniformity, nature of end groups, metal content and degree of polymerization (molecular weight). In very few reports only, sufficient statements regarding these points are made and really structurally uniform polymers were prepared [46]. It should be pointed out that the preparation of structurally uniform polymeric Pc is restricted to well-defined reaction conditions. For various investigations with respect to electrical, photoelectrical, catalytic and photocatalytic properties, the preparation of thin films on flat surfaces (e.g., glass, Ti, glass/ITO (indium-tin oxide), KCl) or coatings on particles (e.g., SiO₂, TiO₂, Al₂O₃) is necessary. Since polymeric Pcs are insoluble and not vaporizable, special techniques must be employed.

1.3.2 Polymeric Phthalocyanines by Electropolymerization

This method allows formation of polymer films when there exists a suitable substituent in the peripheral benzene rings of Pc forming differently structured polymeric films. Lots of work has been done on the study of mechanisms of polymer formations from monomers containing groups such as amino, aniline, pyrrole and thiophene [47-49]. Factors such as solubility of monomer, nature of solvent, electrode size and nature, and ability to form an insoluble polymer govern the polymer growth mechanism. The mechanism of polymer growth of polypyrrole, polythiophene and polyaniline has been studied using cyclic voltammetry, electrochemical quartz crystal microbalance (EQCM) and spectroelectrochemical methods [50-53].

MPc complexes with ring substituents such as amino, pyrrole, sulphonate and mercaptopyrimidine groups have been used to modify various electrodes as polymer films for analytes such as glycine, chlorophenols, dopamine, Lcysteine, hydrazine and oxygen.

1.3.2.1 The Electrochemical Polymerization Strategy

Electrochemical polymerization is an elegant, attractive and easy strategy for the immobilization of metal complexes [54-59] on the surface of electrodes. The principle is based on the electrochemical oxidation (or reduction) of a suitably designed monomer to form a polymeric film incorporating the metal complex. Pyrrole-, thiophene- and aniline-based monomers have been the most commonly used materials [57-60]. Such chemically substituted monomers have many interesting features, including a high flexibility in their molecular design.

Additionally, such materials offer the possibility of using either aqueous or organic solutions to carry out the electropolymerization. The electrochemical deposition process is controlled by the electrode potential. This can be achieved either by controlled potential, controlled current electrolysis or cyclic voltammetry within a well-defined potential range.

Growth of the polymeric films or more precisely, control of the amount of deposited materials (or the polymer film thickness), can be easily achieved by monitoring the total charge passed during the electrooxidative (or reductive) polymerization process. In the general case, the mechanism of electropolymerization of such substituted monomers has still not been completely explained, despite the large quantity of data on this subject.

However, it is now well accepted that in the case of pyrrole and aniline derivatives, the first step in the electropolymerization process is the electrooxidative formation of a radical cation from the chosen monomer [57-60]. This oxidation reaction is followed by a dimerization process, followed by further oxidation and coupling reactions. This leads to the formation of oligomers and polymers on the electrode surface. It also appears that the morphology and the physical properties of the polymer films depend largely upon the electrochemical polymerization conditions. Thus, one can induce a supplementary design parameter during the polymerization step by adjusting the solution composition or the electrode potential.

In this way, electrochemical polymerization can be carefully controlled, resulting in multilayered structures and copolymers from multicomponent solutions.

1.4 Electrochemical Basics

The electrochemical techniques taking place when an electric potential is applied to the system under study give information on the processes.

1.4.1 Cyclic Voltammetry

Cyclic voltammetry is a kind of electrochemical measurement and used for studying the redox properties of chemicals. The three-electrode method is the most widely used because the potential of reference does not change easily during the measurement. This method needs a reference electrode, working electrode, and counter electrode. Electrolyte is added to the compound solution to ensure sufficient conductivity. The combination of the solvent and the electrolyte determines the range of the potential.

The most important electrode in cyclic voltammetry is the working electrode. Electrochemical reactions being studied occur at the working electrode and polymer coating is formed on it. The working electrode can be made from a variety of materials including: platinum, gold, silver, glassy carbon, nickel and palladium. Counter (auxiliary) electrode conducts the electricity from the signal source into the solution, maintaining the correct current. It is usually inert conduct like platinum or graphite. A reference electrode is used in measuring the working electrode potential. A reference electrode should have a constant electrochemical potential as long as no current flows through it. The potential that is cycled is the potential difference between the working electrode and the reference electrode. It is usually made from silver/silver chloride (Ag/AgCl) or saturated calomel electrode (SCE).

In this system, the potential of the electrode is cycled from a starting potential, E_i to a final potential, E_f (the potential is also called the switching potential) and then back to E_i , Figure 1.11. The potential at which the peak current occurs is known as the peak potential, E_p (anodic peak potential (E_{pa}), cathodic peak potential (E_{pc})). At this potential, redox species have been depleted at the electrode surface and the current is diffusion limited. The magnitude of the Faradaic current, I_{pa} (anodic peak current) or I_{pc} (cathodic peak current), is an indication of the rate at which electrons are being transferred between the redox species and the electrode. Cyclic voltammetric processes could be reversible, quasi-reversible and irreversible.

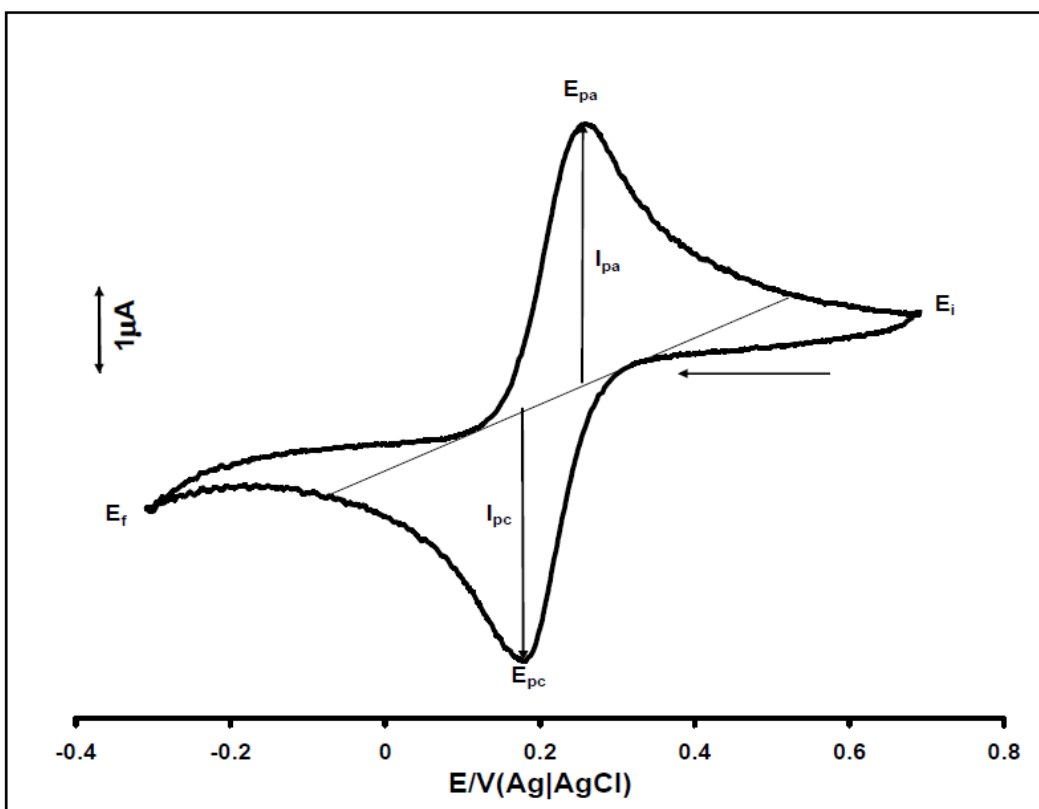


Figure 1.11 Typical cyclic voltammogram for a reversible process.

The voltammogram obtained provides us to understand the electroactivity and redox potential of the material, mechanism of the electrochemical reactions, reversibility of electron transfer, whether the reaction products are further reduced or oxidized. In the case of the polymers, cyclic voltammetry gives basic information on the oxidation potential of the monomers, on film growth, on the redox behavior of the polymer, and on the surface concentration (charge consumed by the polymer).

Conclusions can also be drawn from the cyclic voltammograms regarding the rate of charge transfer, charge transport processes, and the interactions that occur within the polymer segments, at specific sites and between the polymer and the ions and solvent molecules. For very thin films and/or at low scan rates, when the charge transfer at the interfaces and charge transport processes within the film are fast, i.e., electrochemically reversible (equilibrium) behavior prevails, and if no specific interactions (attractive or repulsive) occur between the redox species in the polymer film.

1.4.2 Constant Potential Methods (Potentiostatic)

Potentiostatic method is conducted with a three-electrode system. The potential between the working and reference electrodes is maintained by a potentiostat. An electronic feedback circuit continually compares and controls the working electrode potential with respect to the reference electrode. Several factors should be considered in choosing the appropriate electrolysis potential, including the threshold reaction potential determined by voltammetry, the potential at which interfering reactions may occur and the desired rate of the electrochemical reaction.

The voltage between the working and the reference electrode may be called the polymerization potential. By keeping the potential constant, creation of undesired

species is prevented; hence the initiation becomes selective, that is, through the monomer itself. Chronoamperometry, i.e. measuring the current as a function of time, is the method of choice to study the kinetic of polymerization and especially the first steps.

1.4.3 Constant Current Methods (Galvanostatic)

Galvanostatic method is also named as Chronopotentiometry and carried out by applying a constant current between the working and auxiliary electrodes using a galvanostat. Only a simple, two-electrode configuration is required for galvanostatic electrolysis. The galvanostat ensures a constant current density and thus a controlled rate of the electrochemical reaction.

Common applications of the galvanostat include constant current stripping potentiometry and constant current electrolysis. One advantage of all constant current techniques is that the ohmic drop due to solution resistance is also constant, as it is equal to the product of the current and the solution resistance. However, as the reaction proceeds, the potential on the working electrode may change, new electrochemical processes may occur at different potentials and a change in the composition or character of the product may result and for that reason, complications may arise in initiation and propagation steps.

1.4.4 Differential Pulse Voltammetry (DPV)

This technique is comparable to normal pulse voltammetry in that the applied potentials are an overlapping of a fixed amplitude pulse and a linear potential ramp. However, it differs from normal pulse voltammetry because each potential pulse is

fixed, of small amplitude (10 to 100 mV), and is superimposed on a slowly changing base potential. Current is measured at two points for each pulse, the first point just before the application of the pulse and the second at the end of the pulse. These sampling points are selected to allow for the decay of the nonfaradaic (charging) current. The difference between current measurements at these points for each pulse is determined and plotted against the base potential.

1.4.5 Spectroelectrochemistry

Spectroelectrochemistry combines the use of electrochemistry and spectroscopy. A particular electrochemical cell, called an OTTLE (Optically Transparent Thin Layer Electrode) cell, holds the redox active compound, which is either oxidized or reduced. Product formation is then monitored *in situ* by spectroscopic techniques providing information about the material's band gap and intraband states created upon doping as well as give electrochromic properties of conducting polymers at various applied potentials.

Several spectroscopic techniques have been combined with electrochemical methods. UV/VIS/NIR spectrometries have become routine methods in investigations of conducting polymer films, where they are used to monitor the chemical changes occurring in the surface film [61-65]. In most experiments the transmission mode has been applied. Optically transparent electrodes (OTEs) are usually employed, which are either indium–tin oxide (ITO) or a very thin (less than 100 nm) layer of gold or platinum on a glass or quartz substrate. Another type of electrode used is a partially transparent metal grid or mesh. In some cases the simple grid electrode is replaced by a LIGA structure (LIGA, or lithographic galvanic up-forming, is a technique based on a synchrotron radiation patterned template); however, these systems can be used for

the detection of soluble species. The reflection mode is seldom used in UV/VIS spectroelectrochemistry.

1.4.6 Electrochromism

The term electrochromism is analogous to thermochromism (change in color produced by heat) and photochromism (change in color produced by light) [66] and can be defined as the capability of a material to change its optical properties within the whole electromagnetic spectrum under an applied voltage. Electrochromic materials exhibit a change in absorbance, reflection, or transmission of electromagnetic radiation induced by an electrochemical oxidation–reduction reaction.

Most often, the color change is between a transmissive state and a colored state, but many materials switch between multiple colored states and are referred to as polyelectrochromic materials. Some of the most commonly studied electrochromic materials include transition metal oxides (e.g., tungsten oxide, WO_3) organic molecules (e.g., viologens), and inorganic complexes (e.g., Prussian Blue [PB]) [67-70]. With many of these materials, along with conducting polymers, the electrochromic effect is reversible and can occur not only in the visible region but also in the ultraviolet (UV), infrared (IR), and even microwave regions of the spectrum [71-73]. Compared to other electrochromic materials polymers have some potentially achievable advantages. These polymers offer better processability, faster switching, and color tunability than their inorganic and molecular counterparts. Conjugated polymers can be either anodically coloring (color upon oxidation) or cathodically coloring (color upon reduction), and can exhibit multiple color states in the same material. Through minimal structural modifications, these polymers can be

made soluble in common organic solvents, which allow straightforward preparation of polymer films for large-scale applications.

1.5 Aim of the study

In our laboratory, the novel synthesis of diazophenylene and diazodiphenylene bridged Co/Ni/Cu/Ce/Er Pc polymers were performed by Cemil Alkan [74-76]. With the help of the results of this study, it was aimed:

- Synthesis and characterization of 2,4-di-(2-thienyl)-pyrrole (SNS) substituted phthalocyanine precursor (Figure 1.12).

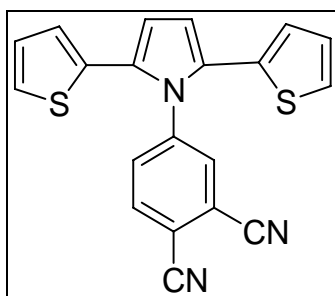


Figure 1.12 Structure of SNS-PN.

- Electrochemical polymerization of a new monomer, 4-(2,5-di-2-thiophen-2-yl-pyrrol-1-yl)-phthalonitrile (SNS-PN) containing an acceptor group bonded to a high spin donor.
- Investigate the electro-optical and electrochromic properties of the polymer film P(SNS-PN) and decide if it can be used in organic lasers and electroluminescent materials.

- Study whether electron withdrawing cyanide groups of P(SNS-PN) can interact with any metal cation through its nitrogen atoms and can be used as cation sensing material.
- Introduce metal-free, zinc and nickel phthalocyanine moieties to the central pyrrole ring of the SNS monomer to form new hybrid materials Figure 1.13.

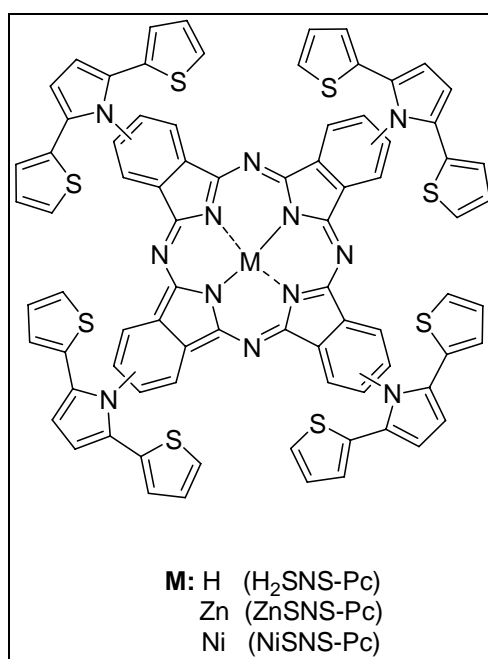


Figure 1.13 Structures of $H_2Pc-SNS$, $ZnPc-SNS$ and $NiPc-SNS$.

- Electropolymerize these new phthalocyanine monomers and characterize the resultant polymer films.

CHAPTER 2

EXPERIMENTAL

2.1 Materials

AlCl₃ (Aldrich), succinyl chloride (Aldrich), thiophene (Merck), *p*-toluenesulfonic acid (PTSA) (Aldrich), 4-nitrophthalonitrile (Across), n-hexanol (Merck), n-pentanol (Merck), 1,8-diazabicyclo[5.4.0]undec-7-ene (DBU) (Merck), zinc (II) acetate 2-hydrate (Merck), nickel (II) chloride (Merck), ethanol (Riedel-de-Haen), methanol (Merck), n-hexane (Merck), diethyl ether (Merck), dimethylsulfoxide (DMSO), hydrochloric acid (HCl) (Merck), sodium hydrogencarbonate (NaHCO₃) (Aldrich), magnesium sulphate (MgSO₄), lithium perchlorate (LiClO₄) (Aldrich), tetrabutylammonium perchlorate (TBAP), iron powder were used as received. Acetonitrile (AN) (Merck), dichloromethane (DCM), and toluene were distilled before use.

2.2 Instrumentation

2.2.1 Nuclear Magnetic Resonance (NMR) Spectrometer

¹H NMR and ¹³C NMR spectra were recorded on a Bruker NMR Spectrometer (DPX-400) in CDCl₃ as the solvent and chemical shifts (δ) were given relative to tetramethylsilane as the internal standard.

2.2.2 Fourier Transform Infrared (FTIR) Spectrometer

Fourier Transform Infrared spectroscopy (FTIR) spectra of the monomers and their polymers were recorded with a Bruker Vertex 70 spectrophotometer.

2.2.3 Fluorescence Spectrophotometer

Fluorescence measurements were recorded on a Varian Cary Eclipse Fluorescence Spectrophotometer.

2.2.4 Scanning Electron Microscopy

The scanning electron microscope (SEM) is a type of electron microscope capable of producing high-resolution images of a sample surface. Due to the manner in which the image is created, SEM images have a characteristic three-dimensional appearance and are useful for judging the surface structure of the sample. The morphological features of the polymer coated ITO electrodes were performed by using QUANTA 400F Field Emission scanning electron microscope.

2.2.5 Elemental Analyzer

Elemental determination of carbon, hydrogen, nitrogen, and sulfur were carried out by LECO CHNS-93 elemental analyzer.

2.3 Electropolymerization and Characterization

2.3.1 Electropolymerization of SNS-PN

The polymers of SNS-PN were synthesized from an electrolytic medium containing 2.0 mM monomer and 0.2 M LiClO₄ in acetonitrile via repetitive cycling at a scan rate of 100 mV/s or constant potential electrolysis at 1.0 V vs Ag wire using Gamry PCI4/300 potentiostat-galvanostat. The polymer was coated on platinum (0.02 cm²) or indium-tin oxide (ITO, Delta Tech. 8–12 Ω, 0.7x5 cm) working electrode. The resulting polymer films were washed with acetonitrile to remove LiClO₄ and unreacted monomers after the electrolysis.

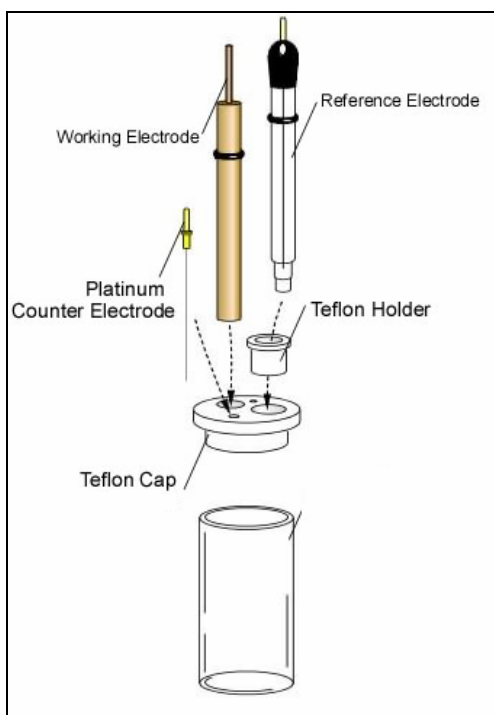


Figure 2.1 Schematic representation of a voltammetric cell.

2.3.2 Electropolymerization of H₂Pc-SNS, ZnPc-SNS and NiPc-SNS

Prior to electrochemical polymerization, redox behavior of the phthalocyanine complexes (H₂Pc-SNS, ZnPc-SNS and NiPc-SNS) were investigated using CV and differential pulse voltammetry (DPV) in DCM solution containing 0.1 M TBAP on platinum electrode.

The monomers were successfully electropolymerized via potentiodynamic or potentiostatic methods using three-electrode system containing a platinum disc (0.02 cm²), a platinum wire as working and counter electrodes, respectively, as well as Ag/AgCl electrode as a reference electrode. Electrochemical behavior of corresponding polymer films, coated on working electrode was investigated in monomer-free electrolytic medium after washing with DCM to remove the oligomeric species and unreacted monomer.

All the solutions were degassed with N₂ and measurements were performed at room temperature under nitrogen atmosphere using Gamry PCI4/300 potentiostat-galvanostat before electrochemical measurements.

2.3.3 Spectroelectrochemistry

Spectroelectrochemical (SPEL) measurements provide key properties of conjugated polymers such as band gap (E_g), the intraband states created upon doping, as well as give electrochromic properties at various applied potentials.

Experimentally, the band gap is related to the wavelength of the first absorption band in the electronic spectrum of the substance. Thus, a photon with λ (wavelength) can

excite an electron from HOMO to LUMO level $\pi \rightarrow \pi^*$ if the energy condition is fulfilled.

$$\Delta E = E(\text{LUMO}) - E(\text{HOMO})$$

$$\Delta E = h\nu = hc/\lambda$$

ΔE = The band gap (Energy gap)

For electro-optical studies, ITO electrodes were coated by the polymer films. Prior to SPEL investigations, the polymer films were switched between their neutral and doped states several times in order to equilibrate redox behavior in monomer-free electrolytic solution. *In-situ* SPEL studies were performed using Hewlett–Packard 8453A diode array spectrometer. A Pt wire was used as a counter electrode and a Ag wire as pseudo-reference electrode which was calibrated externally using 5 mM solution of ferrocene/ferrocenium couple in the electrolytic solution.

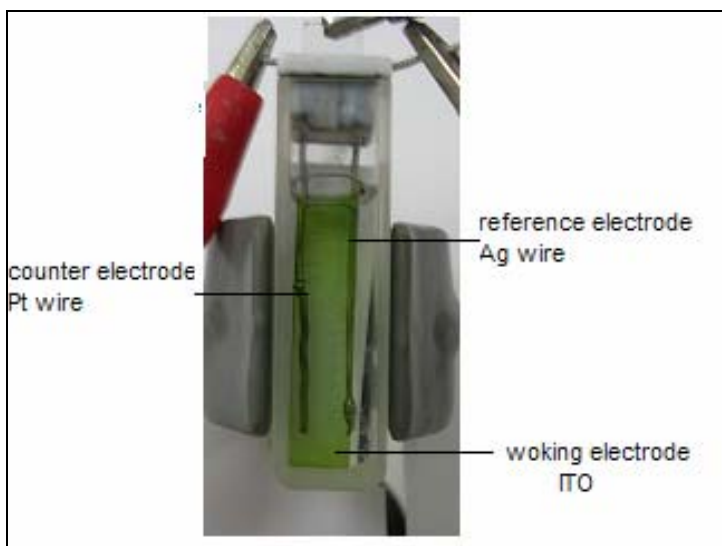


Figure 2.2 Schematic representation of a spectroelectrochemical cell.

2.3.4 Switching Properties of Polymers

Electrochromic switching studies monitor the ability of a polymer to switch rapidly and exhibit a striking color change. It is important for electrochromic applications of the polymer films. For this aim, square wave potential step method was coupled with optical spectroscopy to investigate the switching ability of P(SNS-PN), P(H₂Pc-SNS), P(ZnPc-SNS) and P(NiPc-SNS) between their neutral and oxidized states.

In this double potential step experiment, the potential was set at an initial potential for a set period of time, and was stepped to a second potential for a set period of time, before being switched back to the initial potential again. In order to study switching properties of polymers, they were deposited on ITO-coated glass slides as in the form of thin films.

After coating the polymers on ITO electrode, a potential square wave was applied in the monomer free electrolyte solution while recording the percent transmittance between its neutral and doped states at a fixed maximum absorption wavelength. Switching properties of polymer films were investigated by application of potential square wave technique with a residence time of 10 seconds between their oxidized and reduced potential ranges.

2.4 Experimental Procedure

2.4.1 Synthesis of 4-aminophthalonitrile

Following the general procedure of Griffiths and Roozpeikar [77] a suspension of 4-nitrophthalonitrile (3.89 g, 22.5 mmol) in a mixture of methanol (80 mL) and concentrated hydrochloric acid (17.5 mL) was heated to reflux. Iron powder (4.0 g,

71.42 mmol) was added in small portions over 1 h., and the reaction mixture continued to reflux for an additional 1 h. After cooling to room temperature, the mixture was poured into ice water, and the precipitate formed was collected by filtration, washed with water and dried under vacuum. The crude product was purified by column chromatography (silica: toluene /ethyl acetate 3:1) (Figure 2.3)

Orange solid, the yield was 86%. ¹H NMR (400 MHz, d-acetone): δ/ppm: 6.15-6.2 (s, 2H, NH₂), 7.05 (d, *J*=8.07 Hz, 1H), 7.15 (s, 1H), 7.6 (d, *J*=8.55 Hz, 1H)

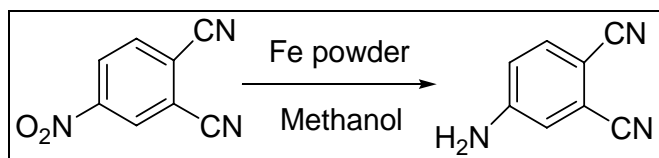


Figure 2.3 Synthetic route of 4-aminophthalonitrile.

2.4.2 Synthesis of 1,4-di(2-thienyl)-1,4-butadione (SOOS)

1,4-di (2-thienyl)-1,4- butanedione was synthesized according to literature procedure [78]. To a suspension of AlCl₃ (16 g, 0.12 mol) in CH₂Cl₂ (15 mL), a solution of thiophene (9.6 mL, 0.12 mol) and succinyl chloride (5.5 mL, 0.05 mol) in CH₂Cl₂ were added dropwise. The mixture was stirred at 18–20 °C for 48 h. This was then poured into ice and concentrated HCl (5 mL) mixture. The dark green organic phase was washed with saturated NaHCO₃ (3 x 25 mL), and dried over MgSO₄. After evaporation of the solvent, a blue green solid was remained which was suspended in ethanol. Filtration and washing with ethanol yielded 1,4-bis(2-thienyl)butane-1,4-dione (Figure 2.4).

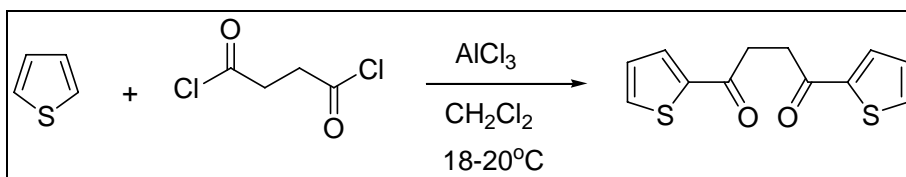


Figure 2.4 Synthetic route of 1,4-di(2-thienyl)-1,4-butanedione.

2.4.3 Synthesis of 4-(2,5-di-2-thiophen-2-yl-pyrrol-1-yl)phthalonitrile (SNS-PN)

The monomer was synthesized by utilizing SOOS and 4-aminophthalonitrile via Knorr-Paal Reaction [78-81]. 0.938 g (3.75 mmol) of SOOS, 0.75 g (5.25 mmol) of the 4-aminophthalonitrile, 0.075 g (0.435 mmol) of PTSA were dissolved in 40 mL of dry toluene. The mixture was stirred and refluxed for 120 h under argon atmosphere. Toluene was evaporated and the product was separated by column chromatography on silica gel (eluent: DCM/hexane (1:1)).

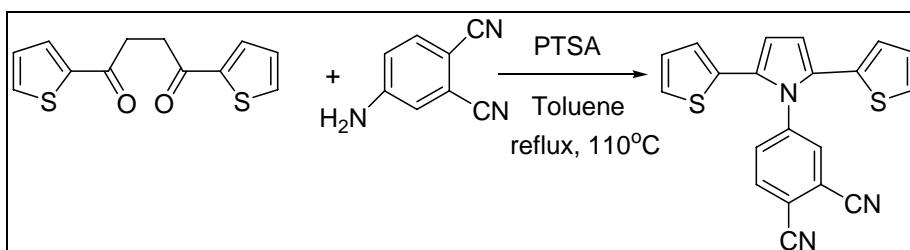


Figure 2.5 Synthetic route of 4-(2,5-di-2-thienyl-1H-pyrrol-1-yl)phthalonitrile.

Yellow solid, 80 % yield. Elemental analysis (%) calcd. For C₂₀H₁₁N₃S₂ : C 67.20, H 3.10, N 11.76, S 17.94; found: C 67.20, H 3.31, N 11.52, S 17.97.

^1H NMR (400 MHz, CDCl_3): δ /ppm: 7.68 (d, $J = 8.27$ Hz, 1H), 7.53 (d, $J = 1.82$ Hz, 1H), 7.45 (d, $J = 1.96$ – 1.80 Hz, 1H), 7.14 (d, $J = 2.68$ Hz, 2H), 6.8 (t, $J = 4.29$ Hz, 2H), 6.53 (d, $J = 2.2$ Hz, 2H), 6.47 (s, 2H).

^{13}C NMR (100 MHz, CDCl_3): δ /ppm: 142.82, 134.13, 134.10, 134.03, 133.04, 129.46, 127.36, 126.61, 126.07, 116.52, 115.19, 114.78, 114.42, 112.35.

2.4.4 Synthesis of tetrakis(4-(2,5-di-2-thiophen-2-yl-pyrrol-1-yl)) phthalocyanine ($\text{H}_2\text{Pc-SNS}$)

SNS-PN (0.28 mmol) was dissolved in n-hexanol (2 mL) under nitrogen in the presence of DBU (0.05 mL) with stirring at 140°C for 2 days under N_2 . The mixture was then cooled to room temperature and the product was precipitated by adding the reaction mixture drop wise into ethanol. The crude product (Figure 2.6) was washed several times with ethanol, methanol and diethyl ether to dissolve unreacted impurities and dried in vacuum oven.

Blue solid, Yield 30%. Elemental analysis (%), calcd. for $\text{C}_{80}\text{H}_{46}\text{N}_{12}\text{S}_8$: C 67.11, H 3.24, N 11.74, S 17.92; found: C 66.42, H 3.84, N 11.74, S 18.00.

2.4.5 Synthesis of tetrakis(4-(2,5-di-2-thiophen-2-yl-pyrrol-1-yl)) phthalocyaninato zinc (ZnPc-SNS)

SNS-PN (0.21 mmol) and zinc (II) acetate 2-hydrate (0.012 g) were dissolved in n-hexanol (2 mL) under nitrogen in the presence of DBU (0.05 mL) and heated with stirring at 140°C for 2 days. The mixture was then cooled to room temperature and the product was precipitated by adding the reaction mixture drop wise into ethanol.

The green crude product (Figure 2.6) was washed with ethanol, methanol, hot ethanol and diethyl ether in order to remove any unreacted metal salts and dried in vacuum oven.

Green solid, Yield 50%. Elemental analysis (%), calcd. for $C_{80}H_{44}N_{12}S_8Zn$: C 64.26, H 2.97, N 11.24, S 17.16; found: C 64.65, H 3.09, N 11.17, S 17.56.

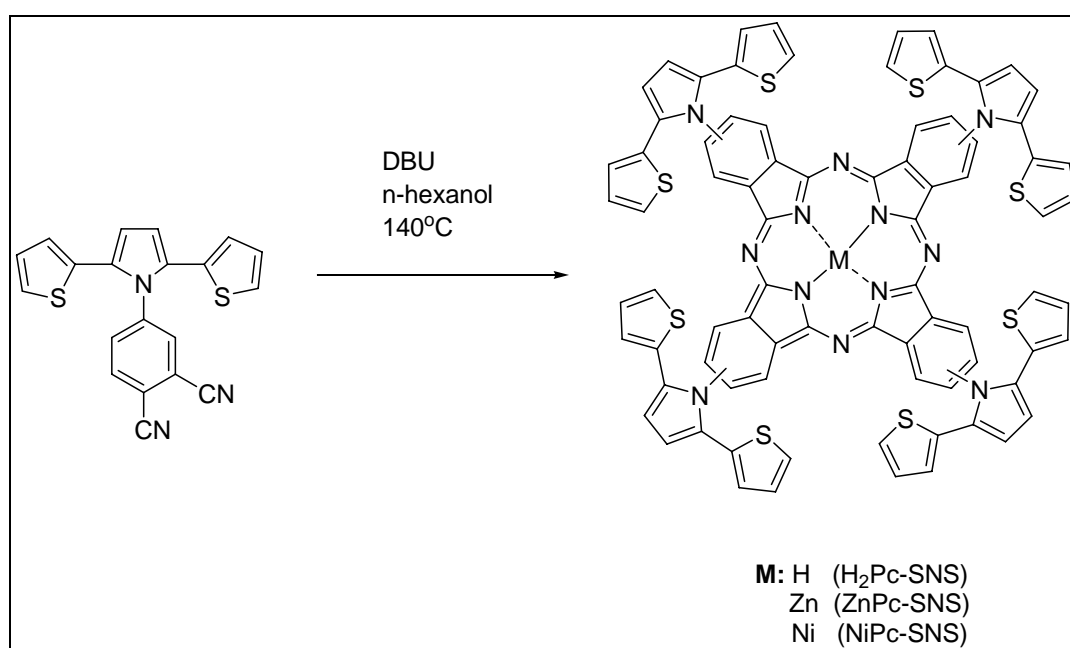


Figure 2.6 Synthetic route of $H_2Pc-SNS$, $ZnPc-SNS$ and $NiPc-SNS$.

2.4.6 Synthesis of tetrakis(4-(2,5-di-2-thiophen-2-yl-pyrrol-1-yl)) phthalocyaninato nickel ($NiPc-SNS$)

$SNS-PN$ (0.28 mmol) and nickel (II) chloride (9.1 mg) were dissolved in pentanol (3 mL) under nitrogen in the presence of DBU (0.05 mL) and heated with stirring at 140 °C for 2 days. The mixture was then cooled to room temperature and the product was precipitated by adding the reaction mixture drop wise into ethanol. The green crude

product (Figure 2.6) was purified using silica gel column chromatography with DCM-hexane (ratio 2:1) as the eluting solvent.

Green solid, Yield 40%. Elemental analysis (%), calcd. for $C_{80}H_{44}N_{12}S_8Ni$: C 64.55, H 2.98, N 11.29, S 17.23; found: C 64.41, H 3.11, N 11.49, S 16.95.

CHAPTER 3

RESULTS AND DISCUSSION

The synthetic route to all of the compounds synthesized is exhibited in Figure 3.1. In this study, the synthesis, structural and electrochemical properties of a series of novel metal-free and metallophthalocyanines were reported. Furthermore, the electropolymerization of the Pc precursor and the newly synthesized Pc derivatives were carried out and the results are presented in this section.

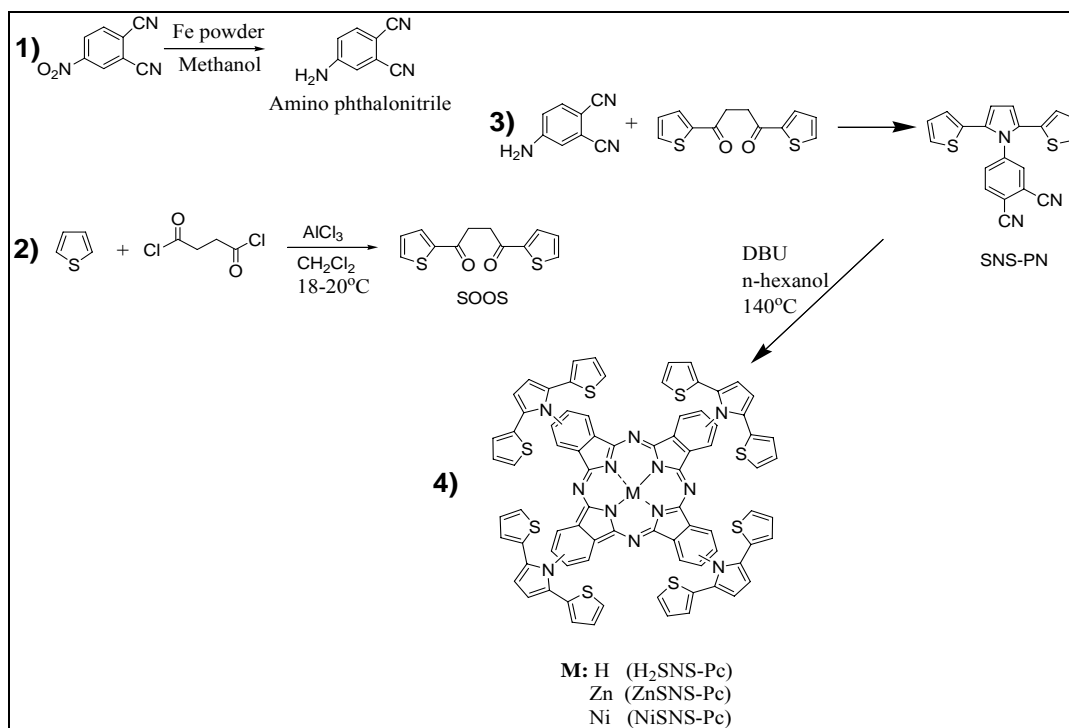


Figure 3.1 Synthesis of all of the compounds.

Substituted phthalocyanines are prepared by cyclotetramerization of substituted phthalonitriles. 2(3),9(10),16(17),23(24) (4-tetrasubstituted) Pcs can be synthesized from 4-substituted phthalonitriles (as in the case of the study) while 1(4),8(11),15(18),22(25) (3-tetrasubstituted) Pcs are obtained from 3-substituted analogues [9]. In both cases, a mixture of four possible structural isomers is obtained and they are differentiated by their molecular symmetry: C_{4h} , C_{2v} , C_s and D_{2h} [82]. The 4-tetrasubstituted compounds always occur in the expected statistical mixture of the isomers as 12.5% C_{4h} , 25% C_{2v} , 50% C_s and 12.5% D_{2h} . However, for the 3-tetrasubstituted Pcs depending on the central metal ion and the structure of the peripheral substituent, the composition of the isomers varies [82].

It is also expected in this study that synthesized 4-tetrasubstituted Pc compounds were prepared as a statistical mixture of four regioisomers. Attempts to separate these isomers with column chromatography method using different solvents were not successful.

3.1 Spectroscopic Characterizations

3.1.1 SNS-PN and P(SNS-PN)

3.1.1.1 ^1H and ^{13}C NMR Spectroscopies

Spectra obtained from ^1H NMR and ^{13}C NMR experiments are very useful to confirm the structural characteristics of the desired SNS-PN (Figure 3.2Figure 3.3)

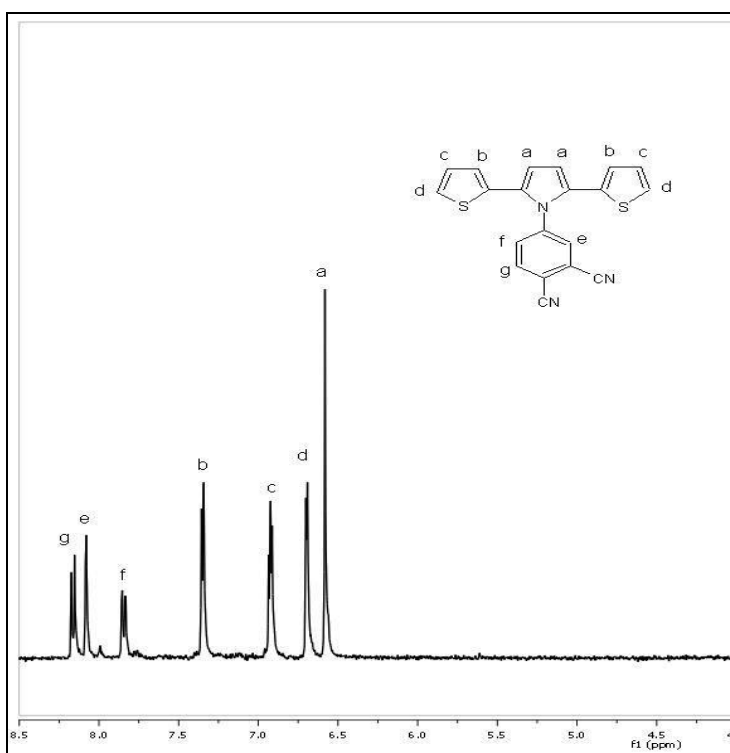


Figure 3.2 ^1H NMR spectrum of SNS-PN.

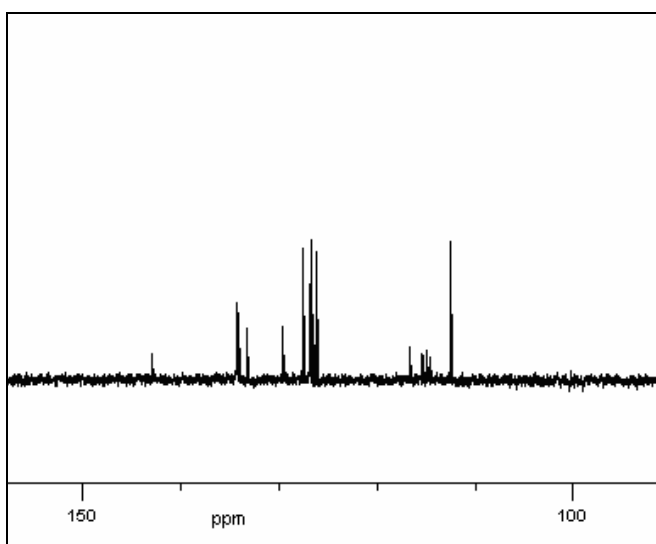


Figure 3.3 ^{13}C NMR spectrum of SNS-PN.

3.1.1.2 Infrared Spectrometry

It is well known that FTIR spectrum of unsubstituted SNS exhibits three strong bands centered at 692, 778 and 841 cm^{-1} due to the C-H out of plane bendings of α -hydrogens of thiophene rings, β -hydrogens of pyrrole ring and β/β' -hydrogens of thiophene rings, respectively [83].

The FTIR spectra of SNS-PN and its polymer P(SNS-PN) are presented in Figure 3.4. SNS-PN also exhibits these three strong peaks at 702 cm^{-1} , 770 cm^{-1} and 836 cm^{-1} due to the C-H bendings of α/β hydrogens of the five-membered aromatic rings. Furthermore, the peaks in the region of 1600-1420 cm^{-1} are assigned skeletal vibrations of benzene ring and the peak at 2240 cm^{-1} is due to the cyanide group.

A close inspection of Figure 3.4 reveals that all these peaks are also present in the FTIR spectrum of P(SNS-PN) except for the peak at 702 cm^{-1} . This peak is due to α -hydrogens of external thiophene rings and its disappearance confirms the formation of linear polymer chains via α - α' linkages.

The broad band observed at around 1650 cm^{-1} proves the presence of polyconjugation [84] and the peaks at 1072 cm^{-1} and 627 cm^{-1} in the polymer spectrum are due to the presence of ClO_4^- dopant [85].

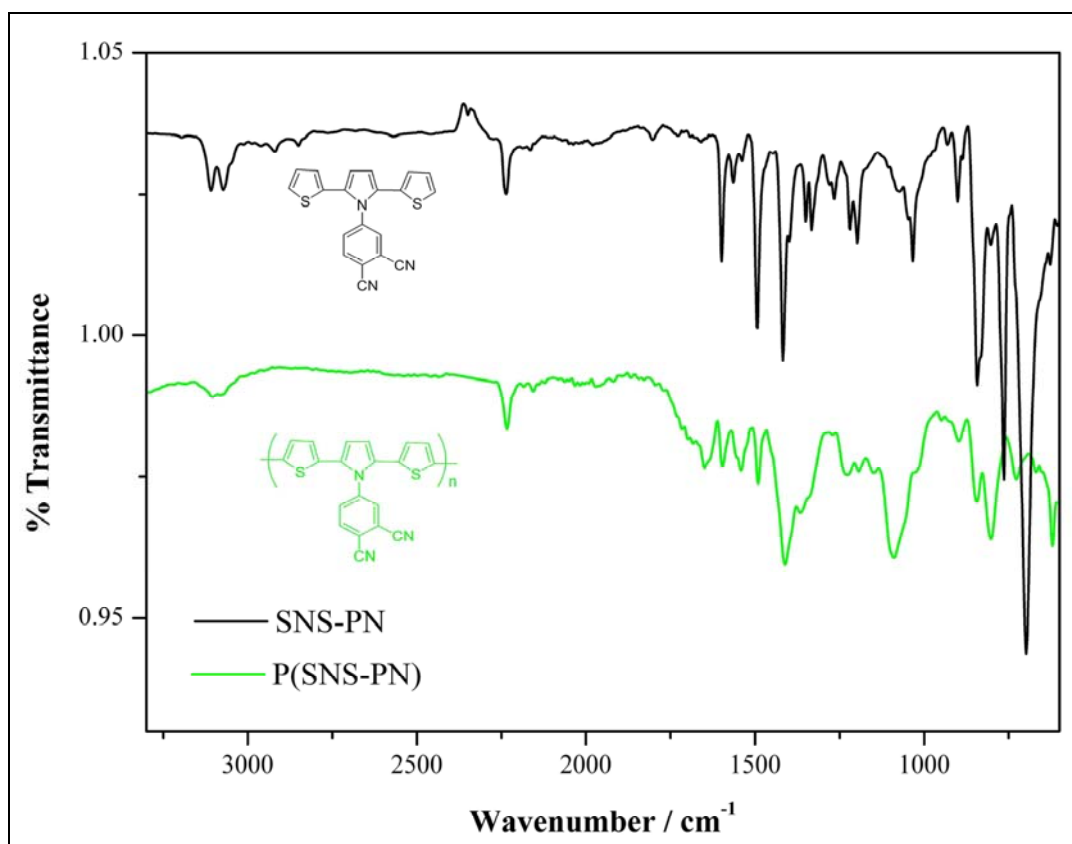


Figure 3.4 FTIR spectra of (a) SNS-PN and (b) P(SNS-PN).

3.1.1.3 Elemental Analysis

SNS-PN was also characterized by elemental analysis. The elemental analysis for the compound gave excellent percentage of carbon value that was the same as the calculated value. For the other elements hydrogen, sulphur and nitrogen, the elemental analysis values were within 2% of the expected values (Table 3.1).

Table 3.1 Elemental analysis data for SNS-PN.

Compound	<i>Calculated</i>				<i>Found</i>			
	<i>C%</i>	<i>H%</i>	<i>N%</i>	<i>S%</i>	<i>C%</i>	<i>H%</i>	<i>N%</i>	<i>S%</i>
SNS-PN	67.20	3.10	11.76	17.94	67.20	3.31	11.52	17.97

3.1.2 H₂Pc-SNS, ZnPc-SNS and NiPc-SNS

3.1.2.1 ¹H and ¹³C -NMR Spectroscopies

NMR Spectra obtained for Pc complexes were unresolvable in the aromatic region due to their poor solubility, high aggregation tendency, which results in a low signal to noise ratio of the spectra, and the compounds being isomerically impure. Thus, formation of the compounds was supported by FTIR Spectroscopy and elemental analyses.

3.1.2.2 Elemental Analysis

Elemental analysis was performed in order to verify the composition and purity of Pc complexes. Percent composition of carbon, hydrogen, nitrogen and sulphur were determined and are reported in Table 3.2.

Table 3.2 Elemental analysis data for Pc complexes.

			<i>Calculated</i>				<i>Found</i>			
<i>Compound</i>	<i>Formula</i>	<i>Mol Wt (g/mol)</i>	<i>C (%)</i>	<i>H (%)</i>	<i>N (%)</i>	<i>S (%)</i>	<i>C (%)</i>	<i>H (%)</i>	<i>N (%)</i>	<i>S (%)</i>
H ₂ Pc-SNS	C ₈₀ H ₄₆ N ₁₂ S ₈	1431.8	67.11	3.24	11.74	17.92	66.42	3.84	11.74	18.00
ZnPc-SNS	C ₈₀ H ₄₄ N ₁₂ S ₈ Zn	1495.2	64.26	2.97	11.24	17.16	64.65	3.09	11.17	17.56
NiPc-SNS	C ₈₀ H ₄₄ N ₁₂ S ₈ Ni	1488.5	64.55	2.98	11.29	17.23	64.41	3.11	11.49	16.95

Generally, a compound is considered to be pure if the determined composition of each element remains within a 0.5 % deviation of the calculated value.

The elemental analyses for compounds H₂Pc-SNS, ZnPc-SNS and NiPc-SNS gave percentage carbon results with a deviation smaller than 1.5 %. For compounds ZnPc-SNS and NiPc-SNS nitrogen and sulphur values were within 2 % of the expected values. The small differences between calculated and determined compositions can be greatly assumed to be due to the large number of carbon and hydrogen atoms present in the molecule. It has been reported before that for large Pc molecules, elemental analyses often gives unsatisfactory results [86].

Elemental compositions can be affected in several ways. The compound can contain impurities, unreacted starting material or undesired by-products. It is also common for compositional determinations to be skewed due to solvent molecules being trapped within structure of the compound.

3.1.2.3 UV-Vis Absorption Spectroscopy

UV-Vis spectroscopy is a very suitable technique to monitor the presence of phthalocyanine groups, their substituents and interactions between them.

UV-Vis spectra of the phthalocyanine complexes exhibit characteristic Q- and B-bands. The Q band in the visible region at 600-750 nm is attributed to the π - π^* transition from HOMO to LUMO of the phthalocyanine ring, and the B-band in the UV region at 300-400 nm arises from the deeper π - π^* transitions [87].

The electronic spectra of the complexes in DCM at room temperature are shown in Figure 3.5. It exhibited a typical Q band at 700 and 665 nm for H₂Pc-SNS, 680 nm for ZnPc-SNS and 670 nm for NiPc-SNS. Compared with H₂Pc, the λ_{max} of the MPcs moved to shorter wavelengths and decreased in the order of ZnPc-SNS, NiPc-SNS, due to the nature of the central metal ion [88].

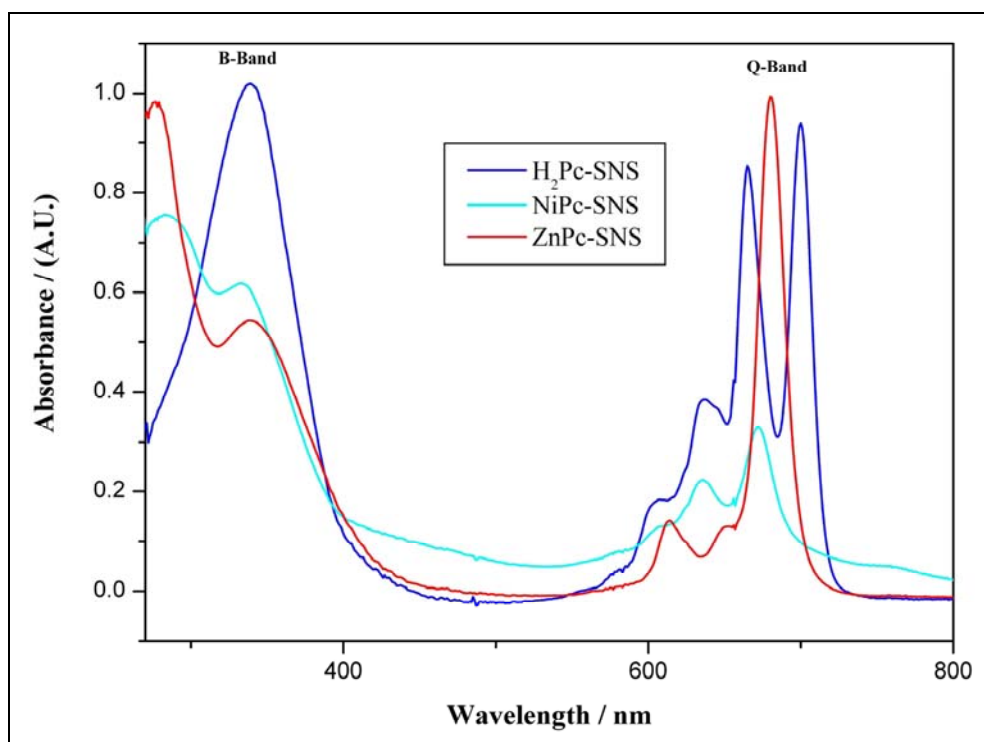


Figure 3.5 UV-vis spectra of 1.0×10^{-4} mol.L⁻¹ for H₂Pc-SNS, ZnPc-SNS and NiPc-SNS in DCM.

The metal-free phthalocyanine complex H₂Pc-SNS gave a doublet (narrow) Q band as a result of the non-degenerate symmetry of metal-free phthalocyanine which is the D_{2h} symmetry [89]. All synthesized complexes exhibited B or Soret band between 300 – 350 nm which results from the transition of the deeper π orbitals (b_{2u} and a_{2u}) to the π^* orbitals (e_g). These bands overlapped with the absorption band of the SNS unit [90]. The small absorption bands that appear around 630 nm might be due to the

aggregation. Aggregation in Pc complexes is typified by a broadened or split Q band, with the high energy band being due to the aggregate and the low energy band due to the monomer [91]. It is usually depicted as a coplanar association of rings progressing from monomer to dimer and higher order complexes. It is dependent on the concentration, nature of the solvent, nature of the substituents, complexed metal ions and temperature [92]. In the aggregated state the electronic structure of the complexed phthalocyanine rings is perturbed resulting in alternation of the ground and excited state electronic structures [93].

3.1.2.4 Infrared Spectrometry

It has widely been accepted that vibrational spectroscopy is a versatile technique for studying the intrinsic properties of Pcs. The FTIR spectra of MPc complexes are generally complex but similar. The main bands are the C-H stretching vibration at around 3030 cm^{-1} , C-C ring skeletal stretching vibrations at around 1600 and 1475 cm^{-1} , C-H out of plane bending vibrations at around $750\text{-}790\text{ cm}^{-1}$ [94], all these bands are from the aromatic ring of the MPc. The unmetallated Pcs can be distinguished from the metallated ones by the presence of N-H stretching vibration at about 3298 cm^{-1} in the former but absence of the band in the latter [95].

In the case of our monomers, the characteristic nitrile ($\text{C}\equiv\text{N}$) stretching at 2240 cm^{-1} of SNS-PN disappeared after conversion, indicative of phthalocyanine formation (Figures 3.6, 3.7 and 3.8)

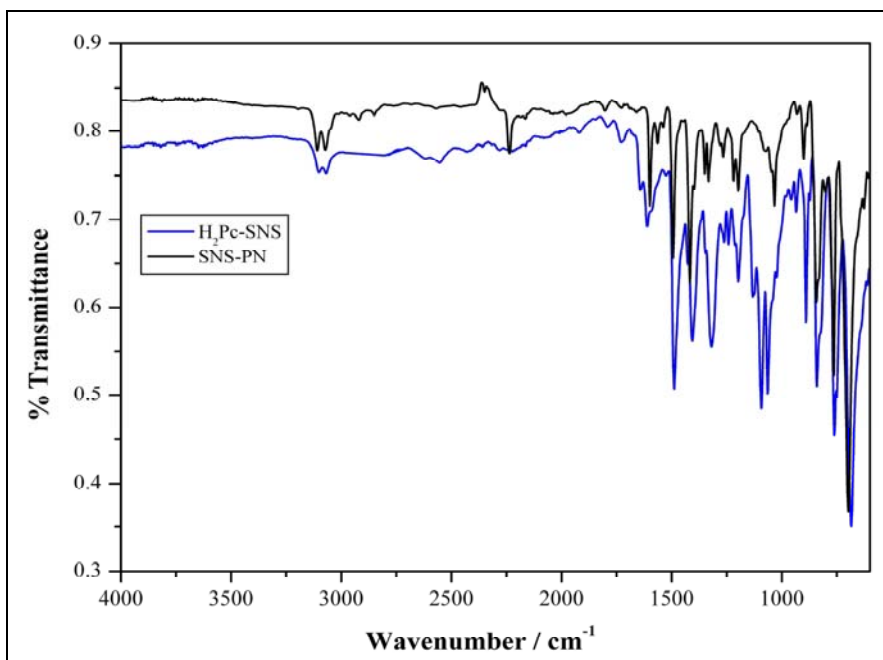


Figure 3.6 FTIR spectra of SNS-PN and H₂Pc-SNS.

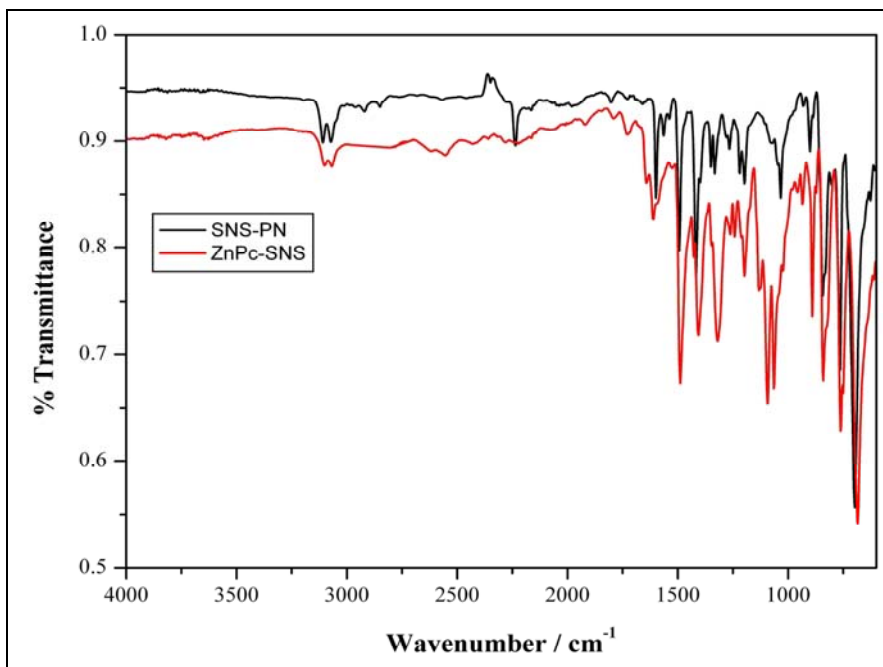


Figure 3.7 FTIR spectra of SNS-PN and ZnPc-SNS.

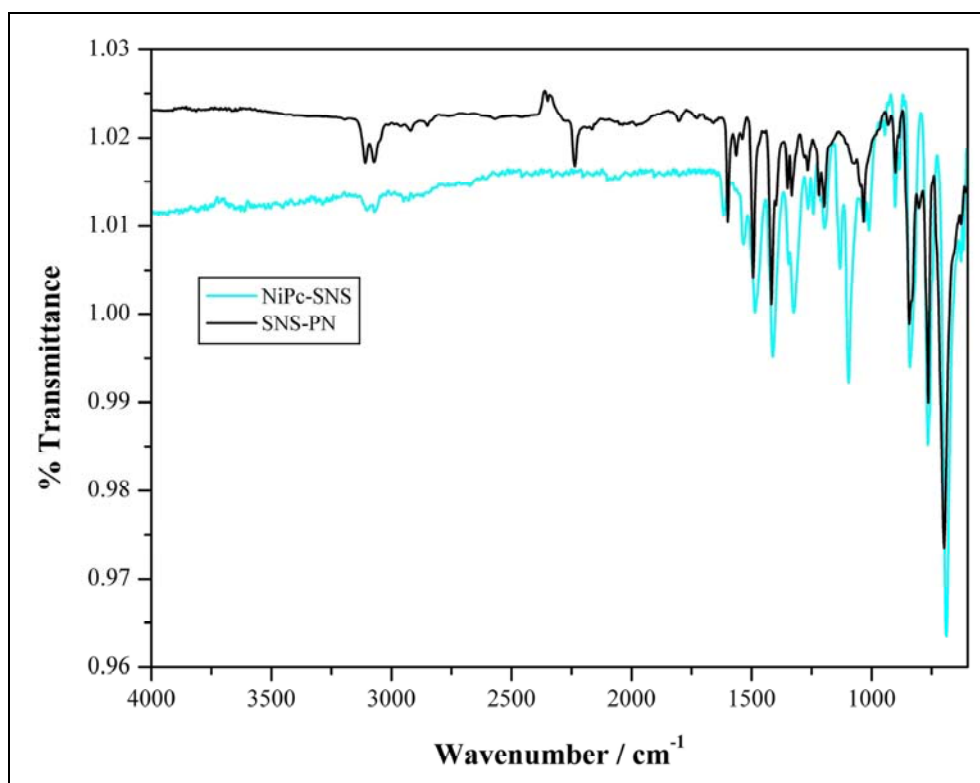


Figure 3.8 FTIR spectra of SNS-PN and NiPc-SNS.

In the FTIR spectra of H₂Pc-SNS, ZnPc-SNS, NiPc-SNS (Figure 3.9), the peaks at 690 cm⁻¹ (for α -hydrogens of thiophene rings), 760 cm⁻¹ (for β -hydrogens of pyrrole ring) and 839 cm⁻¹ (for β/β' -hydrogens of thiophene rings) confirm the presence of SNS substituent through the benzene ring of Pc [90].

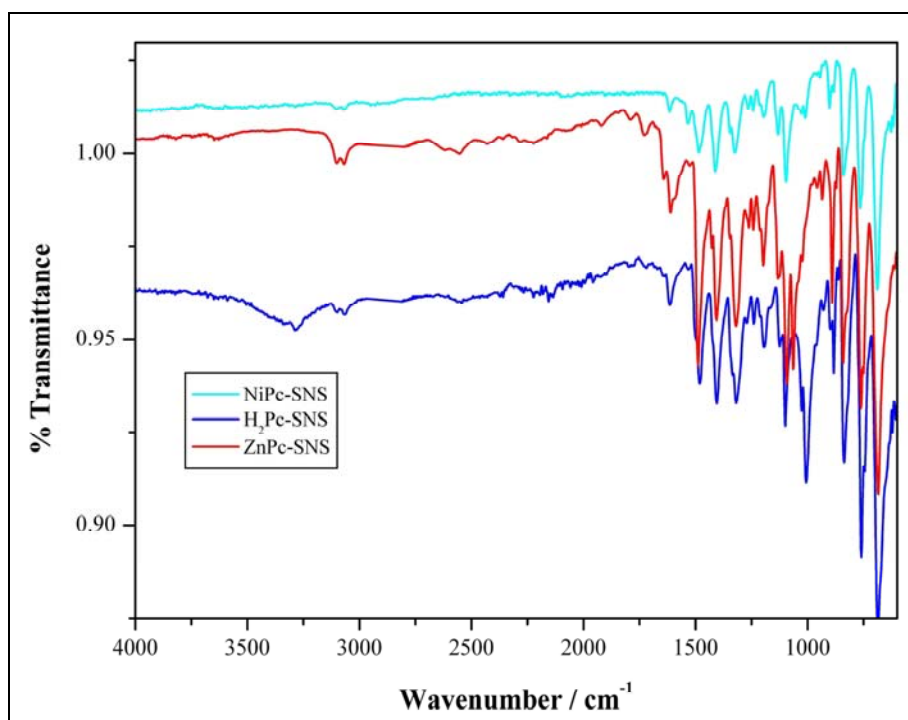


Figure 3.9 FTIR spectra of H₂Pc-SNS, ZnPc-SNS and NiPc-SNS.

The peak at 3060 cm⁻¹ results from stretching of the benzo C-H bonds on the phthalocyanine ring, while aromatic C-H stretching of the thiophene substituents (α -hydrogens of thiophene rings) is ascribed to the peak at 3100 cm⁻¹. Furthermore, the peaks at 1625-1615 cm⁻¹ are attributed to C=C bonds of Pc ring and the peaks in the range 1487-1480 cm⁻¹ are due to C-N aromatic stretching. All the remaining bands observed in the range of 755-740 cm⁻¹ and 600-700 cm⁻¹ may be assigned to various skeletal vibrations of the Pc ring [94]. The FTIR spectra of phthalocyanine complexes are very similar, except for the NH₂ band at 3300 cm⁻¹ which was observed in the FTIR spectrum of H₂Pc-SNS.

3.1.3 P(H₂Pc-SNS), P(ZnPc-SNS) and P(NiPc-SNS)

Upon polymerization for all of the complexes characteristic vibration bands of Pc skeleton in the range of 1100-600 cm⁻¹ remain unchanged. As expected, the peak at 690 cm⁻¹ present in the monomer spectrum disappears in all of the spectra (Figure 3.10, Figure 3.11 and Figure 3.12), which confirms the formation of linear polymer chains via α - α' linkages of thiophene as observed in the polymerization of SNS-PN. The peak at 1086 cm⁻¹ in the polymer spectra are due to the presence of ClO₄⁻ dopant.

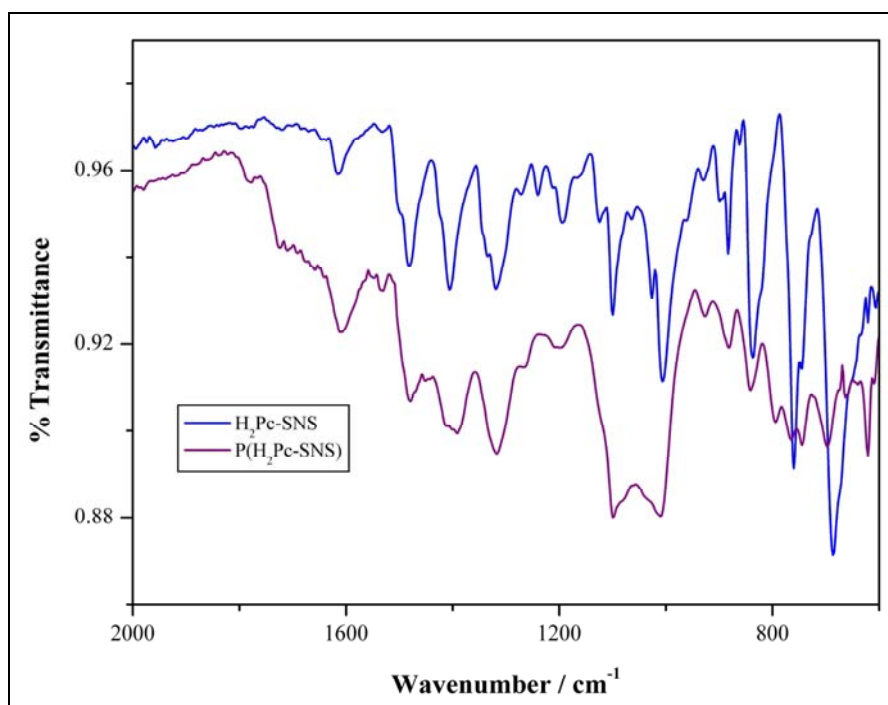


Figure 3.10 FTIR spectra of H₂Pc-SNS and P(H₂Pc-SNS).

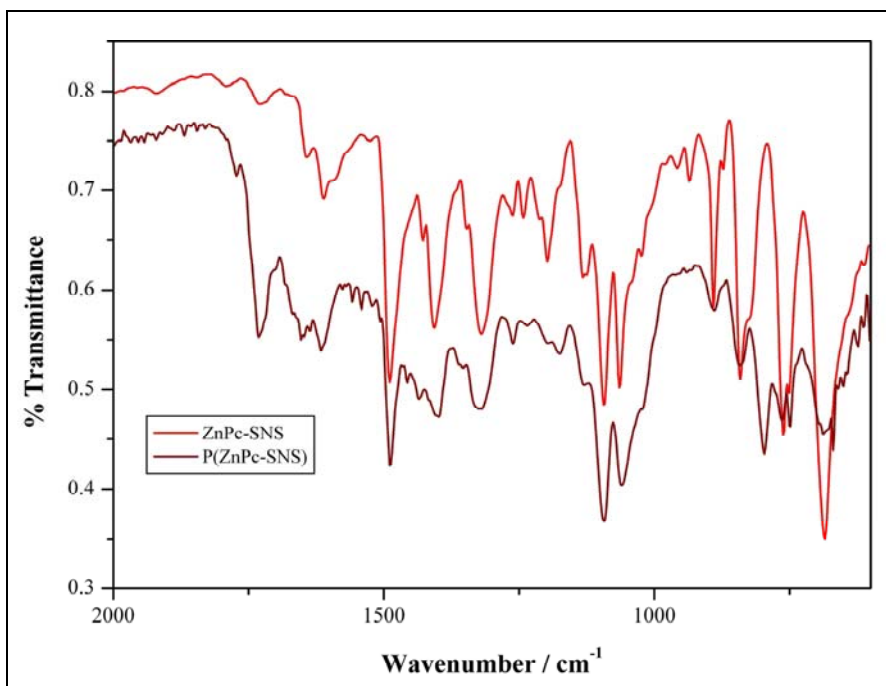


Figure 3.11 FTIR spectra of ZnPc-SNS and P(ZnPc-SNS).

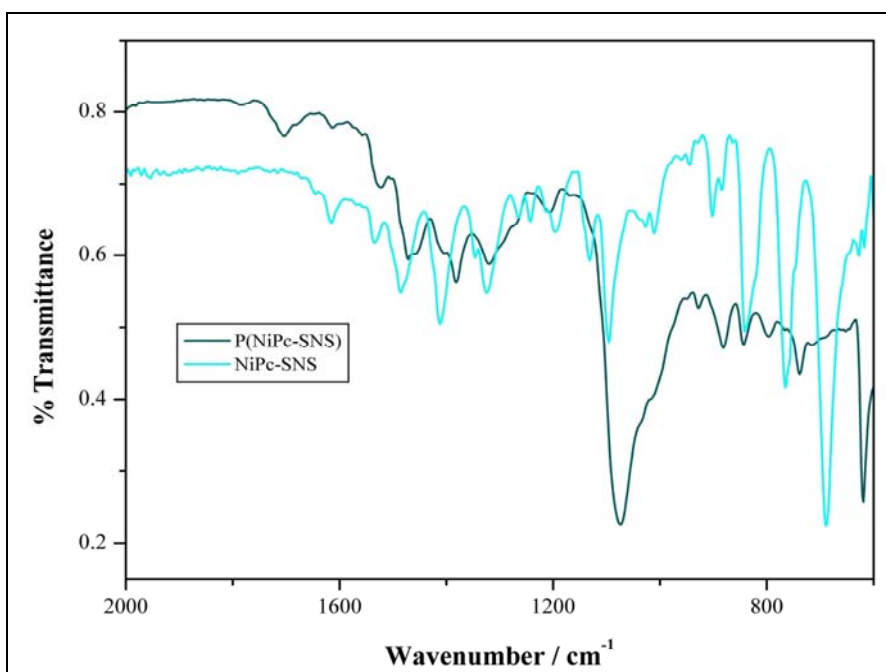


Figure 3.12 FTIR spectra of NiPc-SNS and P(NiPc-SNS).

3.2 Electrochemical Characterization

3.2.1 H₂Pc-SNS, ZnPc-SNS and NiPc-SNS

The solution redox properties of the complexes (0.1 mM) were studied in 0.1 M TBAP/DCM, electrolyte/solvent couple utilizing CV and DPV, before the synthesis of the polymers. The potential values and assignments are summarized in Table 3.3 and the results were depicted in Figure 3.13 to Figure 3.18. A close inspection of these figures reveal that all the complexes have very similar voltammetric responses in solution except potential shift of the redox processes due to the metal centre differences. The voltammetric analyses represent that all complexes display two reversible reduction processes and one oxidation process during the anodic scan vs Ag/AgCl at a scan rate of 100 mVs⁻¹. DPVs support the redox processes recorded with CV.

Figure 3.13 and Figure 3.14 show CV and DPV of the H₂Pc-SNS complex. The compound gives two reduction couples II (-0.57 V) and III (-0.93 V) and one oxidation processes (I). Based on the well-known electrochemical behavior of metal-free phthalocyanines, all the reduction couples are easily assigned to phthalocyanine ring which can be represented as Pc³⁻/Pc²⁻ and Pc⁴⁻/Pc³⁻, respectively. The oxidation peak observed at 0.82 V corresponds to dithienylpyrrole unit (i.e. SNS unit).

The reduction and oxidation behavior of MPc derivatives is due to the interaction between the Pc ring and the central metal ions [96, 97], the Pc ring can undergo successive one-electron reduction and one-electron oxidation to yield the anion and cation radicals, respectively. MPcs having a metal that possess energy levels lying between HOMO and LUMO of the Pc ring, in general, will exhibit redox processes centered on the metal. This is the case for the Pcs of Cr, Mn, Co and Fe, which have open d-shell structures [97]. If the transition metal ion concerned has no accessible d orbital levels lying within the a_{1u} (HOMO) - e_g (LUMO) gap of a phthalocyanine

species, then, its redox chemistry will appear very similar to that of redox inactive MPcs. Zinc and nickel behave in this fashion, with the Zn(II) and Ni(II) central ions being unchanged as the Pc unit is either oxidized or reduced [9].

In this study, it is clearly pointed out that all of these processes can be ascribed to the Pc ring electron transfer reactions. ZnPc-SNS and NiPc-SNS complexes have very similar CV and DPV responses. CV and DPV of the complexes are given in Figure 3.15 to Figure 3.18 to represent the voltammetric response of the MPs having redox inactive metal centre.

Both metal complexes give two reversible reduction couples upon negative potential scan, II (-0.84 V) and III (-1.19 V) for ZnPc-SNS, II (-0.58 V) and III (-0.81 V) for NiPc-SNS. During the positive potential scan as observed for H₂Pc-SNS, the oxidation couple corresponding to dithienylpyrrole unit is seen for both complexes at 0.84 V and 0.88 V, respectively [90].

Since zinc and nickel Pc complexes are known not to show any redox activity, the peak couples observed for ZnPc-SNS and NiPc-SNS are also associated with the ring based processes of Pc.

Table 3.3 Summary of redox potentials ($E_{1/2}$ vs Ag/AgCl) of the Pc complexes in 0.1 M TBAP dissolved in DCM.

<i>Complex</i>	(II) Pc³⁻/Pc²⁻	(III) Pc⁴⁻/Pc³⁻	SNS unit
<i>H₂Pc-SNS</i>	-0.57	-0.93	0.82
<i>ZnPc-SNS</i>	-0.84	-1.19	0.84
<i>NiPc-SNS</i>	-0.59	-0.82	0.88

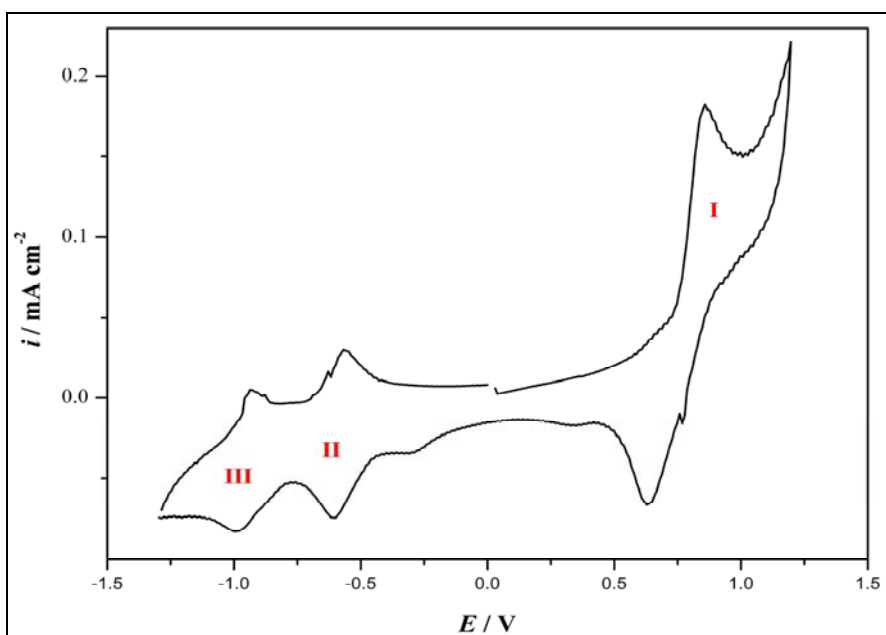


Figure 3.13 Cyclic voltammogram of H₂Pc-SNS on a Pt disc electrode at 100 mVs⁻¹ in 0.1 M TBAP/DCM

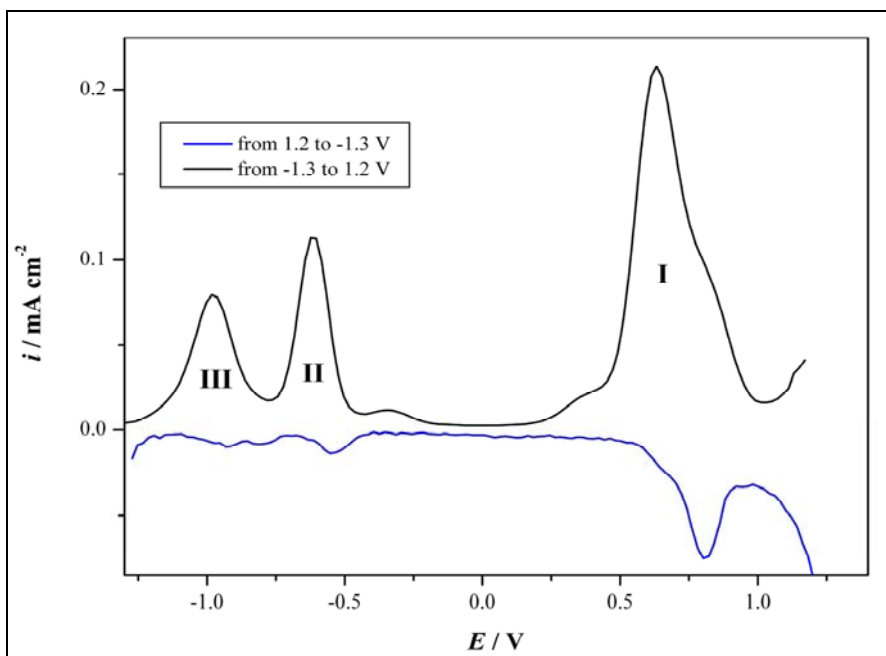


Figure 3.14 DPV of H₂Pc-SNS in 0.1 M TBAP/DCM.

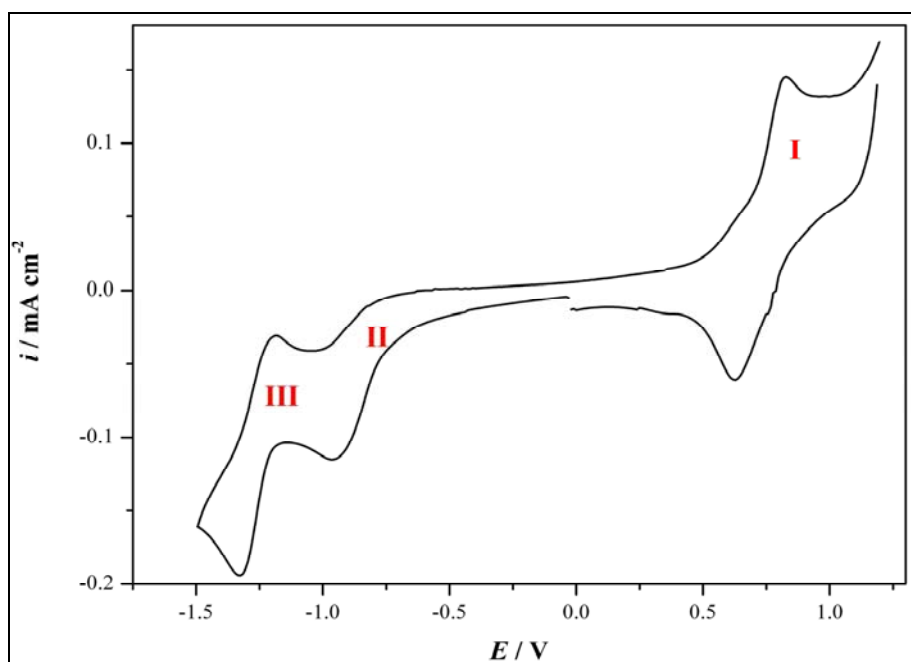


Figure 3.15 Cyclic voltammogram of ZnPc-SNS on a Pt disc electrode at 100 mVs^{-1} in 0.1 M TBAP/DCM .

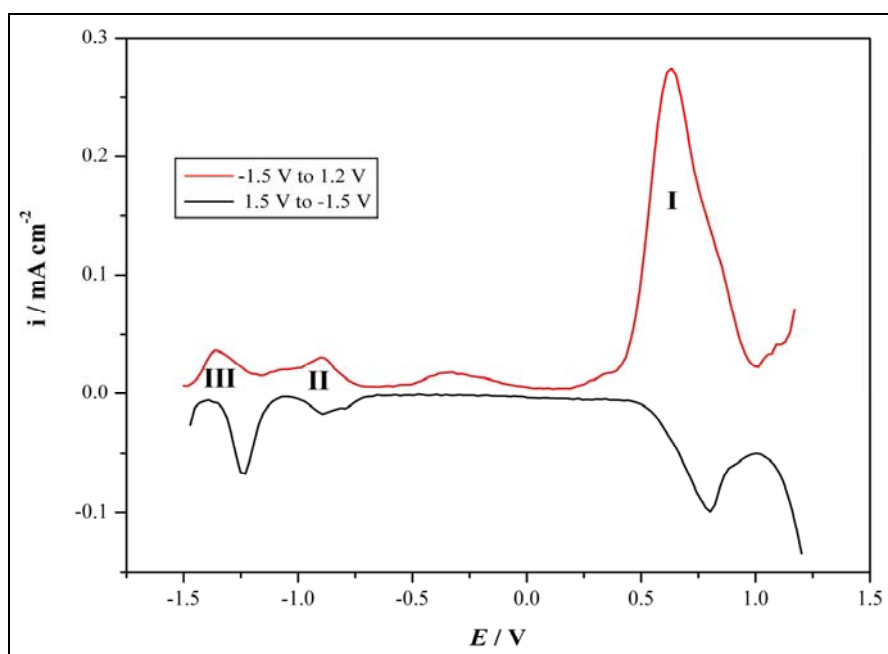


Figure 3.16 DPV of ZnPc-SNS in 0.1 M TBAP / DCM .

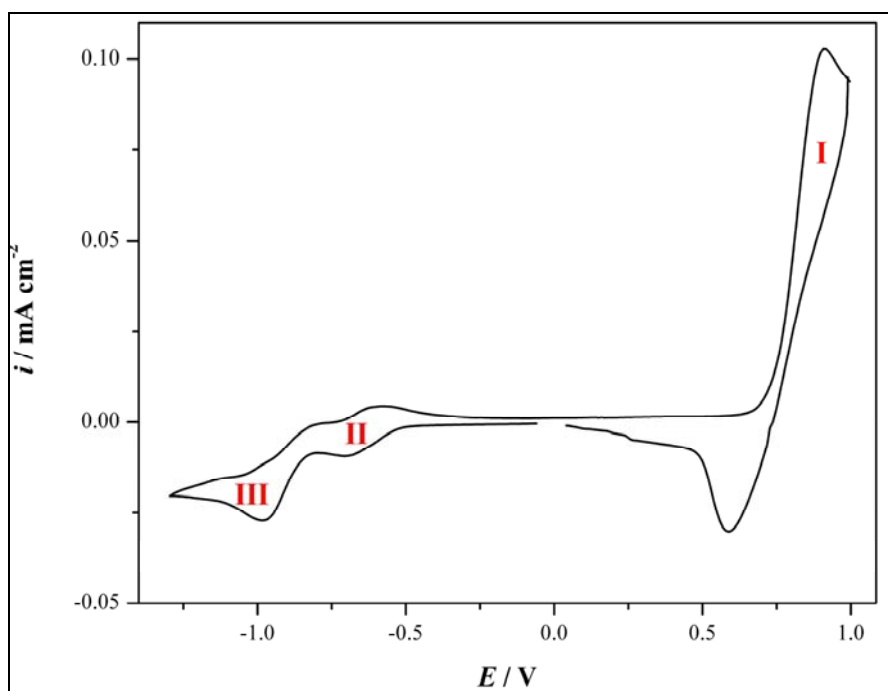


Figure 3.17 Cyclic voltammogram of NiPc-SNS on a Pt disc electrode at 100 mVs^{-1} in 0.1 M TBAP/DCM .

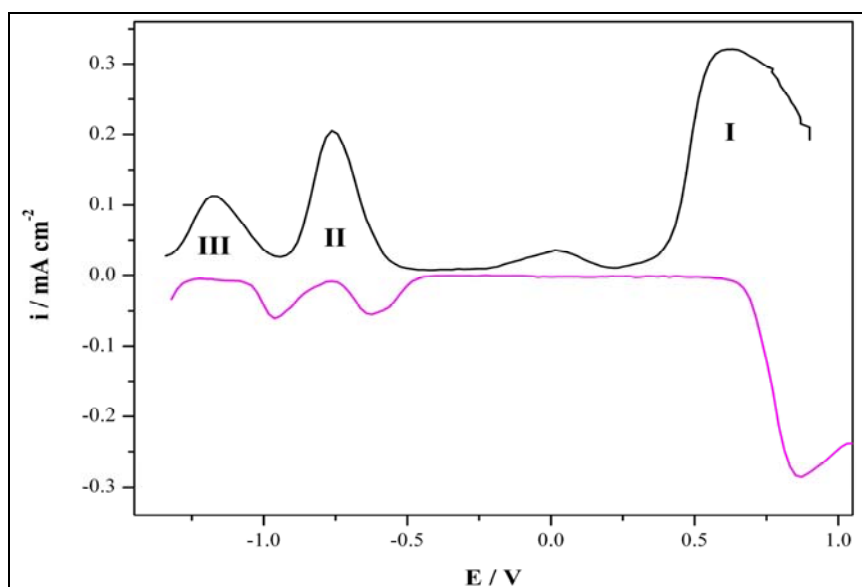


Figure 3.18 DPV of NiPc-SNS in 0.1 M TBAP/DCM .

3.3 Electropolymerization

3.3.1 SNS-PN

Electrochemical behavior of SNS-PN was investigated in 0.2 M LiClO₄/acetonitrile, electrolyte/solvent couple utilizing CV, before the synthesis of the polymers. Cyclic voltammogram of electrolytic solution containing 2.0 mM SNS-PN exhibits one irreversible oxidation peak at 0.92 V vs Ag wire in the first anodic scan. A new reduction peak is also noted during the reverse scan which intensifies upon successive scans in the potential range of 0.0 to 1.15 V.

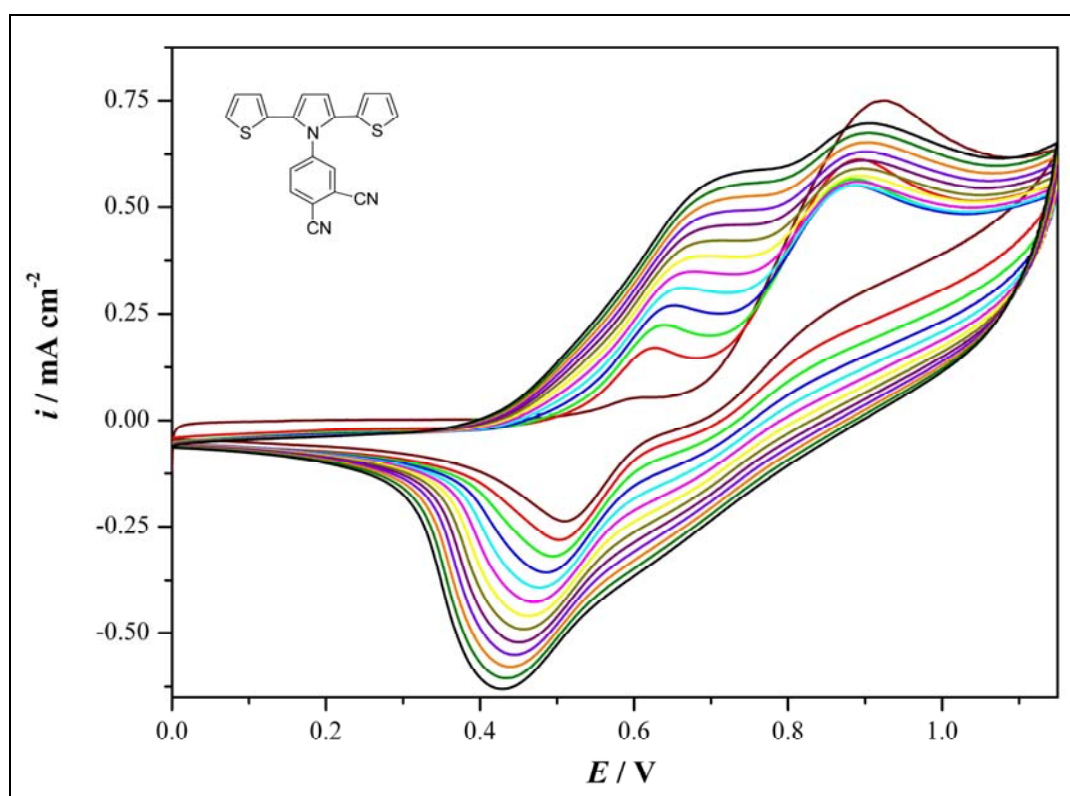


Figure 3.19 Repeated scan electrochemical polymerization of 2.0×10^{-3} M SNS-PN at a scan rate of 100mV/s.

The formation of P(SNS-PN) can be easily seen with the increasing intensity of the reversible redox couple, indicating doping and de-doping of the polymer film (Figure 3.19). Also, electrochemical behavior of the polymer film obtained from SNS-PN after 13 repetitive cycles was investigated in the monomer-free electrolytic solution. Figure 3.20 shows that polymer film exhibits a single and well-defined quasi reversible couple ($E_{pa}= 0.74$ V and $E_{pc}= 0.61$ V) in 0.2 M LiClO₄/acetonitrile solution due to doping and de-doping of the polymer film. Since SNS-PN has two electron withdrawing cyanide groups per monomer unit, the oxidation potential of the monomer and first oxidation potential of the polymer are slightly higher than the reported values for various SNS derivatives [79-80, 83, 85, 98-100].

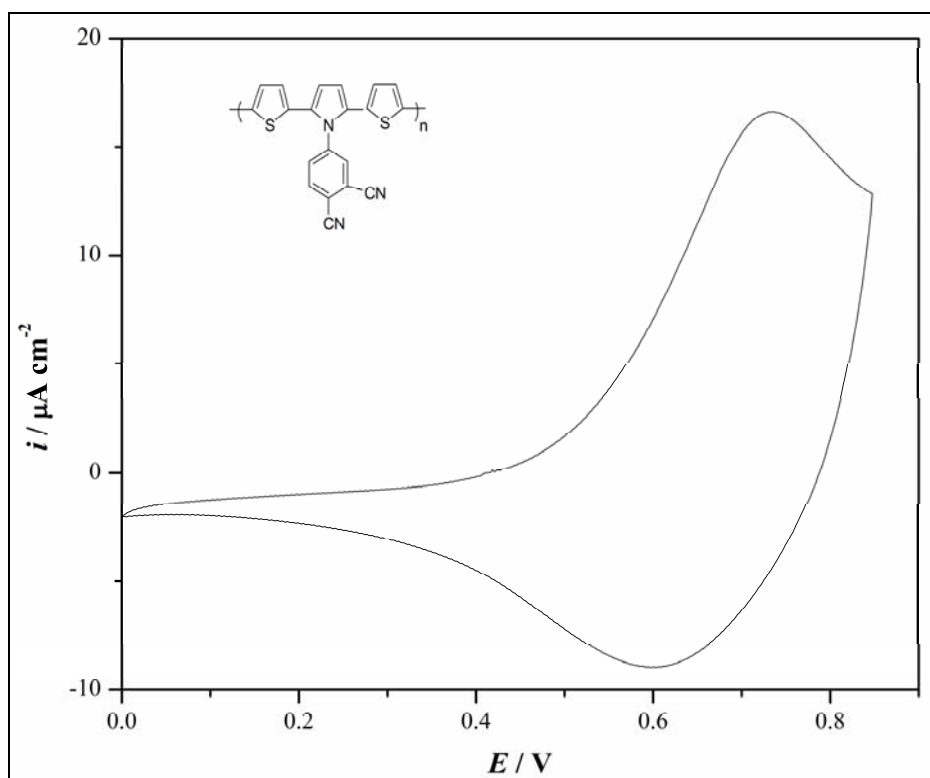


Figure 3.20 Cyclic voltammogram of P(SNS-PN) film on a Pt disc electrode at 100 mV/s in acetonitrile solution containing 0.2 M LiClO₄.

In order to see if these electron withdrawing cyanide groups can interact with any metal cation through nitrogen atoms, cyclic voltammograms of the polymer film were also recorded after keeping the film in contact with a solution containing either TBAP or sodium perchlorate (NaClO_4) for five minutes.

The results are depicted in Figure 3.21. As seen from Figure 3.21, oxidation peak of the polymer film shifted anodically. This result clearly indicates an interaction between cyanide groups present on the polymer chains and cations, thus reducing the electron withdrawing effect of these groups on the polymer film oxidation.

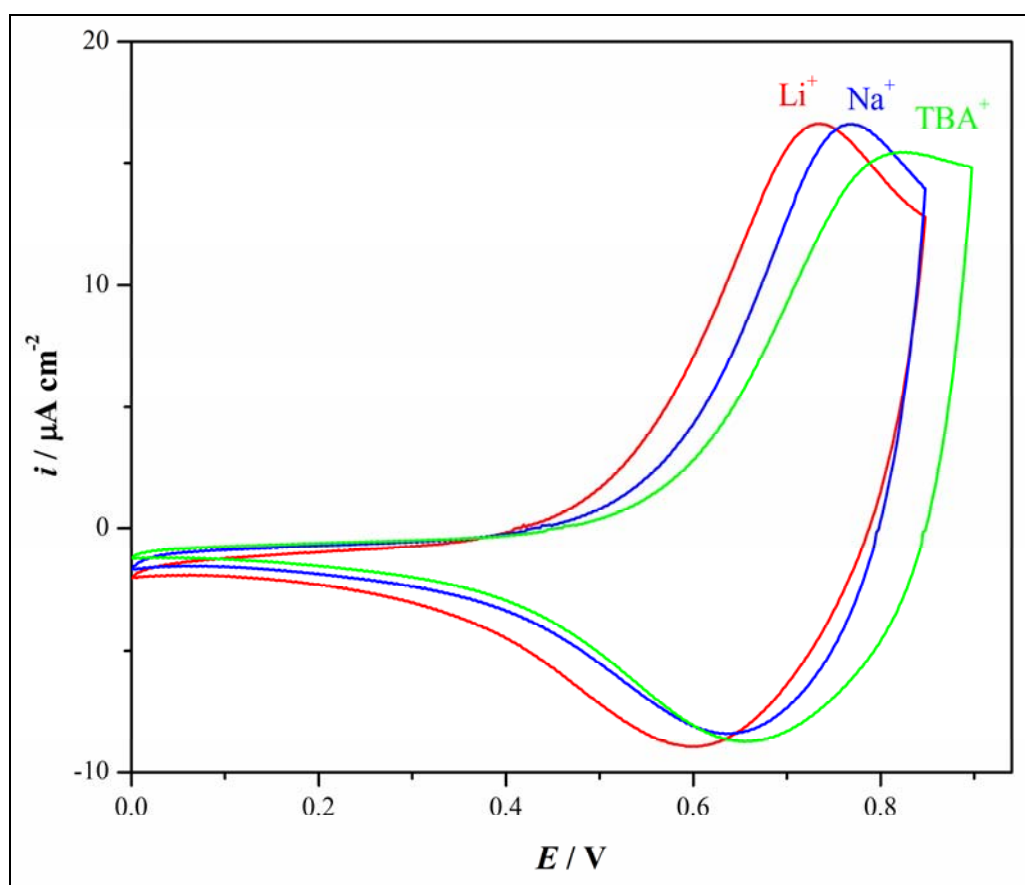


Figure 3.21 Cyclic voltammogram of P(SNS-PN) film (25 mC/cm^2) on a Pt disc electrode in acetonitrile containing 0.2 M LiClO_4 , NaClO_4 , and TBAP.

3.3.2 H₂Pc-SNS, ZnPc-SNS and NiPc-SNS

The oxidative electrochemical polymerization of the complexes were achieved by scanning in the potential ranges 0.0 V to +1.3 V (for H₂Pc-SNS), 0.0 V to 1.15 V (for ZnPc-SNS) and 0.0 V to 1.1 V (for NiPc-SNS) in 0.1 M TBAP/DCM, electrolyte/solvent couple utilizing CV. Cyclic voltammograms of H₂Pc-SNS, ZnPc-SNS and NiPc-SNS exhibit one irreversible oxidation peak at 0.85 V, 0.82 V and 0.88 V in the first anodic scan, respectively (Figure 3.22, Figure 3.23 and Figure 3.24). The slight difference in the peak potentials may be due to the interaction between metal ions and Pc ligand, which shifts the oxidation potential to lower values.

During repetitive cycling of the monomer solutions, in the potential range given above, new reversible redox couples and accompanying increase in the current intensities are observed. This clearly indicates the deposition of electroactive polymer films on Pt disc (0.02 cm²) electrode surface as a consequence of the electrochemical polymerization of SNS units.

After several repetitive scans a new intensifying peak about 0.40 V vs Ag/AgCl is also observed for all of the complexes which shift to more positive potentials upon successive scans. This peak is most probably due to the Pc based oxidation, however, the reversible peak that appears about 0.65 V vs Ag/AgCl is due to doping/dedoping of the electroactive polymer film.

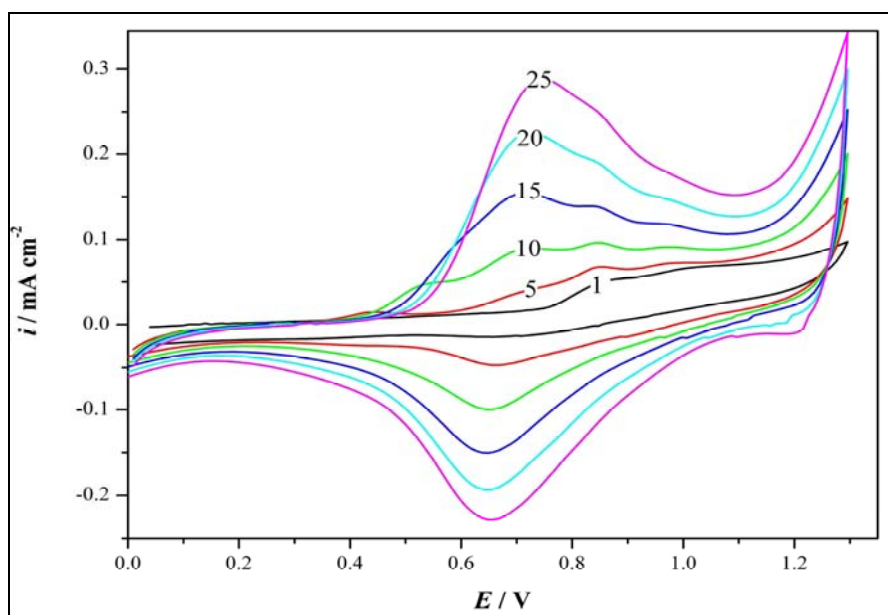


Figure 3.22 Repeated potential scan electropolymerization of 0.1 mM $\text{H}_2\text{Pc-SNS}$ on a Pt disc electrode at 100 mVs^{-1} in 0.1 M TBAP/DCM.

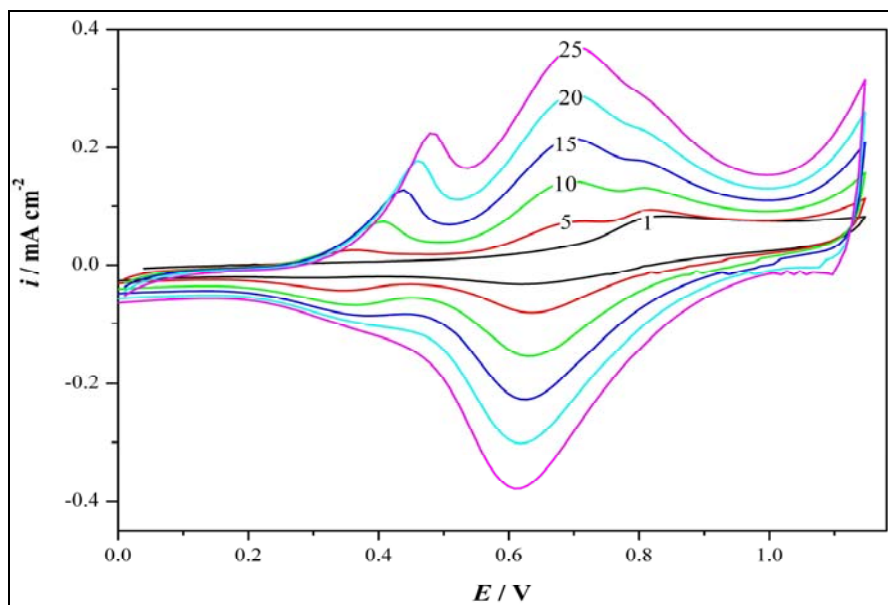


Figure 3.23 Repeated potential scan electropolymerization of 0.1 mM ZnPc-SNS on a Pt disc electrode at 100 mVs^{-1} in 0.1 M TBAP/DCM.

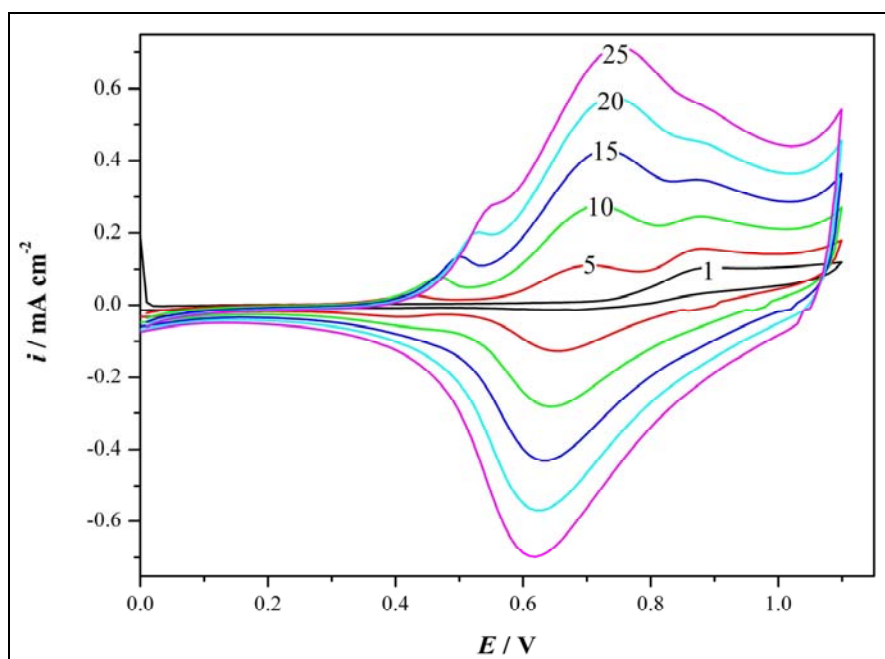


Figure 3.24 Repeated potential scan electropolymerization of 0.1 mM NiPc-SNS on a Pt disc electrode at 100 mVs^{-1} in 0.1 M TBAP/DCM.

The electrochemical behavior of the polymer films [P(H₂Pc-SNS), P(ZnPc-SNS) and P(NiPc-SNS)] obtained from complexes after 25 successive scans is also investigated in the monomer free electrolytic solution. Polymers present well-defined and reversible redox processes in 0.1 M TBAP/DCM.

The polymer films coated on the Pt disc working electrode are cycled between their neutral and oxidized states at various scan rates (20, 40, 60, 80, 100 mV s^{-1}) to elucidate the scan rate dependence of the anodic (I_{ac}) and cathodic (I_{cc}) peak currents (Figure 3.25, Figure 3.26 and Figure 3.27).

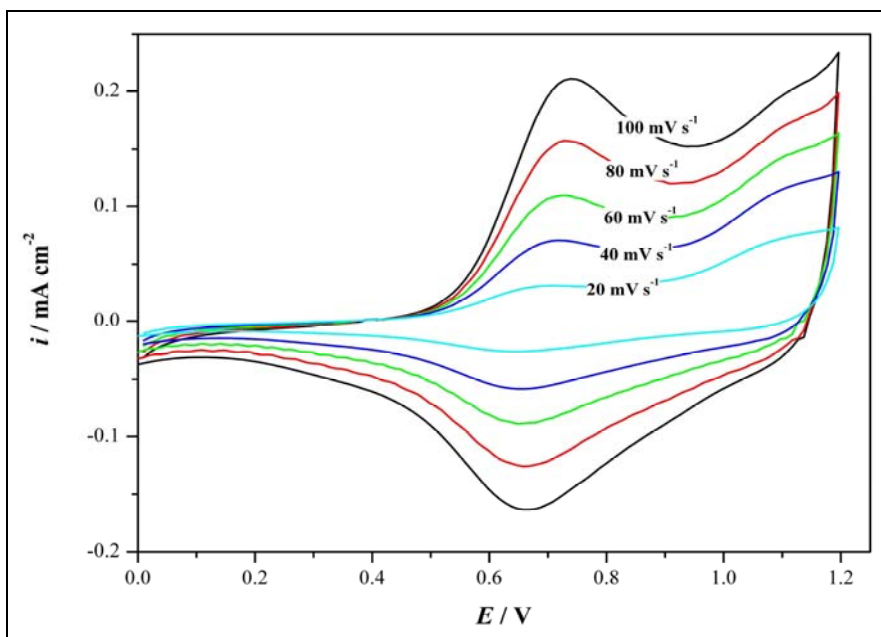


Figure 3.25 Scan rate dependence of P(H₂Pc-SNS) films (25 cycle) on a Pt disc electrode in 0.1M TBAP/DCM at different scan rates between 20 mV/s and 100 mV/s.

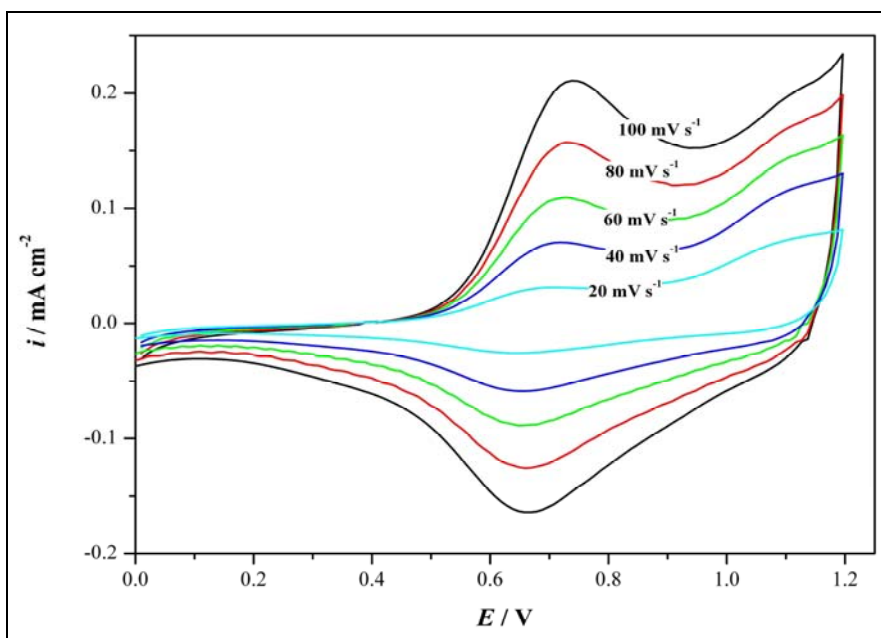


Figure 3.26 Scan rate dependence of P(ZnPc-SNS) film (25 cycle) on a Pt disc electrode in 0.1M TBAP/DCM at different scan rates between 20 mV/s and 100 mV/s.

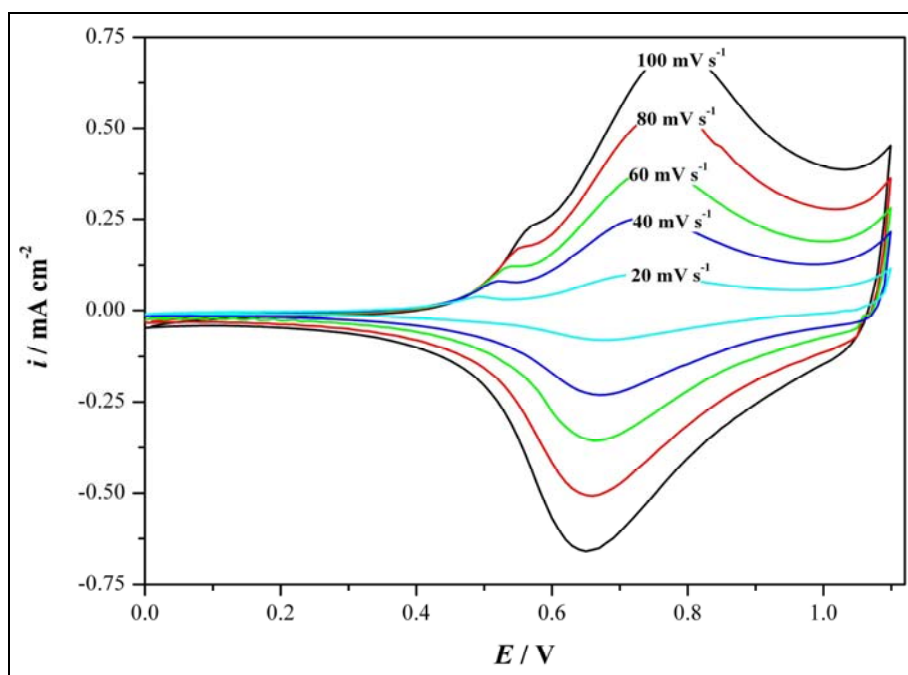


Figure 3.27 Scan rate dependence of P(NiPc-SNS) film (25 cycle) on a Pt disc electrode in 0.1M TBAP/DCM at different scan rates between 20 mV/s and 100 mV/s.

The Randles-Sevcik equation states that the peak current is given by

$$i_p = (2.69 \times 10^5) n^{3/2} A D^{1/2} C_b v^{1/2} \quad (1)$$

where n is the number of electrons in the reaction, A is the surface area of the electrode (cm^2), D is the diffusion coefficient (cm^2s^{-1}), C_b is the bulk concentration of the electroactive species (mol cm^{-3}), v is the scan rate (V s^{-1}). From this equation it can be concluded that for a diffusion-controlled system, the peak current is proportional to the square root of the scan rate in a reversible system. For these processes, it was assumed that the reactants and products are soluble in solution and the surface processes (adsorption of reactants and products) can be neglected. However, the rules change in electroactive polymer electrochemistry, because the polymer is adhered to electrode surface. Therefore, the process is not diffusion-controlled, and cannot be described by the Randles-Sevcik equation discussed above.

Instead, the peak current for a surface bound species is given by the following equation,

$$i_p = n^2 F^2 G v / 4RT \quad (2)$$

where F is the Faradays constant and G is the concentration of surface bound electroactive centers (mol cm^{-2}). Therefore, if a species is surface bound, both the anodic and cathodic peak current will scale linearly with scan rate. Thus, investigation of peak current intensity with respect to scan rate will indicate the nature of electrochemical process being diffusion controlled and the polymer is well-adhered to the electrode surface.

It is found that both anodic and cathodic peak currents depend linearly on scan rate, indicating that the redox process is non-diffusional and the polymer film is well-adhered to the working electrode surface (Figure 3.28, Figure 3.29 and Figure 3.30).

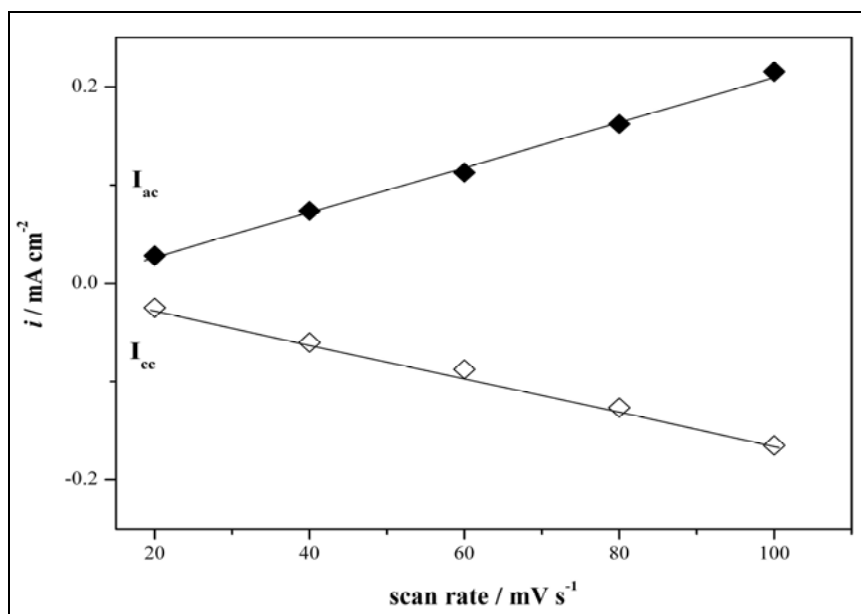


Figure 3.28 Relationship of anodic (I_{ac}) and cathodic (I_{cc}) current peaks as a function of scan rate for neutral and oxidized $\text{H}_2\text{Pc-SNS}$ in 0.1 M TBAP/DCM.

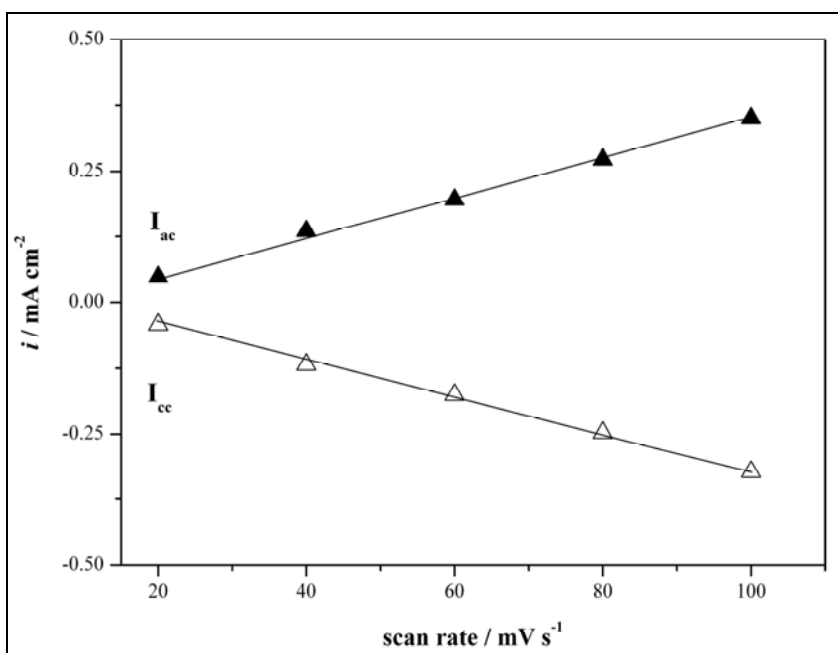


Figure 3.29 Relationship of anodic (I_{ac}) and cathodic (I_{cc}) current peaks as a function of scan rate for neutral and oxidized ZnPc-SNS in 0.1 M TBAP/DCM.

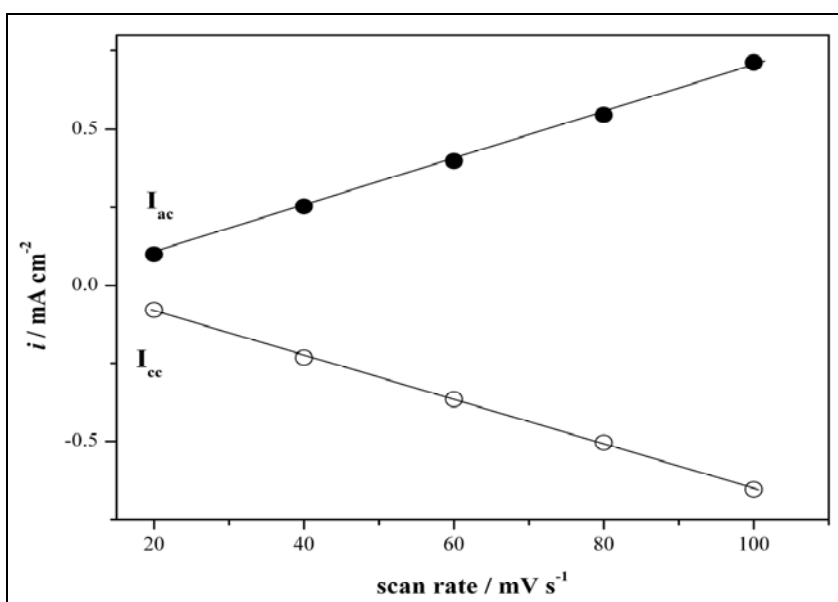


Figure 3.30 Relationship of anodic (I_{ac}) and cathodic (I_{cc}) current peaks as a function of scan rate for neutral and oxidized NiPc-SNS in 0.1 M TBAP/DCM.

In order to see if the cavity of the metal free phthalocyanine ring can interact with any metal cation, cyclic voltammograms of P(H₂Pc-SNS) are also recorded after keeping the film in contact with a solution containing TBAP and zinc (II) acetate solutions for ten minutes.

The results are depicted in Figure 3.31. As seen from Figure 3.31, oxidation peak of the polymer film shifted anodically after being kept in contact with zinc (II) acetate solution. A comparison of this voltammogram with that of recorded for P(ZnPc-SNS) (Figure 3.26) clearly indicates an interaction between zinc (II) ion and Pc ring.

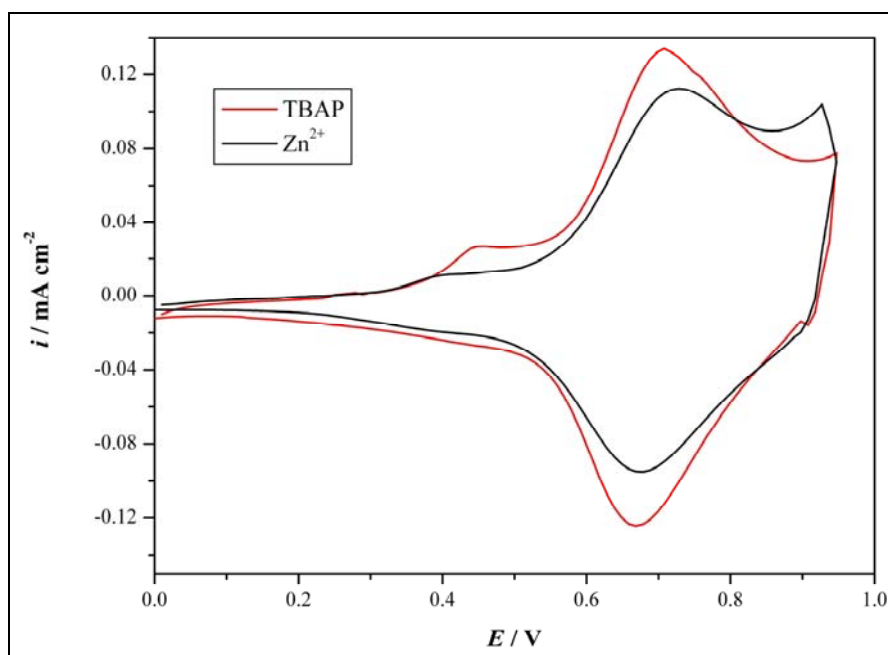


Figure 3.31 Cyclic voltammogram of P(H₂Pc-SNS) film (10 cycle) on a Pt disc electrode in DCM containing 0.1 M zinc (II) acetate and TBAP .

3.4 Spectroelectrochemistry

3.4.1 P(SNS-PN)

The important modifications of the absorption spectra of the polymers are reflected in the electronic transitions between their doped and neutral states of polymers result in. On the basis of these electro-optical properties, the use of the films as active element in smart windows and electrochromic display devices is possible.

For this purpose, P(SNS-PN) film was deposited on ITO and its electrochemical behavior was studied in the monomer-free electrolytic solution containing 0.2 M LiClO₄ and acetonitrile. After polymerization, the films were rinsed with acetonitrile to remove any unreacted monomer. Prior to spectroelectrochemical investigation, the polymer film on ITO was switched between neutral and doped states several times in order to equilibrate its redox behavior in monomer-free electrolytic solution. The changes in electronic absorption spectra recorded *in-situ* at various applied potentials are depicted in Figure 3.32.

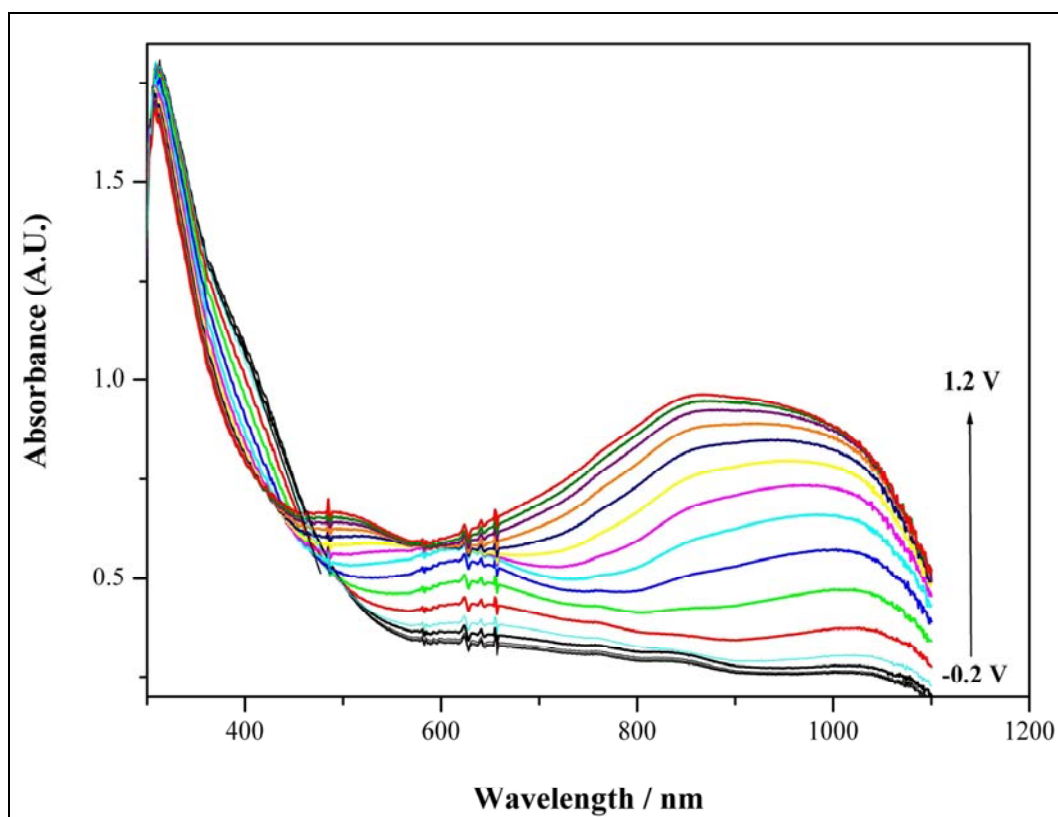


Figure 3.32 *In-situ* absorption spectra of P(SNS-PN) (55 mC/cm^2) recorded in acetonitrile containing 0.2 M LiClO_4 at various applied potentials.

As seen from Figure 3.32, the electronic absorption spectrum of the neutral form of the polymer film exhibits a band at about 389 nm due to $\pi\text{-}\pi^*$ transition and from its commencement on the low energy end the band gap (E_g) was found to be 2.45 eV [79, 84, 98, 99]. This value is slightly lower than the band gap of PSNS (2.6 eV) [83] and this difference may be attributed to the presence of electron withdrawing cyanide groups which induce a decrease in both HOMO and LUMO levels. [103]. Beyond 0.6 V , two new bands at 618 nm ($\sim 2.01 \text{ eV}$) and at 864 nm ($\sim 1.44 \text{ eV}$) start to intensify indicating the formation of polarons [104], and bipolarons, respectively. It is also noteworthy that P(SNS-PN) film can be reversibly switched between its neutral

and oxidized states and exhibits electrochromic behavior; yellow in the neutral and blue in the oxidized state.

3.4.2 P(H₂Pc-SNS), P(ZnPc-SNS) and P(NiPc-SNS)

For spectroelectrochemical investigations, the polymer films were electrodeposited on ITO electrode via constant potential electrolysis at 1.1 V (25 mC/cm²). When 25 mC/cm² achieved the electropolymerization was stopped, the electrodes were then rinsed with DCM to remove the traces of unreacted monomers or oligomeric species and then transferred into monomer-free electrolytic solution.

The changes in the electronic absorption spectrum were recorded during potential scanning from -0.2 V to 1.2 V with a voltage scan rate of 100 mV/s and the results are depicted in Figure 3.33, Figure 3.34 and Figure 3.35.

An inspection of Figure 3.33 reveals that P(H₂Pc-SNS) film, in its neutral state, exhibits three absorption bands at 345 nm, 675 nm and 705 nm which makes the polymer appear in green color. The E_g of the P(H₂Pc-SNS) was found as 2.38 eV by the commencement on the low energy end of the π - π^* transitions at 345 nm. Upon increasing the potential, the color of the P(H₂Pc-SNS) film turns to turquoise green, which is accompanied with the corresponding changes in the absorption bands.

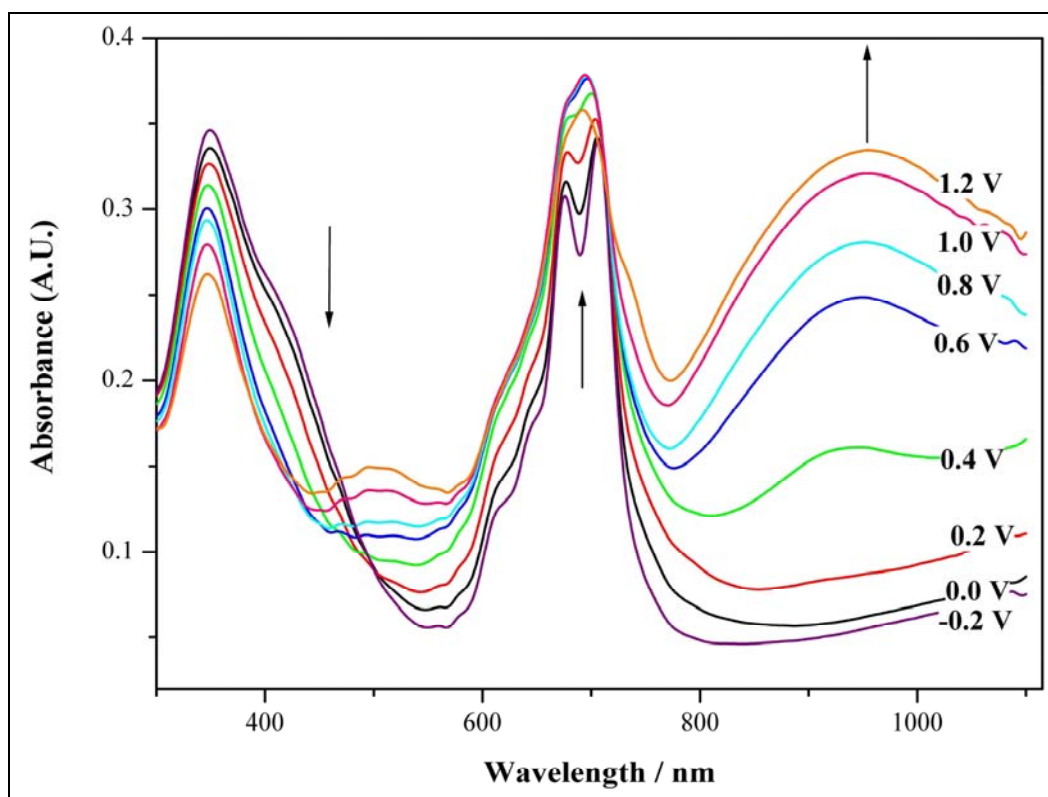


Figure 3.33 Electronic absorption spectra of P(H₂Pc-SNS) on ITO (25mC/cm²) in 0.1 M TBAP/DCM solution during anodic oxidation of the polymer film.

For P(ZnPc-SNS) (Figure 3.34) the absorption bands are observed at 345 nm, 690 nm and 729 nm and E_g of the P(ZnPc-SNS) is found as 2.25 eV. All spectra recorded during potential cycling passes through one clear isosbestic point at 489 nm indicating that P(ZnPc-SNS) is being inter converted between its neutral and oxidized states. Furthermore, a new intensifying absorption band at about 925 nm was also noted, which may be attributed to electronic transitions within the polaron energy band that develops as the P(ZnPc-SNS) film becomes electrically conductive.

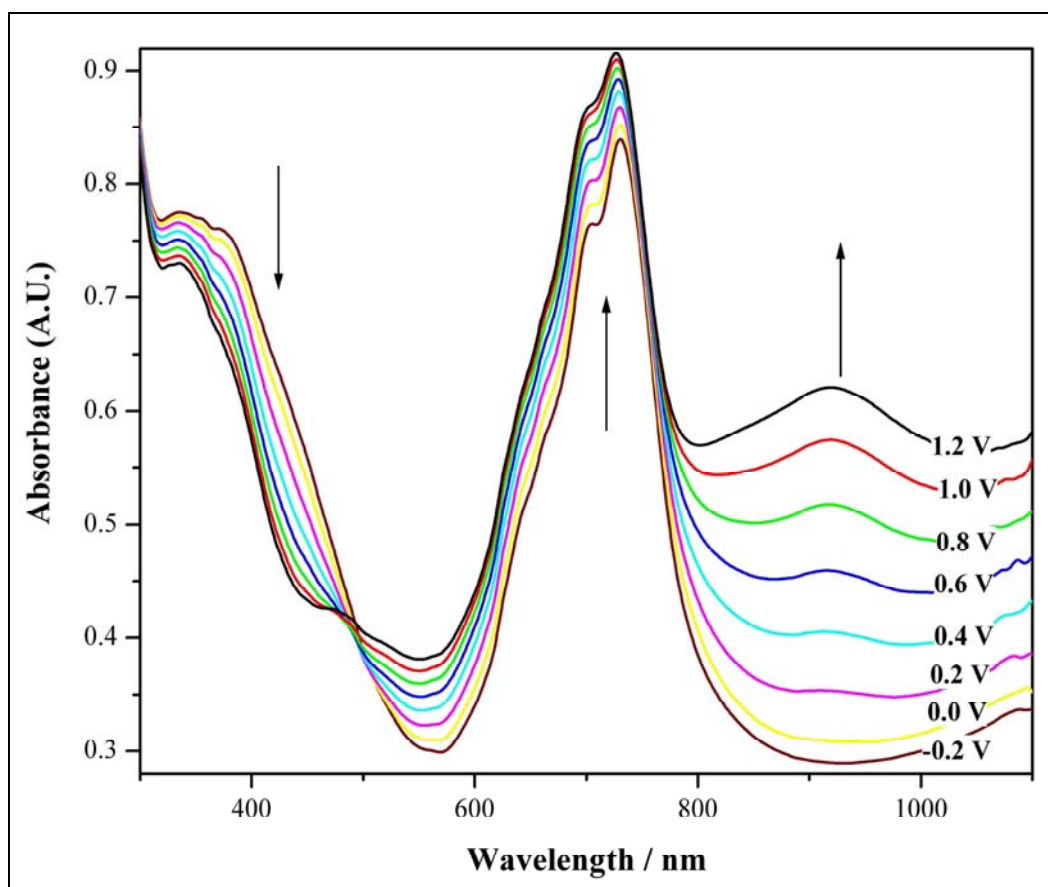


Figure 3.34 Electronic absorption spectra of P(ZnPc-SNS) on ITO ($25\text{mC}/\text{cm}^2$) in 0.1 M TBAP/DCM solution during anodic oxidation of the polymer film.

Figure 3.35 shows the electronic absorption spectra of P(NiPc-SNS) with the bands at 340 nm, 616 nm and 680 nm. By the commencement on the low energy end of the π - π^* transitions at 340 nm, E_g of the P(NiPc-SNS) is found as 2.69 eV. Upon increasing the potential, the green color of the P(NiPc-SNS) film turns to blue.

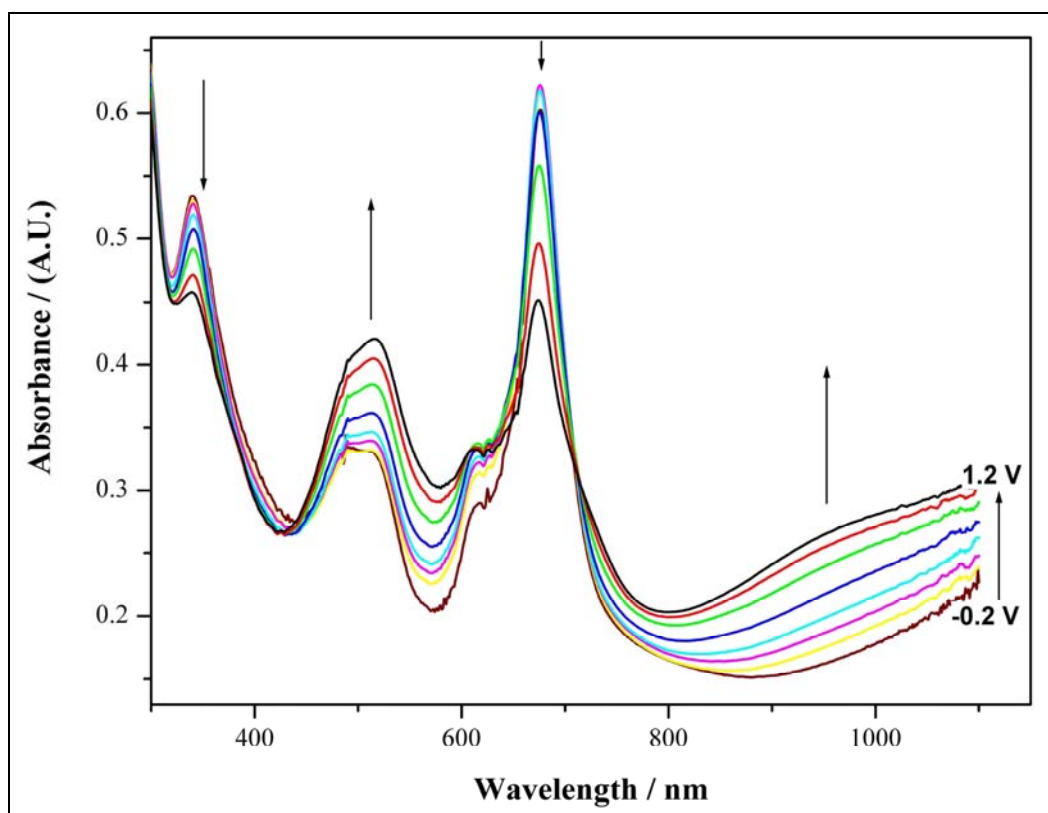


Figure 3.35 Electronic absorption spectra of P(NiPc-SNS) on ITO ($25\text{mC}/\text{cm}^2$) in 0.1 M TBAP/DCM solution during anodic oxidation of the polymer film.

3.5 Electrochromic Switching

For electrochromic applications the ability of a polymer to switch rapidly and exhibit a striking color change is important. Electrochromic switching studies are known to be the easiest and most efficient way to observe these properties.

For electrochromic switching, square wave potential step method was coupled with optical spectroscopy to investigate the switching ability of the polymer films between the neutral and oxidized states in the electrolyte solution.

The coloration efficiency (CE) of the polymer films which is a measure of optical density change (ΔOD) as a function of injected/ejected charge (Q_d) were also calculated utilizing the following equations [105, 106].

$$CE = \Delta OD / Q_d \quad (3)$$

where ΔOD is the change in optical density and Q_d is the charge (C/cm^2) passed during this process. ΔOD is determined from the percent transmittance (%T) before and after a full switch and is calculated using eqn (4), where T_{colored} and T_{bleached} are the transmittance in the oxidized and neutral states, respectively,

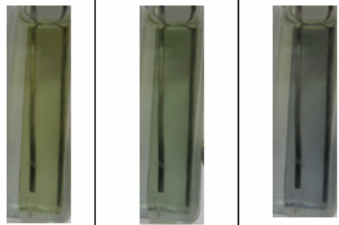
$$\Delta OD = \log (\%T \text{ of bleached state} / \%T \text{ of colored state}) \quad (4)$$

3.5.1 P(SNS-PN)

It was found that P(SNS-PN) film can be reversibly switched between its neutral and oxidized states and exhibits electrochromic behavior; yellow in the neutral and blue in the oxidized state. Switching times and optical contrast in the polymer film on ITO are determined with a change in transmittance at 389, 618 and 864 nm where the maximum transmittance difference between redox states was observed in the visible and near infrared region.

The charge passed at 95 % of the optical switch was used to evaluate CE since beyond which the naked eye cannot sense the color difference. The polymer film coated on ITO (55 mC/cm^2) was switched between 0.0 V and 1.1 V vs Ag-wire and the time required to attain 95 % of the total transmittance difference was found to be 1.7 s for fully oxidized state and 1.5 s for fully neutral state at 389 nm. Also, the value of CE at 864 nm was found as $266 \text{ cm}^2/\text{C}$ (see Table 3.4).

Table 3.4 Voltammetric and spectroelectrochemical data for P(SNS-PN) recorded in AN containing 0.1 M LiClO₄.

λ_{nm} at charge 55mC/cm ²	T _{bleached}	T _{colored}	$\Delta\%T$	ΔOD	CE (cm ² /C)	Neutral State	Intermediate State	Oxidized state
389	35.98	59.87	23.89	0.221	148			
618	45.46	69.71	24.25	0.186	108			
864	31.96	86.45	54.49	0.432	266			

3.5.2 P(H₂Pc-SNS), P(ZnPc-SNS) and P(NiPc-SNS)

The switching ability of the polymer films P(H₂Pc-SNS), P(ZnPc-SNS) and P(NiPc-SNS) between neutral and doped states in the electrolytic solution was investigated and it was observed that the polymer films exhibit electrochromic behavior.

The change in electro-optical responses was recorded in situ while switching between 0.0 V and 1.1 V with a residence time of 10 s. The ΔOD and CE of the polymer films were calculated using equations (3) and (4) (Sec. 3.5).

Values are reported at 90% of a full switch, beyond which the naked eye cannot sense the difference. As seen from Table 3.5, Table 3.6 and Table 3.7 the CE of P(NiPc-SNS) is notably higher than that of P(H₂Pc-SNS) and P(ZnPc-SNS). This can be expressed by different doping levels of phthalocyanine polymers.

Table 3.5 Voltammetric and spectroelectrochemical data for P(H₂Pc-SNS) recorded in DCM containing 0.1 M TBAP.

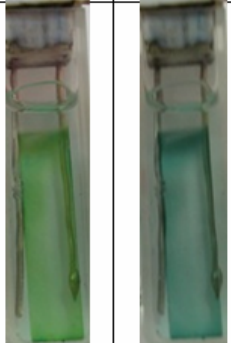
λ/nm at charge $25\text{mC}/\text{cm}^2$	T_{bleached}	T_{colored}	$\Delta\%T$	ΔOD	CE (cm^2/C)	Reduced State	Oxidized state
345	26.1	28.4	2.3	0.037	22.35		
675	27.35	28.64	1.29	0.02	11.71		
705	23.7	24.75	5.91	0.019	10.82		

Table 3.6 Voltammetric and spectroelectrochemical data for P(ZnPc-SNS) recorded in DCM containing 0.1 M TBAP.

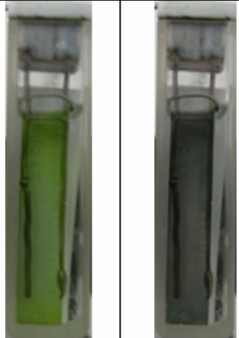


λ/nm at charge $25\text{mC}/\text{cm}^2$	T_{bleached}	T_{colored}	$\Delta\%T$	ΔOD	CE (cm^2/C)	Reduced State	Oxidized state
345	34.4	40.1	5.7	0.067	63.7		
690	27.77	35.6	7.83	0.108	137		
729	39.98	45.7	5.72	0.058	65.2		

Table 3.7 Voltammetric and spectroelectrochemical data for P(NiPc-SNS) recorded in DCM containing 0.1 M TBAP.

λ/nm at charge $25\text{mC}/\text{cm}^2$	T_{bleached}	T_{colored}	$\Delta\%T$	ΔOD	CE (cm^2/C)	Reduced State	Oxidized state
340	23.16	28.63	5.47	0.092	71.9		
500	39.84	49.98	10.14	0.099	86.71		
676	18.86	31.08	12.22	0.217	162.43		

3.6 Fluorescence Study

3.6.1 P(SNS-PN)

Since the electrochemically obtained P(SNS-PN) was found to be soluble in DMF (0.034 g/100 mL) and partially soluble in DMSO, the fluorescence property of both monomer and polymer were investigated in these solvents.

Although the monomer exhibits a weak emission at about 400 nm, its polymer has a relatively intense emission band at the same wavelength when excited at 340 nm, corresponding to blue color (Figure 3.36). These results indicate that this polymer is a blue light emitter and it may find applications in various fields, such as organic lasers and electroluminescent materials.

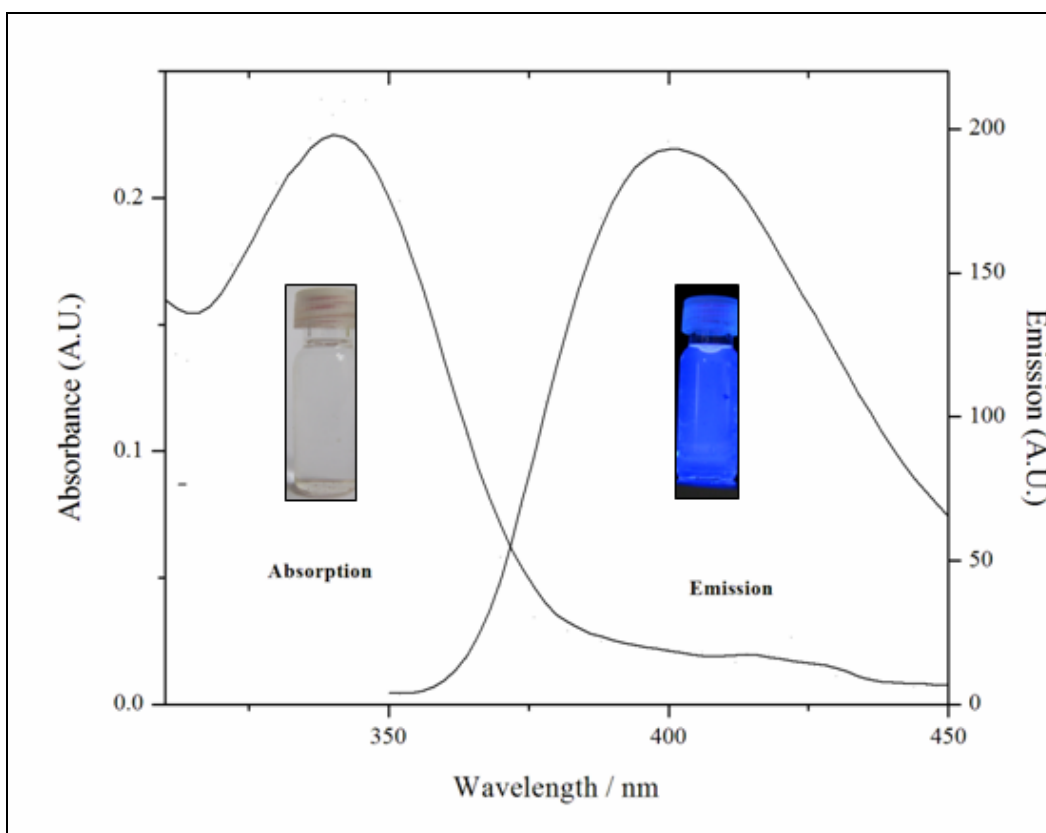


Figure 3.36 Absorption and emission spectra of P(SNS-PN) in DMSO .

It is noteworthy that the emission intensity increases in the presence of Li^+ and Na^+ cations, Figure 3.37. This observation also indicates the presence of an interaction between the cyanide groups of the polymer and the cations and is in accordance with the results obtained from CV studies.

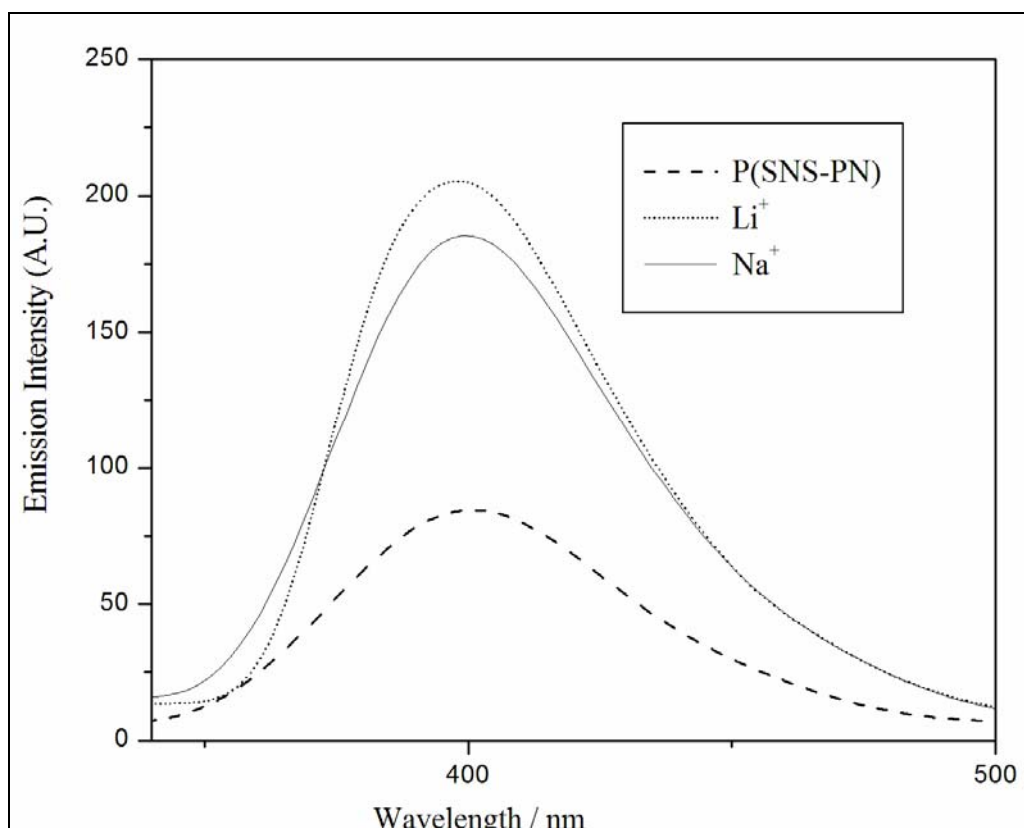


Figure 3.37 Emission spectra of P(SNS-PN) recorded in the presence of 3.3×10^{-5} M LiClO_4 and NaClO_4 in DMF

3.6.2 P(ZnPc-SNS)

The fluorescent property of P(ZnPc-SNS) was studied in DMSO and toluene. Figure 3.38 shows the fluorescence spectra of the polymer in DMSO (a) and toluene (b), respectively. In DMSO, P(ZnPc-SNS) illustrated an emission peak at 407 nm which is attributed to violet color, and in toluene, gave emission band at 590 nm which is orange color. These properties make the polymer a good candidate for practical use such as for light emitting diodes and optical displays.

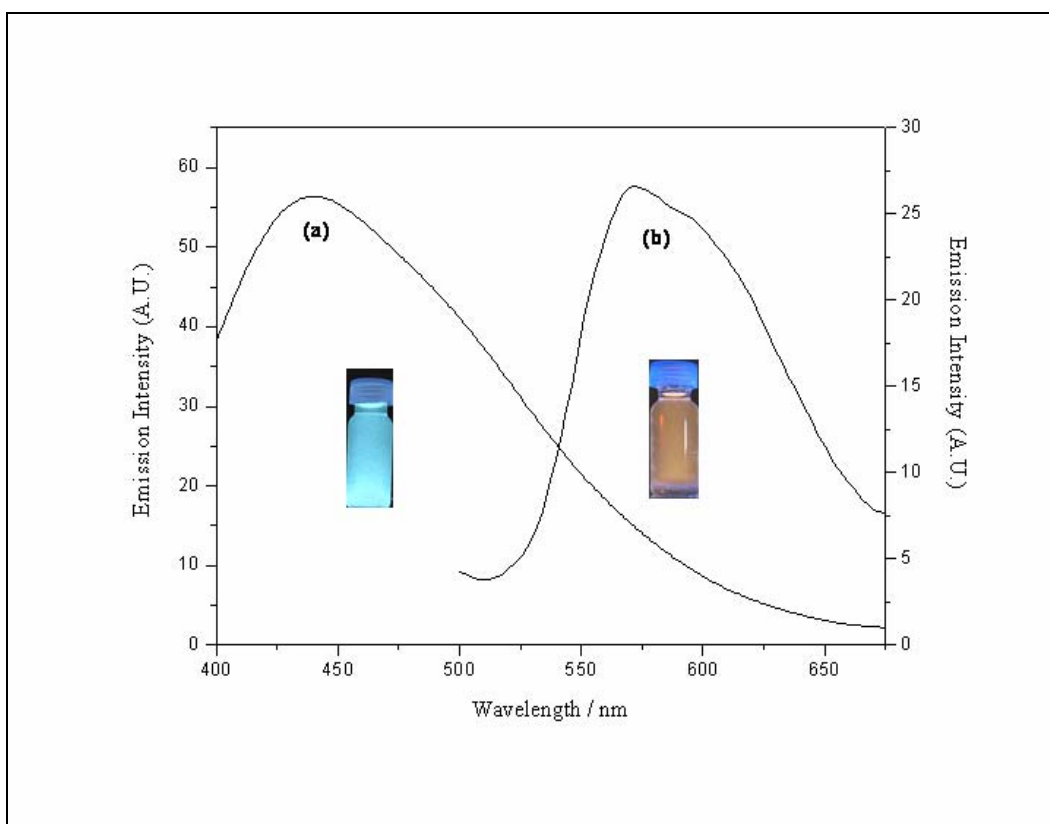
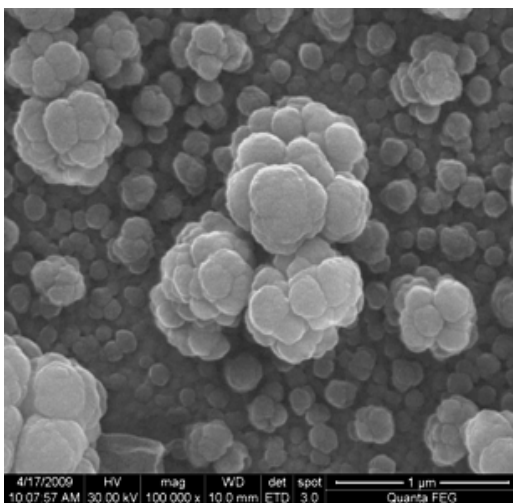


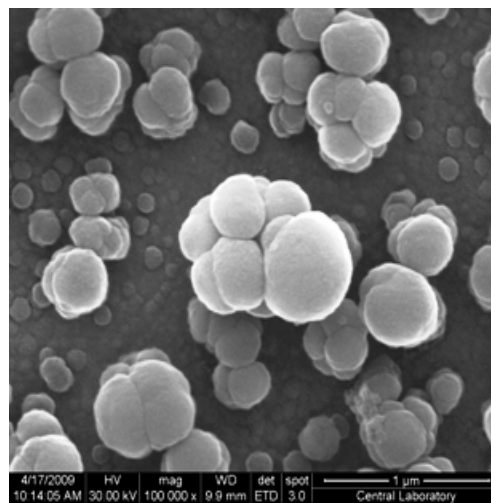
Figure 3.38 Emission spectra of P(ZnPc-SNS) (excited at 370 nm) in (a) DMSO and (b) toluene.

3.7 Morphologies of P(H₂Pc-SNS), P(ZnPc-SNS) and P(NiPc-SNS)

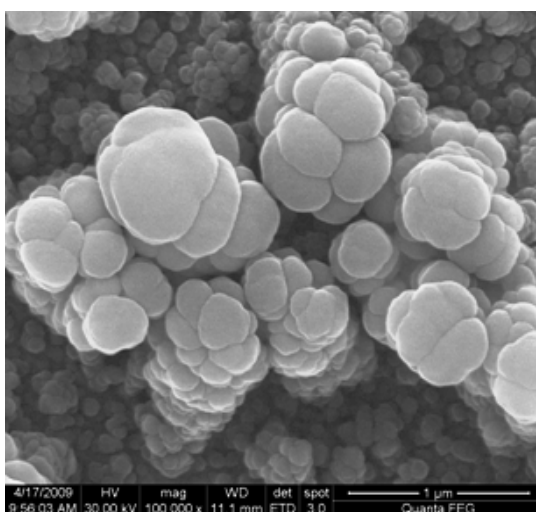
SEM micrographs of P(H₂Pc-SNS), P(ZnPc-SNS) and P(NiPc-SNS) imply that the synthesized monomer is good in film forming, exhibiting homogeneous and compact structure. The solution side of the polymer films revealed similar morphologies having a cauliflowerlike structure (Figure 3.39).



(a)



(b)



(c)

Figure 3.39 SEM micrographs of solution side of (a) P(H₂Pc-SNS) (b) P(ZnPc-SNS) and (c) P(NiPc-SNS)

CHAPTER 4

CONCLUSION

In the first part of this study, the synthesis of a new Pc precursor, SNS-PN, was successfully achieved by utilizing 1,4-di(2-thienyl)-1,4-butadione and 4-aminophthalonitrile via Knorr-Paal Reaction. Characterization of this compound was performed by NMR and FTIR spectroscopies and elemental analysis. Its corresponding polymer was synthesized by electropolymerization in LiClO₄/acetonitrile electrolytic medium and characterized by CV, UV-vis and FTIR spectroscopic techniques. Since SNS-PN has two electron withdrawing cyanide groups per monomer unit, the oxidation potential of the monomer and first oxidation potential of the polymer are slightly higher than the reported values for various SNS derivatives.

Spectroelectrochemical analyses revealed that the polymer of SNS-PN has electronic band gap of 2.45 eV. The time required to attain 95% of the total transmittance difference was found to be 1.7 s for P(SNS-PN). Optical contrast values were measured as 24 %. The polymer film, besides exhibiting a well-defined and reversible redox process in acetonitrile, also exhibits stable electrochromic behavior: yellow in the neutral state and blue in the oxidized state. Soluble part of the polymer in DMSO has the fluorescent property emitting blue light. Moreover, the fluorescence intensity enhances in the presence of several cations, in DMF, due to the interactions between cyanide groups and cations. This result and the shifts in the oxidation potential of the polymer film makes P(SNS-PN) also a candidate in cation sensing, besides its use in organic lasers and electroluminescent materials.

In the second part, novel tetrakis SNS substituted H₂Pc-SNS, ZnPc-SNS and NiPc-SNS complexes were synthesized and characterized by elemental analysis, FTIR and UV-Vis spectroscopies. The oxidative electrochemical polymerization of these complexes were achieved in 0.1 M TBAP/DCM, electrolyte/solvent couple utilizing CV. Cyclic voltammograms of H₂Pc-SNS, ZnPc-SNS and NiPc-SNS exhibited one irreversible oxidation peak at 0.85 V, 0.82 V and 0.88 V in the first anodic scan, respectively. The slight difference in the peak potentials may be due to the interaction between metal ions and Pc ligand, which shifts the oxidation potential to lower values.

Electrochemical and spectroelectrochemical properties of the polymer films were investigated via in-situ spectroelectrochemical and CV techniques in monomer free electrolytic medium. The polymer films were found to exhibit a well-defined and reversible redox processes accompanied by electrochromic changes which make both polymers a candidate for electrochromic material applications. Although all of the polymer films were green in their neutral states, they exhibit different colors in their oxidized state (P(H₂Pc-SNS) turquoise green, P(ZnPc-SNS) black and P(NiPc-SNS) blue). The E_g of the P(H₂Pc-SNS), P(ZnPc-SNS) and P(NiPc-SNS) were found as 2.38 eV, 2.25 eV and 2.69 eV, respectively. The fluorescent property of P(ZnPc-SNS) was studied in DMSO and toluene. Fluorescence measurement showed that the P(ZnPc-SNS) is a good blue and orange light emitter which may find applications in organic lasers and/or LEDs.

REFERENCES

- [1] A. Braun, J. Tscherniac, *Berichte der Deutschen Chemischen Gesellschaft* 40 (1907) 2709.
- [2] H. Diesbach, E. Weid, *Helv. Chim. Acta* 10 (1927) 886.
- [3] A.G. Dandridge, H.A.E. Drescher, A.R. Thomas, *Dyes* 322 (1929) 169.
- [4] C.T.J. Cronshaw, *Endeavour* 1 (1942) 79.
- [5] (a) R. Linstead, A.Lowe, *J. Chem. Soc.* (1934) 1016 (b) M. Hesse, H. Meier, B. Zeeh, *Spektroskopische Methoden in der Organischen Chemie*. Auflage Goerge Thieme Verlag Stuttgart, New York (1991) (c) G. Byrne, R. Linstead, A. Lowe, *J. Chem. Soc.* (1934) 1017 (d) R. Linstead, A. Lowe, *J. Chem. Soc.* (1934) 1022 (e) C. Dent, R. Linstead, *J. Chem. Soc.* (1934) 1027.
- [6] (a) J. Robertson, *J. Chem. Soc.* (1934) 615 (b) J. Robertson, I. Woodward, *J. Chem. Soc.* (1937) 219.
- [7] (a) P. Turek, P. Petit, J. Andre, J. Simon, R. Even, *J. Am. Chem. Soc.* 109 (1987) 5119 (b) P. Moskalev, I. Kirin, *Russ. J. Phys. Chem.* 46 (1972) 1778 (c) J. Andre, K. Holczer, P. Petit, R. Even, *Chem. Phys. Lett.* 115 (1985), 115 463.
- [8] W.M. Sharman, J.E. van Lier, *Synthesis of Phthalocyanine Precursors* in The Porphyrin Handbook, Vol. 15, Academic Press (2003).
- [9] C.C. Leznoff, A.B.P. Lever (Eds.) *Phthalocyanine: Properties and application* Vol.1-4, VCH, New York, (1989-1996).
- [10] N. McKeown *The synthesis of symmetrical phthalocyanines* in The Porphyrin Handbook, Vol. 15, Academic Press, (2003).
- [11] M. Sommerauer, C. Rager, M. Hanack, *J. Am. Chem. Soc.* 118 (1996) 10085
- [12] N. McKeown, *Science of Synthesis*, Vol. 17, Capital 9, Thieme Chemistry, Rochdale, UK, (2005).
- [13] I. Rosenthal, E. Ben-Hur, *Phthalocyanines Properties and Applications*, in C.C. Leznoff, A.B.P. Lever, VCH, Vol. 1, 393-425 (1989).

- [14] I. Rosenthal, *Photochem. Photobiol.* 53 (1991) 859.
- [15] B.W. Henderson, T.J. Dougherty, *Photochem. Photobiol.* 55 (1992) 145.
- [16] M.K. Emmelius, G. Pawlowski, H. Vollman, *Angew. Chem.* 28 (1989) 1445.
- [17] M.M. Nicolson, in C.C. Leznoff, A.B.P. Lever, *Phthalocyanines Properties and Applications*, VCH, New York, Vol. 3, 75-117 (1993).
- [18] K.M. Brown, K.T. Gleim, P. Urban, *Oil Gas* 57 (1959) 73.
- [19] P. Salazar, *Handbook of Petroleum Process*, in R.A. Meyers Part 9, McGraw-Hill, New York.
- [20] G. Schneider, D. Wohrle, W. Spiller, J. Stark, G. Schulz-Ekloff, *Photochem. Photobiol.* 60 (1994) 333.
- [21] R. Gerdes, O. Bartels, G. Schneider, D. Wohrle, G. Schulz-Ekloff, *Int. J. Photoenergy* 1 (1999) 41.
- [22] D. Wohrle, O. Suvorova, R. Gerdes, O. Bartels, L. Lapok, N. Baziakina, S. Makarov, A. Slodek, *Processes of Petrochemistry and Oil Refining* 3 (2002) 30.
- [23] D. Wohrle, D. Meissner, *Adv. Mater.* 3 (1991) 129.
- [24] M.K. Nazeeruddin, M. Humphry-Baker, M. Gratzel, B.A. Murrer, *Chem. Commun.* (1998) 719.
- [25] M.K. Nazeeruddin, M. Humphry-Baker, M. Gratzel, D. Wohrle, G. Schnurpfeil, G. Schneider, A. Hirth, N. Trombach, *J. Porphyrins Phthalocyanines* 3 (1999) 230.
- [26] C. Piechocki, J. Simon, A. Skoulios, D. Guillon, P. Weber, *J. Am. Chem. Soc.* 104 (1982) 5245.
- [27] A.N. Cammidge, M.J. Cook, K.J. Harrison, N.B. McKeown, *J. Chem. Soc., Perkin Trans.* 1 (1991) 3053.
- [28] J. Batey, M.C. Petty, G.G. Roberts, D.R. Wright, *Electron. Lett.* 20 (1984) 489.
- [29] J.H. Zagal, *J. Electroanal. Chem.* 109 (1980) 389.
- [30] T. Kilcuchi, H. Sasaki, S. Toshima, *Chem. Lett.* (1980) 5.
- [31] M.M. Nicolson, *Phthalocyanine: Properties and Applications*, in C.C. Leznoff, A.B.P. Lever, New York, VCH, Vol. 4, 79-181 (1996).

- [32] R.C. Ahuja, K. Hauffe, *Ber. Bunsenges. Phys. Chem.* 84 (1980) 68.
- [33] N.B. McKeown, *Chem. Industry* (1999) 92.
- [34] K.Y. Law, in H.S. Nalwa, *Handbook of Organic Conductive Molecules and Polymers*, Wiley, Chichester, Vol. 1, 487-551 (1997).
- [35] A. Grund, A. Kaltbeitzel, A. Mathy, R. Schwartz, C. Bubeck, P. Vernmehren, M. Hanack, *J. Phys. Chem.* 96 (1992) 7450.
- [36] M.J. Cook, *Pure Appl. Chem.* 71 (2002) 2145.
- [37] X. Lu, K.W. Hipps, X.D. Wang, U. Mazur, *J. Am. Chem. Soc.* 118 (1996) 7197.
- [38] M. Gouterman, in D. Dolphin, *The Porphyrins, Part A. Physical Chemistry*, Academic Press, New York (1978).
- [39] A. J. McHugh, M. Gouterman, C. Weiss, *Theoret. Chim. Acta* 24 (1987) 246.
- [40] A. M. Schaffer, M. Gouterman, E. R. Davidson, *Theoret. Chim. Acta* 30 (1973) 9.
- [41] J.F. Myers, R.G.W. Canham, A.B.P. Lever, *Inorg. Chem.* 14 (1975) 461.
- [42] M.N. Golovin, P. Seymour, K. Jayaraj, Y.S. Fu, A.B.P. Lever, *Inorg. Chem.* 29 (1990) 1719.
- [43] H. S. Nalwa, *Appl. Organomet. Chem.* 5 (1991) 349.
- [44] A.B.P. Lever, *Adv. Inorg. Radiochem.* 7 (1965) 28.
- [45] D. Wöhrle, *Phthalocyanines in Polymer Phases*, in: *Phthalocyanines, Properties and Applications*, in C. C. Leznoff, A. B. P. Lever, VCH, New York (1989).
- [46] D. Wöhrle, U. Marose, R. Knoop, *Makromol. Chem.* 186 (1985) 2209.
- [47] H. Li, T.F. Guarr, *J. Chem. Soc. Chem. Commun.* (1989) 832.
- [48] F. Xu, H. Li, Q. Peng, T.F. Guarr, *Synth. Met.* 55-57 (1993) 1668.
- [49] F. Xu, H. Li, S.J. Cross, T.F. Guarr, *J. Electroanal. Chem.* 368 (1994) 221.
- [50] E.M. Genies, G. Bidan, A.F. Diaz, *J. Electroanal. Chem.* 149 (1983) 101.
- [51] E.W. Paul, A.J. Ricco, M.S. Wrighton, *J. Phys. Chem.* 89 (1985) 1441.
- [52] Y.B. Shim, S.M. Park, *J. Electrochem. Soc.* 144 (1997) 3027.
- [53] H.J. Lee, S.Y. Cui, S.M. Park, *J. Electrochem. Soc.* 148 (2001) D139.

- [54] R.G. Linford, *Electrochemical Science and Technology of Polymers*, Elsevier, London and New York (1987).
- [55] J. Heinze, *Top. Curr. Chem.* 152 (1990) 1.
- [56] A. Merz, *Topics Curr. Chem.* 152 (1990) 49.
- [57] T.A. Skotheim, *Handbook of Conducting Polymers*, Vols. 1 and 2, Marcel Dekker, New York (1986).
- [58] A. Deronzier, J.C. Moutet, *Acc. Chem. Res.* 22 (1989) 249.
- [59] D. Curran, J. Grimshaw, S.D. Perera, *Chem. Soc. Rev.* 20 (1991) 391.
- [60] J. Roncali, *Chem. Rev.* 92 (1992) 711.
- [61] R. Varma, J.R. Selman *Techniques for characterization of electrodes and electrochemical processes*, Wiley, New York (1991).
- [62] M. Kalaji, L.M. Peter, *J. Chem. Soc. Faraday Trans.* 87 (1991) 853.
- [63] C. Bonazzola, E.J. Calvo, *J. Electroanal. Chem.* 449 (1998) 111.
- [64] M.C. Miras, C. Barbero, R. Kötz, O. Haas, V.M. Schmidt, *J. Electroanal. Chem.* 338 (1992) 279.
- [65] P.M.S. Monk, R.J. Mortimer, D.R. Rosseinsky, *Electrochromism*, VCH, Weinheim, 124–143 (1995).
- [66] J.R. Platt, *J. Chem. Phys.* 34 (1961) 862.
- [67] P.M.S. Monk, R.J. Mortimer, D.R. Rosseinsky, *Electrochromism: Fundamentals and applications*, Weinheim, Germany, Wiley, VCH (1995).
- [68] R.J. Mortimer, *Chem. Soc. Rev.* 26 (1997) 147.
- [69] D.R. Rosseinsky, R.J. Mortimer, *Adv. Mater.* 13 (2001) 783.
- [70] P.R. Somani, S. Radhakrishnan, *Mater. Chem. Phys.* 77 (2002) 117.
- [71] T.L. Rose, S. D'Antonio, M.H. Jillson, A.B. Kon, R. Suresh, F. Wang, *Synth. Met.* 85 (1997) 1439.
- [72] E.B. Franke, C.L. Trimble, J.S. Hale, M. Schubert, J.A. Woollam, *J. Appl. Phys.* 88 (2000) 5777.
- [73] P. Topart, P. Hourquebie, *Thin Solid Films* 352 (1999) 243.
- [74] C. Alkan, L. Aras, G. Gündüz *J. Appl. Polym. Sci.* 106 (2007) 378.

- [75] C. Alkan, L. Aras, G. Gündüz *J. Appl. Polym. Sci. Part A: Polym. Chem.* 44 (2006) 5692.
- [76] C. Alkan, L. Aras, G. Gündüz, *e-Polymers* no.070 (2004).
- [77] J. Griffiths, B. Roozpeikar, *J. Chem. Soc. Perkin Trans. 1* (1976) 42.
- [78] A. Merz, F. Ellinger, *Synthesis* 6 (1991) 462.
- [79] S. Tarkuç, E. Sahmetlioğlu, C. Tanyeli, I.M. Akhmedov, L. Toppare, *Electrochim. Acta* 51 (2006) 5412.
- [80] F. Alğı, A. Cihaner, *Tetrahedron Lett.* 49 (2008) 3530.
- [81] P.E. Just, K.I. Chane-Ching, P.C. Lacaze, *Tetrahedron* 58 (2002) 3467.
- [82] M. Durmuş, S. Yeşilot, V. Ahsen, *New J. Chem.* 30 (2006) 675.
- [83] J.P. Ferraris, T.R. Hanlon, *Polymer* 30 (1989) 1319.
- [84] E. Şahin, E. Sahmetlioglu, I.M. Akhmedov, C. Tanyeli, L. Toppare, *Organic Electronics* 7 (2006) 351.
- [85] A. Cihaner, F. Alğı, *Electrochim. Acta* 53 (2008) 2574.
- [86] S. Marcuccio, P.I. Svirskaya, S. Greenberg, A.B.P. Lever, *Can.J.Chem.* 63 (1985) 3057.
- [87] M. Gouterman, *The porphyrins*. In: D. Dolphin, editor 3, New York, Academic, 1 (1978).
- [88] S. Wie, D. Huang, L. Li, Q. Meng, *Dyes Pigments* 51 (2003) 51.
- [89] M.J. Stillman, T. Nyokong, *Phthalocyanines: properties and applications*, in: C.C. Leznoff, A.B.P. Lever (Eds.), chapter 3, VCH, New York, Vol. 1 (1989).
- [90] A. Yavuz, B. Bezgin, M.A. Önal, *J. Appl. Polym. Sci.* in Press, (2009) DOI: 10.1002/app.30269.
- [91] H. Enkelkamp, R.J.M. Nolte, *J. Porphyrins Phthalocyanines* 4 (2000) 454.
- [92] D.D. Dominguez, A.W. Snow, J.S. Shirkn, R.G.S. Pong, *J. Porphyrins Phthalocyanines* 5 (2001) 582.
- [93] W.J. Kroenke, M.E. Kenney, *Inorg. Chem.* 3 (1964) 696.
- [94] A.N. Sidorov, I.P. Kotlyar, *Opt. I. Spektr.* 11 (1961) 175.

- [95] T.F Guarr, *Handbook of Organic Conductive Molecules and Polymers*, in: H.S. Nalwa (Ed.), Wiley, Chichester, vol.4, 461, (1997).
- [96] D.P. Goldberg, L.J.S. Michel, A.J.P. White, D.J. Williams, A.G.M. Barrett, B.M. Hoffman, *Inorg. Chem.* 37 (1998) 2100.
- [97] A.B.P. Lever, E.R. Milaeva, G. Speier, *The Redox Chemistry of Metallophthalocyanines in Solution in Phthalocyanines: Properties and Applications*, in: C.C. Leznoff, A.B.P. Lever (Eds.), vol. 3, VCH, New York, (1993)
- [98] S. Tarkuç, E. Sahmetlioğlu, C. Tanyeli, I.M. Akhmedov, L. Toppare, *Sensor Actuat. B: Chem.* 121 (2007) 622.
- [99] S. Variş, M. Ak, C. Tanyeli, I.M. Akhmedov, L. Toppare, *Eur. Polym. J.* 42 (2006) 2352.
- [100] A. Cihaner, F. Algi, *J. Electroanal. Chem.* 614 (2008) 101.
- [101] R.F. Lane, A. T. Hubbard, *J. Phys. Chem.* 77 (1973) 1401.
- [102] E. Lavion, *J. Electroanal. Chem.* 39 (1972) 1.
- [103] J. Roncali, *J. Macromol. Rapid Commun.* 28 (2007) 1761.
- [104] T. Yamamoto, *J. Chem. Soc. Chem. Commun.* (1981) 187.
- [105] C.L. Gaupp, D.M. Welsh, R.D. Rauh, J.R. Reynolds, *Chem. Mater.* 14 (2002) 3964.
- [106] B.D. Reeves, C.R.G Grenier, A.A. Argun, A. Çırpan, T.D. Mccarley, J.R. Reynolds, *Macromolecules* 37 (2004) 7559.

CURRICULUM VITAE

PERSONAL INFORMATION

Surname, Name: Yavuz, Arzu
Nationality: Turkish (TC)
Date and Place of Birth: 2 March 1979 , Karaman
Marital Status: Married
Phone: +90 312 210 32 09
Fax: +90 312 210 32 00
email: arzubuyukyagci@yahoo.com

EDUCATION

Degree	Institution	Year of Graduation
MS METU	Chemistry	2004
BS METU	Chemistry	2001
High School	Karaman Anadolu High School	1997

WORK EXPERIENCE

Year	Place	Enrollment
2008-Present	MTA Genel Müdürlüğü, Ankara	Analyst
2001-2008	METU Department of Chemistry	Research Assistant

FOREIGN LANGUAGES

Advanced English

PUBLICATIONS

1. A. Yavuz, B. Bezgin, A. M. Önal "Synthesis and Characterization of a New Conducting Polymer Based on 4-(2,5-di-2-thiophen-2-ylpyrrol- 1-yl)-phthalonitrile", Journal of Applied Polymer Science, in Press (2009) DOI: 10.1002/app.30269.

2. A. Yavuz, G. Tuzcu, L. Aras "Synthesis of copolymers of methoxy polyethylene glycol acrylate and 2-acrylamido-2-methyl-1-propanesulfonic acid: Its characterization and application as superplasticizer in concrete" Cement and Concrete Research, 39 (2009) 629.

HOBBIES

Movies, Swimming, Tennis.